NAVAL POSTGRADUATE SCHOOL

MONTEREY, CALIFORNIA

THESIS

AIRCRAFT EVALUATION USING STOCHASTIC DUELS

by

Jason W.C. Gay

September 2017

Thesis Advisor:	Moshe Kress
Co-Advisor:	Michael Atkinson
Second Reader:	Roberto Szechtman

THIS PAGE INTENTIONALLY LEFT BLANK

REPORT DOCUMENTATION PAGE			*Form Approved OMB No. 0704-0188*
Public reporting burden for this collection of information is estimated to average 1 hour per response, including the time for reviewing instruction, searching existing data sources, gathering and maintaining the data needed, and completing and reviewing the collection of information. Send comments regarding this burden estimate or any other aspect of this collection of information, including suggestions for reducing this burden, to Washington headquarters Services, Directorate for Information Operations and Reports, 1215 Jefferson Davis Highway, Suite 1204, Arlington, VA 22202-4302, and to the Office of Management and Budget, Paperwork Reduction Project (0704-0188) Washington DC 20503.			
1. AGENCY USE ONLY ***(Leave blank)***	**2. REPORT DATE** September 2017	**3. REPORT TYPE AND DATES COVERED** Master's thesis	
4. TITLE AND SUBTITLE AIRCRAFT EVALUATION USING STOCHASTIC DUELS			
6. AUTHOR(S) Jason W.C. Gay			
7. PERFORMING ORGANIZATION NAME(S) AND ADDRESS(ES) Naval Postgraduate School Monterey, CA 93943-5000			**8. PERFORMING ORGANIZATION REPORT NUMBER**
9. SPONSORING /MONITORING AGENCY NAME(S) AND ADDRESS(ES) N/A			**10. SPONSORING / MONITORING AGENCY REPORT NUMBER**
11. SUPPLEMENTARY NOTES The views expressed in this thesis are those of the author and do not reflect the official policy or position of the Department of Defense or the U.S. Government. IRB number ____N/A____.			
12a. DISTRIBUTION / AVAILABILITY STATEMENT Approved for public release. Distribution is unlimited.			**12b. DISTRIBUTION CODE**

13. ABSTRACT (maximum 200 words)

Our thesis presents a modeling paradigm that uses stochastic duels to evaluate the performance of fighter aircraft in one-on-one air combats. The main thrust distinguishing our work is the combination of stochastic models, kinematics, and flight theories to represent the dynamics of a one-on-one air duel between two opposing fighter aircraft. We consider the duel in two phases, starting from a beyond-visual-range engagement to a close-range dogfight. The main contribution of our research is a stochastic model that directly relates physical characteristics of the two aircraft to compute their mission-level performance. The model is able to capture sufficient fidelity of the air duel without losing its analytical tractability. We illustrate our model using a numerical example featuring two actual dissimilar fighter aircraft, followed by a sensitivity analysis using smart experimental design methods. Our analysis reveals that the engagement time at beyond-visual range, single shot kill probability, aircraft velocity, flight velocity during a dogfight, and the maximum load factor of an aircraft are influential in determining the win probability of each aircraft in an air duel.

air combat, stochastic duels, Markov chains				**15. NUMBER OF PAGES** 131
				16. PRICE CODE
17. SECURITY CLASSIFICATION OF REPORT Unclassified	**18. SECURITY CLASSIFICATION OF THIS PAGE** Unclassified	**19. SECURITY CLASSIFICATION OF ABSTRACT** Unclassified	**20. LIMITATION OF ABSTRACT** UU	

NSN 7540-01-280-5500 Standard Form 298 (Rev. 2-89)
Prescribed by ANSI Std. 239-18

THIS PAGE INTENTIONALLY LEFT BLANK

Approved for public release. Distribution is unlimited.

AIRCRAFT EVALUATION USING STOCHASTIC DUELS

Jason W.C. Gay
Captain, Singapore Army
B.Eng, University of Queensland, 2013

Submitted in partial fulfillment of the
requirements for the degree of

MASTER OF SCIENCE IN OPERATIONS RESEARCH

from the

NAVAL POSTGRADUATE SCHOOL
September 2017

Approved by: Moshe Kress
Thesis Advisor

Michael Atkinson
Co-Advisor

Roberto Szechtman
Second Reader

Patricia Jacobs
Chair, Department of Operations Research

THIS PAGE INTENTIONALLY LEFT BLANK

ABSTRACT

Our thesis presents a modeling paradigm that uses stochastic duels to evaluate the performance of fighter aircraft in one-on-one air combats. The main thrust distinguishing our work is the combination of stochastic models, kinematics, and flight theories to represent the dynamics of a one-on-one air duel between two opposing fighter aircraft. We consider the duel in two phases, starting from a beyond-visual-range engagement to a close-range dogfight. The main contribution of our research is a stochastic model that directly relates physical characteristics of the two aircraft to compute their mission-level performance. The model is able to capture sufficient fidelity of the air duel without losing its analytical tractability. We illustrate our model using a numerical example featuring two actual dissimilar fighter aircraft, followed by a sensitivity analysis using smart experimental design methods. Our analysis reveals that the engagement time at beyond-visual range, single shot kill probability, aircraft velocity, flight velocity during a dogfight, and the maximum load factor of an aircraft are influential in determining the win probability of each aircraft in an air duel.

THIS PAGE INTENTIONALLY LEFT BLANK

TABLE OF CONTENTS

THIS PAGE INTENTIONALLY LEFT BLANK

LIST OF FIGURES

THIS PAGE INTENTIONALLY LEFT BLANK

LIST OF TABLES

THIS PAGE INTENTIONALLY LEFT BLANK

LIST OF ACRONYMS AND ABBREVIATIONS

BIC	Bayesian Information Criterion
BVR	Beyond-Visual Range
CTMC	Continuous-Time Markov Chain
DOE	Design of Experiments
DTMC	Discrete-Time Markov Chain
MOP	Measure of performance
NOLH	Nearly Orthogonal Latin Hypercube
OODA	Observe, Orient, Decide, Act
SSKP	Single Shot Kill Probability

THIS PAGE INTENTIONALLY LEFT BLANK

EXECUTIVE SUMMARY

In this thesis, we present a modeling paradigm for evaluating fighter aircraft using stochastic duels. Fighter aircraft systems and weapons designs are known to involve substantial capital investment. Due to possible budget constraints in the U.S. Navy, the number of fighter aircraft may face force-size reductions in the future. The U.S. Navy must continue to strive to meet its operational requirements in a fiscally austere environment. The ability to make smarter and cost-effective decisions in aircraft procurements and upgrades remains a key driver of the U.S. Navy's ability to fight effectively now and into the future. Our model aims to provide "first-order" insights into the performance of fighter aircraft to analysts and decision-makers before they invest further resources into larger-scale, higher-resolution simulations for evaluations.

Our model considers a two-phase one-on-one duel between two opposing fighter aircraft, starting from a beyond-visual range engagement to a close-range dogfight. The first phase is the approach phase where the two aircraft enter the duel at a range beyond visual contact. During the first phase, both aircraft race to detect and fire at each other with the main goal of shooting the opponent down. If the two aircraft survive the first phase, they will enter the second phase where they engage each other in a dogfight. Once in the dogfight, the two aircraft will contest to out-maneuver each other and to shoot each other down. The dogfight features one side as the Pursuer—the aircraft pursuing its opponent from the rear and attempting to shoot the opponent down—and an evader—the aircraft in front of the Pursuer attempting to break off—on the other side.

For the first phase, we use a probability model to represent the missile exchange between two approaching aircraft and incorporated the kinematics of both aircraft and missiles. The resulting model captures the dynamics of a missile exchange at beyond-visual range to determine the likely outcomes given the specifications of both the aircraft and missiles.

For the second phase, we use a discrete-time Markov chain to model the dogfight. We augment the underlying formulation of the Markovian model with flight theories that

are relevant to the aircraft's measure of performance. Specifically, we combine the relationships of the aircraft's specifications, such as the turn performance, to the key tactical maneuvers in the state transition of the Markov chain. This, allows us to capture greater resolution of the dogfight's dynamics without significantly reducing the analytical tractability of the model.

We illustrate the result of our model using a numerical example featuring two actual, dissimilar aircraft and their specifications. Specifically, we used the EF-2000 Eurofighter as the blue aircraft and the Multi-role Su-30 FLANKER-F as the red aircraft. Our model reveals that both aircraft have comparable capabilities during the first phase, albeit the EF-2000 has a reasonable advantage over the Su-30. However, once the two aircraft enter the dogfight, the EF-2000 dominates the Su-30 because of its superiority in aircraft maneuverability.

We complete the numerical example with a sensitivity analysis of the model using smart experimental design methods. Our analysis reveals that in Phase 1 the time to detect and fire at the enemy, the single shot kill probability of the aircraft's missile, and the aircraft's velocity have significant effects in influencing the probability of win of an aircraft. Furthermore, we find that increasing the single shot kill probability and velocity of an aircraft may also diminish the win probability of the opponent. For the overall duel, we discover that the single shot kill probability, aircraft velocity in Phase 1, flight velocity in Phase 2, and the maximum load factor of the aircraft to be most influential in increasing the win probability of one side and decreasing the win probability of the opponent.

ACKNOWLEDGMENTS

This thesis would have never been completed without the extensive assistance and advice from my team of advisors. I would like to sincerely thank my advisor, Dr. Moshe Kress, and my co-advisor, Dr. Michael Atkinson, for their unwavering support in this project. I would also like to extend my heartfelt appreciation to my second reader, Dr. Roberto Szechtman, for his valuable insights.

No man is an island. In order to go fast, one must go alone; in order to go far, one must go as a team. This journey will never be the same with the mutual support from the Singaporean community here in Monterey, California. To the Singaporean community, thank you.

Finally, to the most important woman in my life: Mum, thank you for everything.

THIS PAGE INTENTIONALLY LEFT BLANK

I. INTRODUCTION

A. BACKGROUND AND MOTIVATION

The main motivation for this thesis is to develop a modeling paradigm of air combats that can provide insights about the mission performance of a fighter aircraft based on its characteristics.

Fighter aircraft systems and weapons designs are known to involve substantial capital investment. According to Zabinski (2015), the number of fighter aircraft such as the F/A-18 variants and the F-35 variants is expected to face force-size reductions and budgetary constraints, while the U.S. Navy continues to strive to satisfy its operational requirement. The ability to make smarter and cost-effective decisions in aircraft procurements and upgrades remains a key driver of the U.S. Navy's ability to fight effectively now and into the future.

While it is a common practice to perform high-resolution simulations to compute precise results in determining the performance of fighter aircraft in various missions, these simulations can often be costly in terms of both money and time. An analytical model that provides sufficiently useful insights into air combat by examining an aircraft's performance against its potential adversary will be instrumental for air combat analysis. Analysts and decision-makers may use this analytical model to gain insights into the performance of a fighter aircraft, thus allowing them to better streamline their resources into larger-scale, higher-order evaluations.

B. SCOPE AND OBJECTIVES

Our main aim in this thesis is to develop an analytical model for evaluating fighter aircraft performance using stochastic duels. The key thrust of our work is the development of a mathematical model that captures the key characteristics of modern one-on-one air duels. We balance analytical tractability and model fidelity through incorporating disciplines such as kinematics and flight theory in our mathematical formulations. Our approach allows us to directly relate the physical specifications of the aircraft to their mission performance.

Our model focuses on the one-on-one duel between two fighter aircraft. When two fighter aircraft enter a duel from a distance beyond the visual range of the pilots, the pilots will attempt to fire at each other using long-range missiles, supported by their onboard radar systems to gain situational awareness of their target. The main characteristic of this part of the duel is the ability to detect an opponent faster and fire more accurately than one's opponent. If the two aircraft survive the missile exchange during the initial approach and fly close enough to visually recognize their opponents, they transition into an air combat maneuver phase, also known as a dogfight. During the dogfight, the two aircraft's characteristics are paramount in determining the outcome of the duel. Characteristics such as the turn performance, flight velocity control, structural load factors, and weapon effectiveness are influential in determining the winner in the dogfight. Our model is designed to determine the factors that are important to invest in for an aircraft to gain superiority over an opponent.

Chapter II discusses our review of existing literature relevant to both air combat models and stochastic duels, coupled with our assessments of the key modeling challenges. Chapter III presents the tactical settings and model assumptions. We present our model in Chapter IV, comprising a two-phase stochastic duel. Following our model, we present a numerical example of our model in Chapter V featuring two actual fighter aircraft followed by a sensitivity analysis using smart experimental design methods. We conclude our work in Chapter VI with a summary and a short compilation of potential future research using our modeling approach.

II. LITERATURE REVIEW

A. AIR COMBAT MODELS

The origin of air combat modeling traces back to the use of differential equations to model the attrition in air combat by Lanchester (1916) when he first investigated the principle of force concentration using a set of differential equations on the conditions of ancient and modern warfare. Over the ensuing hundred years, many people have attempted to model air-to-air combat. Notable uses of the Lanchester equations include Johnson and MacKay's (2008) model for the Battle of Britain in 1940 between the British and German air forces.

The underlying formulations of these models vary from simple differential equations to Markov chains, to Game Theory, and to influence diagrams. Previous work covers a broad spectrum of applications; some models apply to very low-resolution theatre-level strategic air operations, while other models focus on higher resolution applications such as missile control designs. Our aim in this chapter is to provide a review of some of the significant past works to guide our own model's development.

Feigin and Shinar (1984) proposed a simple Markov model to analyze air combat involving a moderate number of participants. A continuous-time Markov chain (CTMC) is used in their model to compute the performance of two opposing squadrons engaged in an air-to-air combat. Feigin and Shinar recognized the weaknesses of contemporary models at that time that disregard the existence of individual duels during air combat and thus leading to an oversimplified perspective. This led to their proposed Markov model that seeks to capture the micro-effects of individual duels between two aircraft as part of a larger air combat. Low fidelity rate parameters such as the rate of detection, the rate of moving into firing positions, and the rate of breaking off from a pursuit are used to compute the states in the Markov chain. State vectors are used to represent the number of aircraft in various states such as a pursuer, an evader, or as is free, at every instantaneous point in time. Feigin and Shinar showed that enumerating the model, the solutions from the CTMC may provide insights into the attrition ratios, expected number of kills on each

side, and the expected duration of the battle. However, for the model to be useful in real-life applications for air combat analysts, the input parameters required by Feigin and Shinar's model are extremely difficult to obtain. Notwithstanding, we are inspired by the use of a Markov model to track the various states that an aircraft may follow during air combat, and this serves as one of the critical building blocks to our model.

One of the more recent uses of Lanchester equations for modeling air-to-air combat was proposed by Gilbert (2011). His work studies the strategic implications of fighter force reductions by using Lanchester attrition equations to model combat between a heterogeneous blue force comprising two different fighter-aircraft against a homogenous red force that has electronic attack capabilities—these attacks are conducted using electronic means to degrade the opponent's radar or radio systems. Despite recognizing the difficulty and importance of formulating sufficiently appropriate attrition coefficients for the Lanchester equation, Gilbert demonstrated how these coefficients may be determined by setting up a scoring system to characterize the performance of the two opposing air forces based on several qualitative measures. While the models and simulations done by Gilbert provide insights to the attrition ratio of the two dissimilar opposing forces, the formulation of these scores remains subjective and arbitrary, and therefore, the final results can change drastically depending on the analysts' opinions.

With a greater focus on the Pursuer-Evader problem in an air duel, Moritz et al. (1987) demonstrated the use of a differential game to model the one-on-one combat using medium range missiles. The main feats of their work are the use of kinematic differential equations and missile guidance law in conjunction with differential game theory to compute solutions to maneuver solutions. They illustrated the usefulness of connecting physical characteristics of the aircraft to tactical decisions in maneuvers. Notwithstanding, the model may not necessarily capture the tactical conditions involved in a typical air-to-air combat because of the extremely high-resolution perspectives.

Another notable work is the study of the Markov Game approach to tactical air maneuvers by Baron et.al (1972). The study is focused on modeling and solving air combat decision-making problems between two opponents using a Markov Game. In their model, a two-dimensional air combat problem is first characterized by the equations

of motion of the aircraft followed by a Markov game with a finite state space. Although our thesis does not focus on the decision-making processes between two opponents in an air combat, Baron et. al's work illustrated how the fidelity of air combat model may be improved by incorporating physical relationship, such as the equations of motion in the model, without significantly losing the tractability of the model.

In a more recent research, Virtanen et al. (2006) presented an excellent work on modeling the maneuvering decisions of pilots in a one-on-one combat using an influence diagram with a moving horizon. Their model illustrates the combination of air maneuver kinematics, decision processes, and uncertainties to analyze optimal air combat maneuvers and to contribute greater autonomy to decision making systems for selecting maneuvers in air combat simulators. However, the time efficiency of solving the model was not discussed in their paper and it remains contentious whether the model can be used for air combat analysis without investing significant amount of computational time.

B. STOCHASTIC DUELS

Ancker's work on stochastic duels, starting from 1963 to the late '80s, formed the foundations to stochastic modeling involving duels with differing number of participants. The fundamental duel had its beginning in work by Williams and Ancker (1963) where they illustrated the use stochastic models to gain insights into the impact of kill probabilities and rate of fire between two opposing firers on the outcome of the engagement.

Extensions to the one-on-one stochastic duels were done by many others as well. These range from the two-on-one duel conceived by Ancker and Gafarian (1983) to the general many-on-many duel for a mountain battle developed by Kress (1992). These later works carefully analyze the physical and tactical characteristics of the battles to provide an appropriate mathematical formulation of these traits.

Recent research also features the augmentation of stochastic duels with other contemporary dimensions in modern warfare. Li and Liu (2012) developed a stochastic model for a many-on-one duel with information sharing, where they illustrate how the time-to-kill may be formulated as a random variable that is a function of information

sharing across the units in the duel, thus yielding a density function of the time-to-kill within the many-to-one stochastic duel. Liu (2006) offered a change in the tactical conditions from the fundamental duel to a model for guerrilla warfare, where the main distinctive feature is the "ambush" like scenario, coupled with topographical considerations. The model was derived from the fundamental duel and incorporated both searching and mixed stochastic duels to illustrate the unique characteristics of guerilla warfare.

C. CHALLENGES IN MODELING AIR COMBAT USING STOCHASTIC DUELS

1. Our General Approach

We have seen in our extensive literature review the suite of methods that were explored to model both air combats and stochastic duels for various purposes. Most of the existing models attempt to balance the resolution of the combat model with the computational cost associated with higher- resolution techniques.

In our thesis, there are three key considerations, namely 1) stochastic modeling, 2) air combat, and 3) aircraft evaluation. The notion of evaluation obliges us to place substantial focus on the aircraft performance and specifications in our model. These key considerations are underpinned with the need to ensure that the model can be computed within a reasonably short period of time.

Table 1 presents a summary of modeling approaches and potential areas of application observed from our literature review on both air combat and stochastic duels. The need to balance these approaches in terms of analytic tractability, the level of resolution, and physical and tactical details of air combat dynamics is apparent.

Table 1 Summary of past approaches and their applicability in different levels of resolutions.

Past Modeling Approaches	Level of Resolution		
	Theater level	**Tactical Many on Many**	**Tactical One on One**
Stochastic duels using Probabilistic models	Not applicable.	Yes, but is an evolution of Many on One duel with limited frontage.	Yes, but does not account for rational behaviors. Will need adaption to air combat situations
Influence Diagram approach	No.	Not preferred. Too much computational effort required.	Yes. Explicit representation of micro effects and maneuver decisions. Difficult to replicate multiple times.
Lanchester models	Yes. Suitable for analyses of large-scale strategic air combat.	Yes, but loses resolution on micro effects because they neglect the dynamics of separate duels.	No.
Differential game theory (zero-sum or non-zero-sum)	No.	Possible but heavy on computation efforts.	Yes.

Our review of existing works reveals the potential use of probabilistic models, similar to the fundamental duel, to describe the posture and tactical conditions unique to air-to-air combats. Next, we identify several key differences between a fundamental stochastic duel and an air-to-air duel.

First, all of the stochastic duels that feature land-based firers assume negligible time between firing until a projectile hits its target. This is chiefly due to the relatively higher velocity of modern weapons as compared to the dynamics of the battle. Even in the work by Feigin and Shinar, the relative velocities of weapons' projectiles were not explicitly considered in the model, albeit this is still a valid assumption as their model is specifically designed for the close-range dogfight and air-to-air missiles may not be widely proliferated at the time of their work. However, the same assumption may not be applicable to a modern air-to-air duel, especially when the ability to fire at beyond visual

range becomes more prominent to modern aircraft. Aircraft fly at much higher speeds than land-based firers. Modern fighter-aircraft, with advanced aviation technologies, can operate in the range of supersonic to hypersonic speeds. Furthermore, this trait is accentuated by the prolific use of air-to-air missiles in air battles. These air-to-air missiles operate with similar velocities as the aircraft. Therefore, it is necessary for our stochastic model to explicitly consider the dynamics of these two different elements—the aircraft and the missile in flight—in an air duel.

Secondly, we recognize that both physical space and time play significant roles in determining the outcome in an air duel. Aircraft combating each other need to maneuver through space and are bounded temporally in terms of their tactical decisions. This contrasts with most of the stochastic duel models as they primarily consider only the temporal factor in terms of inter-firing time distribution, thus implicitly amalgamating the effects of physical space.

While a probabilistic model may sufficiently model an air duel between two firers, it does not capture the dynamics of a dogfight—a prominent aspect of air combat ever since the introduction of air warfare. Existing literature shows us how different mathematical approaches will lead to different levels of resolution of the combat model. In our case, it is critical to capture sufficient characteristics of the dogfight in order to maintain sufficient fidelity of the real combat in our model.

We direct our attention to the use of a Markovian model, inspired by Feigin and Shinar's (1984) work on modeling multiple air combats, to model the dynamics of a dogfight. We also gain insights from both the work of Moritz et al. (1987); and Virtanen et al. (2006) to incorporate elements of maneuver dynamics and kinematics into the model, thus resulting in a higher level of realism and fidelity.

2. Model Evolution and Lesson Learned

In the early stage of our model development, we went through several iterations of modeling approaches before culminating with the One-on-one duel model proposed in this thesis. These earlier iterations provided insights about the structural and

mathematical challenges facing us in developing a model that could capture the dynamics of the duel sufficiently while maintaining analytical tractability.

We started developing the model using a continuous-time Markov chain to account for some of the key states that occur during a one-on-one air duel. The results of these simpler Markovian models provided us with some insights into the interactions between various key performance measures and how they may affect the aircraft's ability to win an air duel.

Two key challenges remained persistent in the earlier models. First, the inputs were, similar to some of the past works on air combats, rate parameters as a form of aggregated performance measures to characterize the aircraft. Although these models are analytically tractable, they are difficult to be used for aircraft evaluation because it is difficult to obtain accurate data on these rate parameters. Second, to ensure realism in the model, the physical kinematics between the aircraft and their missiles need to be modeled explicitly.

These key lessons learned led us to incorporate a higher-resolution modeling approach that can bridge engineering-level specifications to mission-level performance through the combination of kinematics, flight theories, and stochastic modeling.

THIS PAGE INTENTIONALLY LEFT BLANK

III. SCENARIO AND ASSUMPTIONS

In this chapter, we present the scenario used to develop the combat model for evaluating the one-on-one air duel. We elaborate how the tactical air combats are framed into a scenario, and state several realistic assumptions, which are sufficient for constructing meaningful analytical models of one-on-one air duels.

A. THE SCENARIO

Consider two opposing, dissimilar aircraft entering the combat zone from opposite directions. Full hostility is declared in the combat zone; meaning that there are no neutral or civilian aircraft in the combat zone.

The whole duel is categorized into two phases, namely the approach in Phase 1 and the dogfight in Phase 2. Phase 1 begins when the two aircraft are 60 to 100km apart, while Phase 2 begins when the two aircraft are approximately 35km apart, as shown in Figure 1. The primary objective of the two aircraft in both phases is to shoot the opponent down while avoiding being shot down.

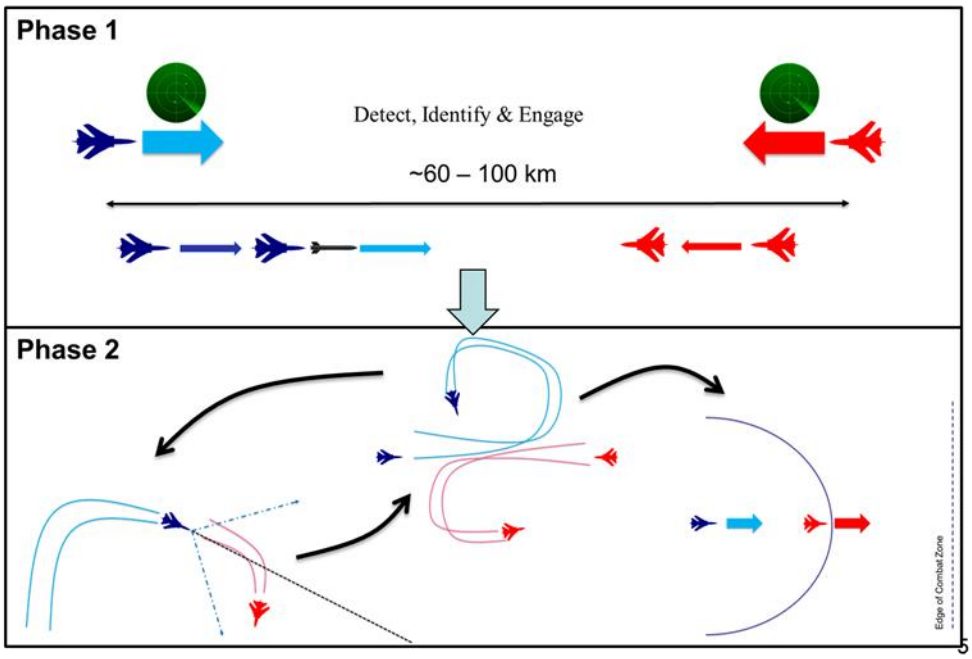

Figure 1 Overview of the one-on-one duel in two phases. Phase 1 refers to the Approach phase where the aircraft approach each other in a straight-line trajectory. Phase 2 refers to the close-range dogfight.

1. Tactical Conditions

We make the following assumptions regarding the tactical conditions under which the duel occurs.

1. The weapons onboard the aircraft are only missiles, thus excluding the use of guns. This assumption serves to focus on the more prominent and lethal weapons currently employed in air combat.

2. The duel begins with both aircraft having no knowledge of each other's physical location and intended actions, but they are aware of each other's presence in the combat zone.

3. Fuel is assumed to be unlimited in the duel. With the advances in modern combat aviation, we assume that the aircraft participating in the duel have sufficient fuel to last longer than the fight.

4. During the Approach phase, each aircraft is limited to firing at most one missile. This is because we assume that the two aircraft will have complete awareness of each other's position after the first missile exchange given the short duration of the phase, and both aircraft will

transit into tactical maneuvers thereafter corresponding to the dogfight phase.

2. General Assumptions

Air-to-air combat takes place in a three-dimensional space. We model this combat in a two-dimensional space. Although there may be some loss in resolution of the combat dynamics and governing physics in terms of aircraft performance, the reduction in dimensionality facilitates models that are more transparent and simpler analyses.

The Observe, Orient, Decide, Act (OODA) loop of a trained pilot affects the outcome of an air combat. Although this is an area of extensive research in the field of air combat, missile control and guidance, and combat simulations, the scope of our model does not extend to analyzing the complex decision-making process of the fighter pilot. Therefore, we develop our model without moving into Game Theory, Decision-Analysis, and other higher-resolution decision sciences.

Several attributes in the scenario retain the influence of human factors. One of these attributes relates to the tactics used by the pilots to turn during a dogfight as they maneuver into positions. Another aspect is how well the aircraft and pilot can achieve the desired velocity during certain maneuvers. By considering these attributes, we retain some flexibility in the model to factor in these attributes. For example, by performing a sensitivity analysis of the model of an F-18 operated by an experienced pilot against a specific adversary, analysts can determine how well an F-18 will perform in dogfights that are dominated by a certain type of maneuver tactics.

B. PHASE 1—APPROACH

In Phase 1, the two aircraft approach each other in a straight-line trajectory, starting at a range of 60 to 100 km. At this distance, both aircraft do not have visual contact with each other; therefore, they are unaware of the opponent's physical location or intended actions. However, they are aware of each other's presence in the combat zone. We denote this range between the two aircraft as the beyond-visual-range (BVR).

Each aircraft is supported by its own tactical support systems, which facilitates overall situational awareness and provides tactical intelligence to the aircraft. Systems,

such as Early Warning aircraft, ground sensors and radars, and satellite communications, augment the onboard detection system of the aircraft assisting the fighter pilot in obtaining a positive identification of the opponent. Once a positive identification is obtained, the aircraft may fire at its opponent. Figure 2 illustrates the initial conditions under which the duel begins in Phase 1.

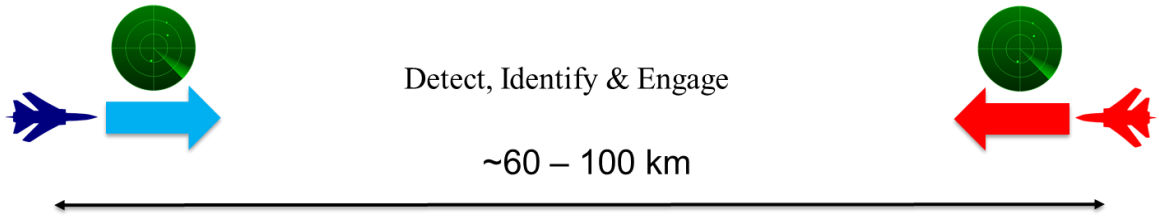

Figure 2 The start of the duel where two opposing aircraft approaches each other. The two aircraft are assumed to approach each other in a straight-line trajectory without prior knowledge of their opponent's location and intended actions.

An important factor at this phase of the duel, which is unique to modern air combat, is the relative speeds of the missiles and the aircraft. Unlike in classic duels and combat models for land-based battles, where the muzzle velocities of the projectiles are so high compared to the dynamics on the battlefield that the time-of-flight of a projectile is assumed negligible, the comparable velocities of the missile and aircraft play a role in the outcome of an air battle. Because of the relatively slower missile velocities, it is possible for two aircraft to simultaneously shoot each other down, even if the missiles on both sides are not launched at the same time. These observations regarding the relative velocities between aircraft and missiles lead to the assumption that each aircraft may only fire one missile during this phase of the duel.

Due to the advances in contemporary aviation technologies, our model assumes that an aircraft will gain almost immediate awareness that it is being fired upon, and it will attempt to fire its own missile in retaliation while trying to avoid being hit by its opponent's incoming missile. This gives the aircraft being fired upon an opportunity to counter-attack its opponent. However, due to the shortened distance between the two

aircraft after the first missile is fired, the aircraft firing back may have very short time to respond before the two aircraft transition into Phase 2—dogfight.

The possible outcomes at the end of the Approach phase are 1) blue is shot down, 2) red is shot down, 3) both aircraft are shot down, 4) transition to Phase 2—accounting for the number of missiles fired on each side.

C. PHASE 2—DOGFIGHT

If neither aircraft is shot down in Phase 1, the duel will transit into Phase 2 when the distance between the two aircraft is approximately 35km. At this distance, the two aircraft could positively identify each other visually. This phase is much more dynamic than Phase 1, where the two aircraft can maneuver, evade, pursue, and attempt to shoot each other down.

During the dogfight in Phase 2, each aircraft may take on two primary roles: Pursuer and Evader. In addition, it is possible for both aircraft to be in a state of neutrality where both are maneuvering to get into a position of the Pursuer. After maneuvering in this neutral state, eventually one of the aircraft becomes the Pursuer and the other the Evader.

The Pursuer is the aircraft flying behind its opponent—the Evader—in pursuit, attempting to acquire it as a target and then shoot it down. The Pursuer has the advantage of firing its weapon once the pilot acquires the target (Evader). The Pursuer, however, loses the initiative to decide the direction and velocity of the pursuit. Its primary challenge is to maintain itself at the rear of the Evader, attempting to fire at it. The Pursuer is subjected to changes in direction and velocity dictated by the Evader.

The Evader, on the other hand, is at the front of the two aircraft. Because of its position, the Evader is unable to fire its weapon at its opponent. The main objective of the Evader is to break away from the pursuit as soon as possible before the Pursuer fires its missile at it. Furthermore, only by breaking away from the pursuit can the Evader subsequently regain the opportunity to maneuver itself into the Pursuer role.

During a dogfight in Phase 2, it is not possible to model every possible move that the two aircraft may take while maintaining the tractability of the model. However, based on the illustrations of basic fighter maneuvers presented by Shaw (1985), it is possible to broadly categorize the kinds of combat maneuvers that may occur. We categorize these combat maneuvers into three main parts, namely 1) lead turns and turn types, 2) pursuit and break-off, and 3) disengagements.

1. Lead Turns and Turn Types

The first category of maneuvers is the lead turn (Shaw 1985). This maneuver features two planes flying towards each other, crossing paths, with the intent of performing a turn to get into a firing position to fire at their opponent. At the end of the lead turn, it is most likely that one of the aircraft becomes the Pursuer, while the other becomes the Evader. This maneuver is fundamental for gaining an advantageous position. Throughout the lead turn, both aircraft are assumed to be in a state of neutrality. The tactics and techniques adopted by the pilots affect the tactical advantage one may have once this maneuver is over.

The lead turn manifests a very fundamental situation when two aircraft approach and pass each other. The lead turn is most likely to occur when transitioning from Phase 1 to Phase 2 and during the multiple attempts in Phase 2 where the two aircraft race to obtain an advantageous position as the Pursuer. Therefore, we use the lead turn maneuver shown in Figure 3 to model how two aircraft may transit from a neutral state to a Pursuer-Evader state.

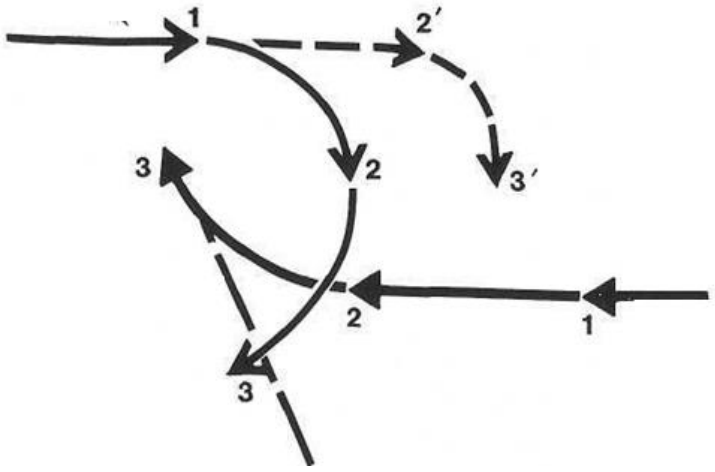

Figure 3 A lead turn between two aircraft. Source: Shaw (1985). The two trajectories (top and bottom) illustrate the path each aircraft takes at different instances of time. At (1), the top aircraft made an earlier clock-wise turn, attempting to pursue its opponent. (2) and (3) show the relative position between the two aircraft after the turn was initiated. (2') and (3') on the top aircraft's trajectory illustrate the alternative path it would take if it did not turn at (1). The dashed line on the bottom aircraft is used to indicate the rearward direction to exemplify the tactical advantage that the top aircraft has by (3).

The actual tactics executed by the two aircraft, as shown in Figure 3 are much more complex in reality; some tactical considerations include the flight-path separation distance—the lateral distance between two parallel flight-paths—at which the turn occurs, the skills and experience of the pilot, the relative positions at which the turn occur, and the overall tactical plan of the pilot. However, to simplify the scenario, we assume that the two aircraft turn at the same instance, thus reducing the lead turn to a simpler approximation of two circular trajectories. Notwithstanding, our model retains a critical factor characterizing a lead turn: the types of turn executed by the two aircraft.

There are two main types of lead turns (Shaw 1985). In the first type, the two aircraft turn in opposite directions (one clockwise, the other counter-clockwise). This is defined as the nose-to-nose turn. In the other type, the two aircraft turn in the same direction, which is defined as a nose-to-tail turn. The flight paths for these two turn types are illustrated in Figure 4.

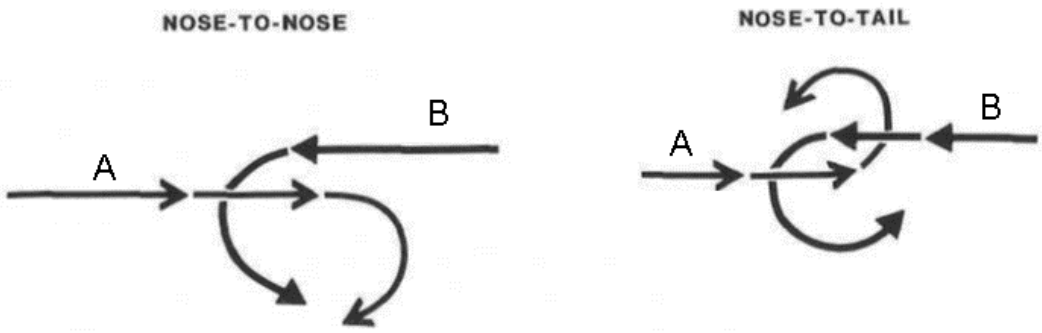

Figure 4 Flight paths of the two aircraft in a nose-to-nose turn and nose-to-tail turn. Source: Shaw (1985). In a nose-to-nose tail, both aircraft turn in an opposing direction. In the figure, Aircraft A turns in a clockwise direction while Aircraft B turns in a counter-clockwise direction. In a nose-to-tail turn, both aircraft turns in the same direction. In the figure, both A and B turns in a counter-clockwise direction.

Both turn types are, in fact, a "race" between two circular trajectories. The distinction, however, lies in the characteristics of the race. In the nose-to-nose turn, according to Shaw (1985), the relative turn radius of the aircraft plays a significant role in determining the potential angular advantage of either side. The turn rate—the angular velocity at which the aircraft executes a turn (a higher turn rate corresponds to changing the aircraft's angular orientation faster)—is relatively insignificant. This property is illustrated in Figure 5 where Case 1 and 2 demonstrate how, regardless of the turn rate, the side with the smaller turn radius will have a better chance of becoming the Pursuer. In Case 1, Aircraft A has a higher turn rate, covering a larger turn angle relative to the Aircraft B. In Case 2, Aircraft A has a lower turn rate relative to the Aircraft B. Nonetheless, in both cases, Aircraft A has the better chance of becoming the Pursuer at the end of the lead turn because of a smaller turn radius.

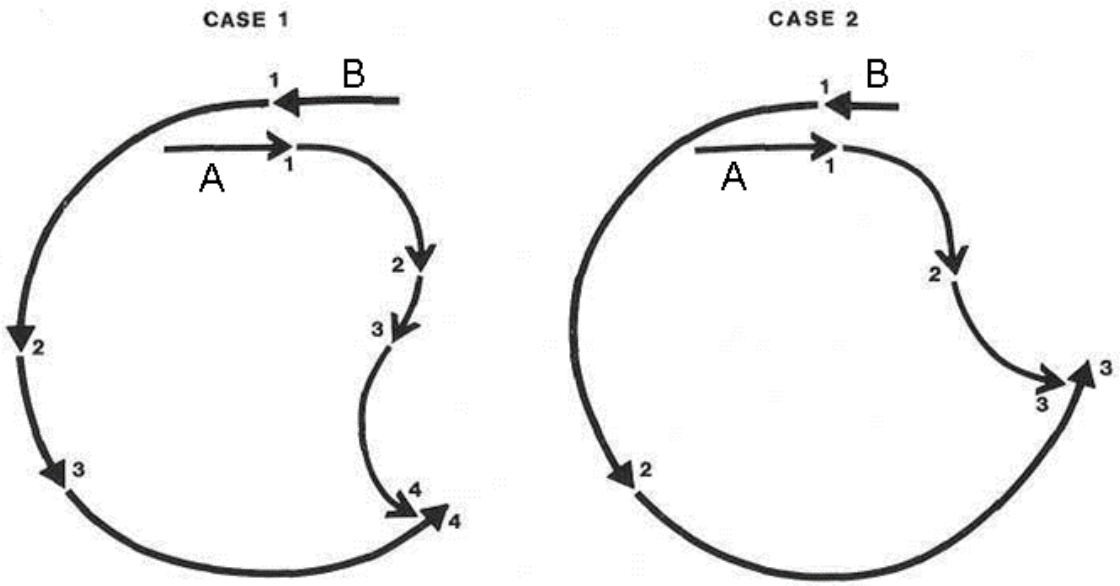

Figure 5 Two possible cases of a nose-to-nose turn. Source: Shaw (1985). The aircraft with the lower turn radius will almost always have the higher probability to become the Pursuer. In Case 1, Aircraft A has a comparable turning rate to Aircraft B; but because of its small turn radius, it will become a Pursuer of B at the end of the turn. In Case 2, Aircraft A has a relatively lower turning rate than Aircraft B; notwithstanding, it will become the Pursuer of B at the of the turn.

On the other hand, in the case of a nose-to-tail turn, the impacts of the turn radius and turn rate are reversed. During a nose-to-tail turn, both aircraft need to turn and face the opponent in the fastest possible manner. As such, a smaller turn radius may not necessarily benefit an aircraft (Shaw 1985). Instead, in this turn type, the aircraft with a higher turn rate will have the greater potential of becoming the Pursuer of its opponent. This is illustrated in Figure 6 where Case 1 shows how, even with a small turn radius, Aircraft A may not necessarily become the Pursuer. Case 2 demonstrates that a better turn rate will benefit Aircraft A when both aircraft perform the turn with the same radius.

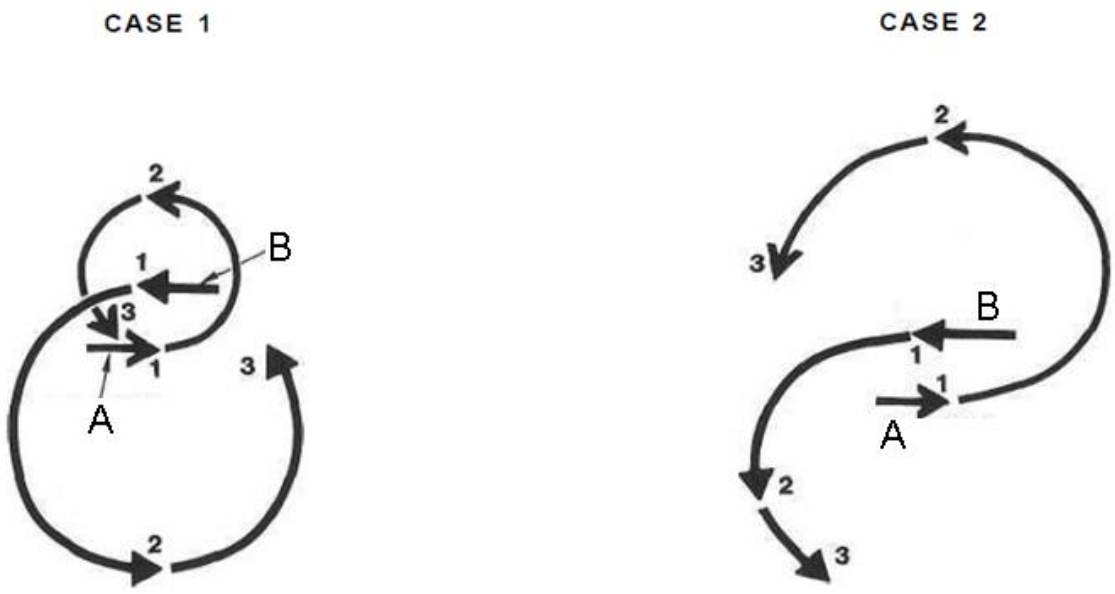

Figure 6 Two possible cases of a nose-to-tail turn. Source: Shaw (1985). In Case 1, Aircraft A performs the turn with a smaller turning radius compared to Aircraft B. In Case 2, Aircraft A performs the turn with a larger turning radius compared to Aircraft B. Both cases have Aircraft A turning at a higher rate. These illustrate how an aircraft with the higher turn rate, regardless of its turning radius, will have a high probability of becoming the Pursuer at the end of the turn.

The lead turn maneuver and the geometrical relationships that emerge from the two possible types of turns, generate two possible "races" between two circular trajectories of the aircraft, with the goal of each aircraft to become the Pursuer.

2. Pursuits and Break-offs

Another major dynamic of the dogfight is the pursuit of the Evader by the Pursuer. According to Shaw (1985), there are three forms of pursuits—lead, pure, and lag pursuits. The different forms of pursuits distinguish themselves by the orientation of the Pursuer's velocity vector ahead of, directly toward, or behind the target aircraft. In a lead pursuit, the Pursuer's nose is positioned ahead of the Evader; while in a lag pursuit, the Pursuer's nose is positioned behind the Evader. In our model, we use the pure pursuit to model the dynamics of the Pursuer and Evader in the pursuit curve. This is the form where the Pursuer's nose is held directly towards the Evader (Shaw 1985).

Because the Evader is positioned in the front, it has the advantage of initiating the direction and velocity of the pursuit curve albeit it is susceptible to being fired upon and has a limited view of the Pursuer. On the other hand, the Pursuer faces the challenge of continuously maintaining itself behind the Evader. An Evader with a significant turning speed advantage may break-off from the pursuit with a higher probability than one with a lower turning speed.

By considering only pure pursuits in the model, it is possible to estimate the probability of the Evader breaking off the pursuit curve based on the relative turn-rates of the two aircraft. We assume that once the Evader manages to turn out of a certain angle relative to the Pursuer, the latter will lose sight of the Evader and, therefore, effectively allowing the Evader to break-off. We justify this assumption as our model uses a two-dimensional approximation of the pursuit and break-off; and that there exists an angle beyond which the Pursuer may no longer effectively be in pursuit of the Evader, limited by the field of view of the pursuing pilot's target acquisition system.

3. Disengagements

Because of the limited number of missiles loaded on both aircraft at the start of the duel, it is possible that an aircraft expends all its payload of missiles while both aircraft are still alive. Since we assume only missile engagements, an aircraft without any missiles will attempt to disengage from the duel. While this may not necessarily represent the most likely outcome when an aircraft runs out of missiles in actual combats—it may continue the battle using other weapons—this assumption serves to provide the additional information on how effective an aircraft may disengage itself from a combat zone, if necessary.

To disengage, the Evader tries to break off from any ongoing pursuit and move in a straight-line trajectory away from the Pursuer to disengage itself from the combat zone. The Pursuer, on the other hand, is assumed to always chase its disengaging opponent, and the Pursuer may fire one last missile before the duel ends.

To bind the mission-level conditions of the duel, we assume that each aircraft may only operate within a designated sector, beyond which, the aircraft may lose tactical

support and coordination by friendly forces, or move into another sector that may place itself in a different duel or combat. We define this as the maximum pursuit distance. Furthermore, we also assume that the Pursuer's weapon has a maximum engagement range, beyond which the weapon cannot be fired. This presents the Pursuer with two constraints for it to successfully shoot down the Evader during the disengagement. First, the Pursuer cannot travel beyond the designated combat zone, which implies that there is a limit to the amount of time available for the Pursuer to execute its firing drill during the pursuit. Second, the Pursuer's weapon system has a maximum engagement range, which implies that it must fire at the Evader before the latter is too far away.

Because of these two constraints, the relative velocities of the two aircraft are significant factors in the disengagement stage; the initial separation distance—the initial distance between the two aircraft at which the straight-line disengagement pursuit begins—plays an important role in determining the probability of a successful disengagement. However, due to the non-deterministic nature of a pursuit curve, there is uncertainty about the initial flight separation distance at which the disengagement attempt begins.

The disengagement from the dogfight is analogous to the Approach phase, except that there is no need to distinguish the side with the firing initiative since both aircraft are flying in the same direction and only the Pursuer can shoot. Figure 7 illustrates a disengagement pursuit with the Red aircraft as the Evader.

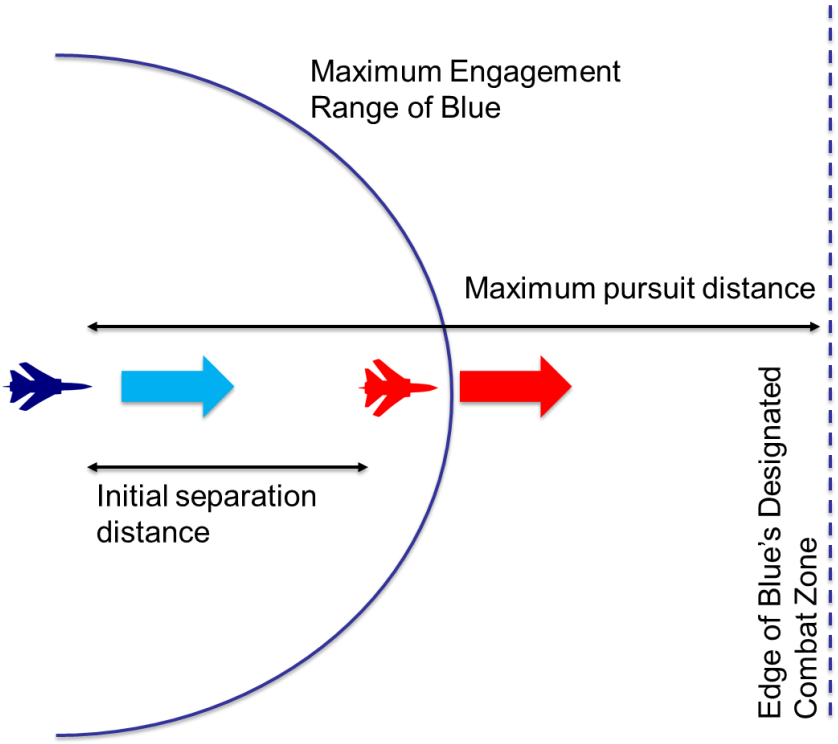

Figure 7 A disengagement pursuit where the Red aircraft attempts to disengage from the duel. The blue curvature represents the maximum engagement range of Blue's weapon, and the distance from Blue to the dotted lines represents its maximum pursuit distance. At the start of the disengagement, both aircraft are separated at a distance—this is defined as the initial separation distance.

D. MEASURE OF PERFORMANCE (MOP)

In this section, we discuss the general characteristics of the duel, from which we define our measure of performance (MOPs). These MOPs are used as the building blocks in determining the parameters and structures of our analytical model and are critical connecting our model to actual air duels.

The following characteristics of the duel are used to support the definitions of our MOPs subsequently:

1. **Situation Awareness**. During the Approach phase, the situation awareness of the pilot of an aircraft is crucial in determining the side that will have the firing initiative at beyond visual range. An aircraft that can detect, identify, and fire faster than its opponent will tend to have a better

chance winning the fight in Phase 1. The ability to fire faster does not only depend on the aircraft's onboard targeting and radar systems but also on its supporting units in the tactical air combat such as supporting ground sensors and early warning systems.

2. **Aircraft Maneuverability and Performance Specifications**. During Phase 2—the dogfight—the aircraft maneuverability is crucial in determining the outcome of the battle. An aircraft engaged in a close-range dogfight requires substantial maneuverability advantage over its opponent to successfully take on the role of the Pursuer. Specifically, an aircraft's turn performance is most influential in this phase of the duel. This is evident in two of the three maneuvers that were discussed, namely 1) lead turns, and 2) pursuits and break-offs. In short, an aircraft's ability to make turns faster and sharper will tend to give it an advantage during the dogfight. However, we also note at this point that parameters used to characterize this characteristic are often difficult to obtain for air combat. This is one of the major obstructions to improving the fidelity of air combat models.

3. **Offensive and Defensive Weapon Systems.** The last performance factors are the accuracy, range, and lethality of the weapons onboard the aircraft. They determine the terminal effect of the battle.

Using these general characteristics of the duel, we define the following MOPs for our model:

1. **Time to Engage**. The time to engage characterizes the aircraft's ability to lock on and fire at a target. This MOP is influenced by several factors, such as the aircraft's target acquisition system, the situation awareness of the pilot, and the skill of the pilot. The ability to fire fast is crucial in both the first and second phase of the duel. In the first phase, the aircraft has to identify a distant target at beyond visual range followed by firing a missile at it. In addition, should an aircraft be fired upon, its ability to fire back quickly before the initial missile terminates is critical in denying the survivability of its opponent. Furthermore, in the second phase, the time for an aircraft to engage will determine whether it can successfully fire a missile and shoot its opponent down before the latter breaks away from a pursuit.

2. **Aircraft Turn Performance**. The aircraft turn performance strongly influences its maneuverability and the dynamics during dogfight in the second phase of the duel. An aircraft with good maneuverability is expected to yield a higher probability of becoming the Pursuer, thus giving it a higher chance of successfully firing its missile at its opponent. On the other hand, an aircraft with poor turn performance will subject itself to greater susceptibility of getting fired at by its opponent. Even with

successful break-offs from a pursuit curve, the aircraft may not be able to pursue its opponent for prolonged durations. This then reduces its opportunity to aim and fire, thus depriving it of shooting down its opponent.

3. **Missile Performance**. The missile performance of the aircraft determines the terminal effects of the duel in both the first and second phase. At beyond visual range, the missile's guidance system, flight characteristics, and lethality will determine whether an aircraft may successfully shoot its opponent down, given that it manages to fire a missile. In the second phase, the same effects apply, except that the flight characteristics of the missile may not be significant due to the shorter ranges typical of a dogfight.

THIS PAGE INTENTIONALLY LEFT BLANK

IV. THE MODEL

In the One-on-One duel model, we consider two opposing aircraft; B representing the Blue aircraft and R representing the Red aircraft. The two aircraft begin the duel in Phase 1—the Approach phase—where they fly towards each other while attempting to shoot each other down. If both aircraft survive this phase, they transit into Phase 2—the dogfight. We model the duel by using a probability model for Phase 1, interconnected with a Discrete-Time Markov Chain (DTMC) for Phase 2.

The probability model for Phase 1 focuses on the missile exchange between the two aircraft as they approach each other and shorten the distance between themselves. We define variables in conjunction with the kinematic relationships between the missiles and aircraft to capture both the spatial and temporal characteristics of this phase. From the Phase 1 model, we determine the probability distribution of the outcomes comprising: 1) A win by either aircraft, 2) both aircraft mutually shot down and 3) transition to Phase 2 with the number of missiles fired accounted for.

The DTMC model for Phase 2 concentrates on the dynamics of the dogfight while keeping track of the number of missiles remaining onboard each aircraft. The DTMC model incorporates basic flight dynamics in the stochastic model to provide an appropriate approximation of the dogfight. This formulation allows us to use engineering-level specifications of the aircraft to compute mission performance and gain insights into the mission-level performance of the two aircraft in the duel. Solving the Phase 2 DTMC yields the probability of the mutually exclusive outcomes comprising 1) win by either aircraft, 2) disengagement from the dogfight by either aircraft when one of the aircraft fully expends its missile payload, and 3) mutual disengagement when both aircraft run out of missiles.

We note that the dogfight can also be modeled as a Continuous Time Markov Chain (CTMC) (See Chapter II); however, the main advantage of the DTMC model, as compared to the CTMC model, is the ability to directly use engineering-level aircraft specifications for most of the input parameters. As a result, the underlying probability

formulation in the DTMC model is slightly more complex than in the CTMC, albeit it is still sufficiently simple to compute numerically. The benefits of enabling a link between engineering-level specifications to mission-level performance, however, clearly outweigh the slight increase in complexity of the underlying arguments.

A. PHASE 1—APPROACH

1. Methodology

The Approach phase has a fixed, well-defined duration that is determined by the velocities of the two aircraft. When the two aircraft approach each other closer than a certain minimum distance (approximately 35km) they are no longer considered to be at BVR. Thus, the duration of the approach confines Phase 1 to a deterministic temporal boundary. The two main events of Phase 1 are 1) engagement initiative of either side, 2) counter-fire by the aircraft being fired upon. Each of these main events, coupled with their respective missile's probabilities of kill, leads to the outcomes for Phase 1.

We need to distinguish between the two main events—fire and counter-fire—during Phase 1. When an aircraft gains the initiative to fire a missile, we assume that the performance of that missile is at its fullest potential based on the missile's specifications. However, if a missile is fired by a counter-firing aircraft, we assume that the pilot is adopting an immediate-action-drill to react to the incoming threat at the cost of loss in accuracy. We define the first case as Aimed Shot and the second case (counter-fire) as an un-aimed shot.

To model this phase, we explicitly define the physical events that may occur. During the approach, both aircraft are closing the distance between each other while attempting to fire their missiles. We assume that each aircraft may fire at most one missile during the approach. This assumption is appropriate considering the short period of time before both aircraft transits into a dogfight at close range. The missile velocities, which are relatively close to the aircraft velocities by approximately three to four factors, need to be accounted for during the missile exchange.

2. Phase 1 Parameters

We use nine parameters to construct the Phase 1 model. Two of them are random variables with distributions with non-negative support, and seven are deterministic inputs. Table 2 summarizes these nine parameters used in the Phase 1 model.

Table 2 Parameters used for Phase 1 model.

	S/N	PARAMETERS	NOTATION [UNITS]
	1	BVR Engagement Time	$X_B,\ X_R$ [seconds]
	2	Counter-firing Time	Y_B, Y_R [seconds]
	1	Single Shot Kill Probability of Aimed Shot	p_B^A, p_R^A
	2	Single Shot Kill Probability of Un-aimed Shot	p_B^U, p_R^U
	3	Approach Velocity of the aircraft	u_B, u_R [meters per second]
	4	Missile Velocity	w_B, w_R [meters per second]
	5	Missile Capacity of the aircraft	m_B, m_R [integer]
	6	Distance of Approach	D_a [meters]
	7	Minimum Distance at the end of Approach	$D_{\min}$ [meters]

a. Random Variables

The two random variables characterizing the firing capabilities of each aircraft are described as follows:

1. **BVR Engagement Time**, $X_B(X_R)$, measured in seconds. This is a random variable defined as the time between in the beginning of the Approach phase until the Blue (Red) aircraft is first to fire a missile at the opponent. It is the time required to detect, positively identify, and execute a missile firing-drill.

2. **Counter-firing Time**, $Y_B(Y_R)$, measured in seconds. This is a random variable defined as the time from the moment of firing a missile at the opponent, to the time the counter-fire occurs. We expect this variable to be shorter than the BVR Engagement Time because of the immediate-action drill assumption.

We assume that all four random variables are independent.

b. Inputs

The seven deterministic input parameters used in Phase 1 are:

1. **Single Shot Kill Probability of an Aimed Shot**, $p_B^A(p_R^A)$. This is the probability of kill of an aimed shot fired by Blue (Red) who gained the firing initiative. Apart from considering the aircraft, pilot, and weapon characteristics of the shooter, this parameter also takes into account the counter-measures used by the defender, such as flares, jamming systems, and stealth technologies. We denote $\overline{p}_X^A = 1 - p_X^A, X = B, R.$

2. **Single Shot Kill Probability of an Un-aimed Shot**, $p_B^U(p_R^U)$.This is the probability of kill of an un-aimed shot fired by Blue (Red) during counter-fire. Again, both the performance of the shooter and the defender must be taken into account in this parameter. We denote $\overline{p}_X^U = 1 - p_X^U, X = B, R.$

3. **Approach Velocity**, $u_B(u_R)$, measured in meters per second. This is the speed the Blue (Red) aircraft approaches its opponent in Phase 1. This parameter is determined by the aircraft characteristics, air-combat tactics, and historical data.

4. **Missile Velocity**, $w_B(w_R)$, measured in meters per second. This is the cruising speed of Blue's (Red's) air-to-air missiles. We assume that $Min\{w_B, w_R\} > Max\{u_B, u_R\}$. This parameter is estimated from missile technical specifications.

5. **Distance of Approach**, D_a, measured in meters. This is the starting distance of Phase 1 when the duel begins.

6. **Minimum Distance at the End of Approach**, $D_{\min}$, measured in meters. This is the distance between the two aircraft at the end of the approach phase and the beginning of Phase 2—dogfight.

7. **Missile Capacity**, $m_B(m_R)$. The number of missiles Blue (Red) can carry onboard the aircraft. We assume that Blue (Red) starts the duel with the maximum number of missiles onboard.

c. Functions

From the input parameters, we further develop two essential functions that are used in Phase 1:

1. **Time until Approach Ends**, T_a, measured in seconds. This is a time parameter derived from the approach distance, D_a, and the relative approach velocities of the two aircraft, u_B and u_R. This function is used as the temporal boundary for the duration of Phase 1. Formally:

$$T_a = \frac{D_a - D_{\min}}{u_B + u_R}$$

2. **Missile Termination Time**, $\tau_B(\tau_R)$ measured in seconds. This is a random variable defined as the time between Blue (Red) firing a missile until the missile terminates at its target. It is the time limit for the target, Red (Blue)—the counter-firing aircraft—to fire back before the first missile terminates. This random variable is a linear function of the random variable, $X_B(X_R)$. Formally:

$$\tau_B = \frac{D_a - (u_B + u_R)X_B}{w_B + u_R}$$

3. Events in Phase 1

We define the model of the Approach phase by combining the information from the scenario discussed in Chapter III.B with the parameters and functions defined in Section 2 above.

a. Overview of the Sequence of Events

A sequence of events involving possible missile exchanges describes Phase 1—the Approach phase. The sequence begins with the initial conditions, comprising the distance of the approach and the respective aircraft's input parameters, under which the two aircraft enter the duel. Once the duel begins, both aircraft attempt to fire a missile at each other. When one of the aircraft initiates a shot, the other will attempt to fire back a missile, while avoiding being hit by the incoming missile. If the counter-firing aircraft manages to fire back, both aircraft are susceptible to being shot down by each other's missile. Otherwise, if the counter-firing aircraft cannot fire back before the incoming

missile terminates (and obviously, misses), the counter-firing aircraft may still fire its missile using an aimed shot before the end of Phase 1.

The sequence of all possible events characterizing Phase 1 is shown in Figure 8. From the figure, we observe three distinct groups of critical events as the duel in Phase 1 unfolds. These three critical events are 1) firing initiatives, 2) pre-termination counter-fire, and 3) post termination counter-fire.

In the first and second critical events, all possible outcomes in Phase 1 may occur. When one of the aircraft fires a missile and the opponent fires back, both aircraft are susceptible to being shot down or, if they survive, to transition to the second phase. However, in the third critical event where an aircraft fires back at its opponent after the opponent's missile terminates, only the opponent is susceptible to be shot down.

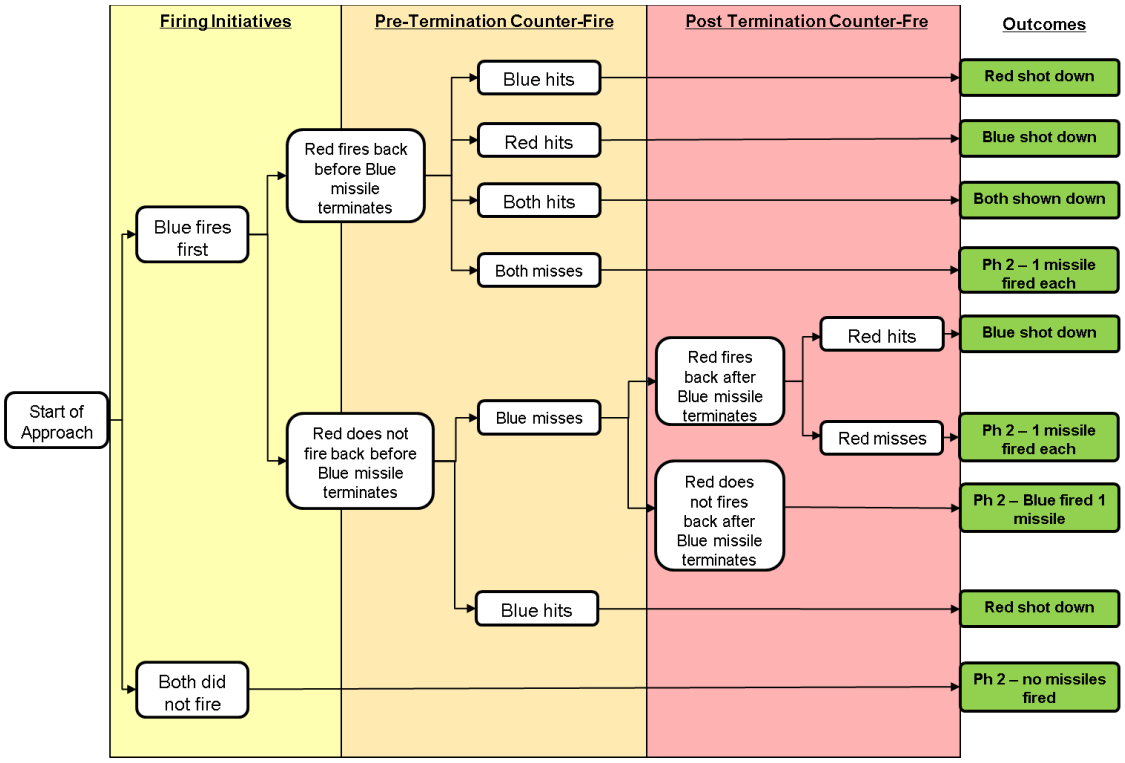

Figure 8 A tree diagram showing the possible events during Phase 1 assuming Blue fires first. (Note that the events are symmetric when Red fires first.) Three key critical events are in the tree diagram, namely 1) firing initiatives (highlighted in yellow), 2) pre-termination counter-fire (highlighted in orange), and 3) post termination counter-fire (highlighted in red). Green nodes correspond to the outcomes.

We may also examine the sequence of events using a timeline. The timeline informs us the temporal relationships among the critical events as the duel unfolds. These temporal relationships further allow us to formulate our probabilistic model with time as a key consideration. Using Blue's viewpoints, the timeline of events during Phase 1 is illustrated in Figure 9.

With reference to Figure 9, after Blue fires the first missile, Red has two windows of opportunities to fire back. The first window is the time between Blue's launch missile termination this is the missile termination time as previously defined in 2.c. If Red does not fire back before Blue's missile terminates, Red may be shot down before having a chance to respond. If Red survives, it has the remaining time interval, computed by

taking the difference between the approach time limit and Blue's engagement time, to fire back using an aimed shot.

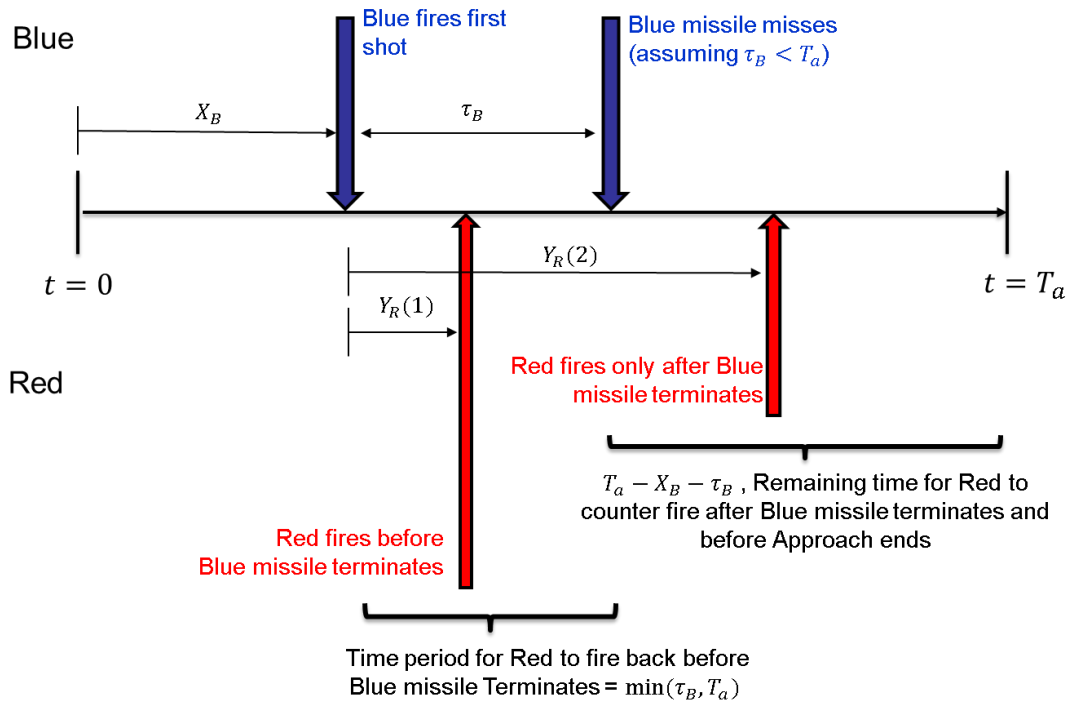

Figure 9 Timeline of the events occurring after Blue fires first. The blue arrows indicate the firing and termination of Blue's missile, while the red arrows indicate two possible scenarios where Red manages to fire back before the Approach ends. $Y_R(1)$ illustrates the instance when Red fires back at Blue before Blue's missile terminates. $Y_R(2)$ indicates the instance when Red fires back at Blue after Blue's missile misses Red.

b. Critical Event 1: Firing Initiative

The initial conditions at the start of the sequence are as shown in Figure 10. Once the sequence of event begins, both aircraft race to become the first shooter.

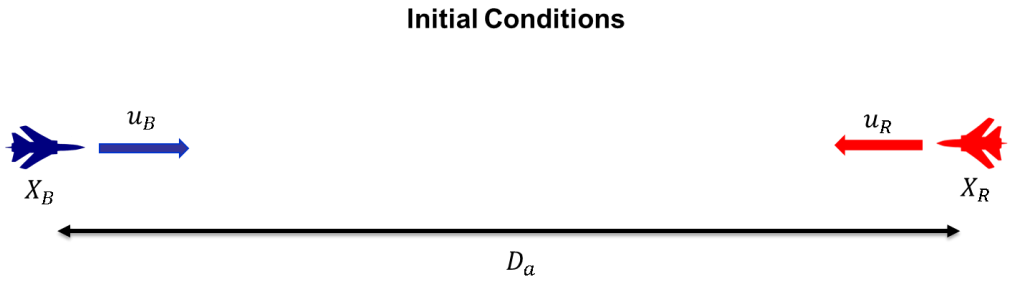

Figure 10 Initial conditions at the beginning of Phase 1. Both aircraft approach each other at D_a meters apart with their respective approach velocities, u_B and u_R. The BVR engagement times, X_B and X_R, are used to determine which aircraft fires first.

There are three possible outcomes from this critical event. If both aircraft cannot fire a missile before the Approach time ends, the duel will move on to Phase 2 with no missiles fired. Otherwise, one of the aircraft will fire the first missile.

As described above, without loss of generality we assume that the first shooter is the Blue aircraft. When the Blue aircraft fires the initial missile as shown in Figure 11, the fight moves on to the next critical event. Two parameters affect the following events: the remaining time in the Approach phase after the missile is fired, and the missile termination time. These two parameters determine the probabilities of the ensuing critical events.

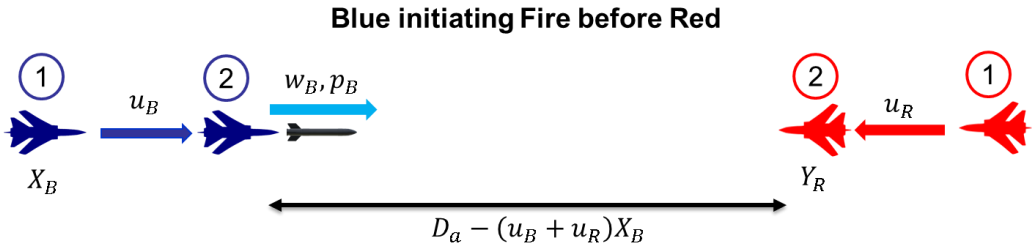

Figure 11 Instance after Blue initiates a missile fire. The remaining distance of the approach after the initial missile is fired is derived using the aircraft velocities, u_B and u_R, Blue's missile velocity, w_B, and Blue' engagement time, X_B. (1) corresponds to the initial conditions and (2) is the instance when Blue initiates the fire.

c. Critical Event 2: Pre-Termination Counter-firing

The next critical event determines whether the aircraft being fired upon may fire back before the attacking missile terminates. If the counter-firing aircraft manages to fire back before the missile terminates, both aircraft may be shot down by each other's missiles. Note that in this case, the first missile has a probability of kill of an aimed shot, while the counter-fired missile has a probability of kill of an unaimed shot. Figure 12 illustrates the case of Red counter-firing successfully, given that Blue having the firing initiative.

If the aircraft being fired upon does not fire back before the attacking missile terminates, but survives the attack, the duel continues to the next critical event—Post Termination Counter-Fire, as described in the next subsection.

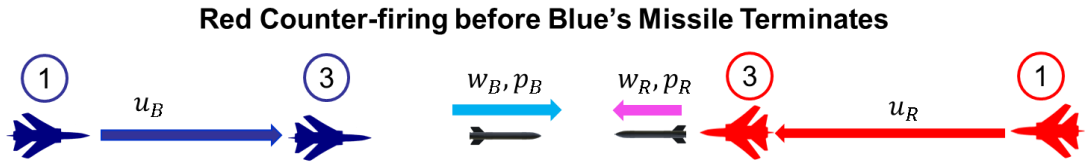

Figure 12 The instance where Red fires back successfully after Blue initiated a fire. In this case, both the missiles are in the air, therefore, subjecting both aircraft to be shot down. The condition for this scenario is for Red to fire back before Blue's missile terminates.

d. Critical Event 3: Post Termination Counter-firing

In the case of post-termination counter-fire, the Red aircraft applies aimed fire. If the Blue aircraft is not shot down, the duel will transit to Phase 2. Figure 13 illustrates the case of Red firing back after Blue's missile terminates.

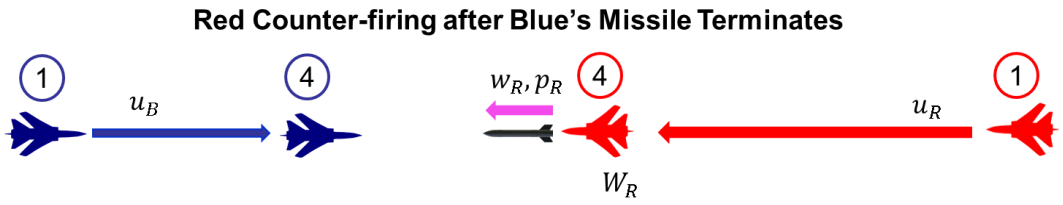

Figure 13 The instance when Red fires back successfully after Blue's missile terminates. At (4), it implies that Red manages to fire back before the remaining time of approach ends, but only after Blue's missile terminates. Mathematically, the counter-firing time of Red satisfies: $\tau_B < Y_R < T_a - X_B$.

4. Probability Model

Based on the discussion in Section 3 above, we now present the probability model for Phase 1.

a. Red Shot Down, Blue Survives

We define the probability of the outcome where Red is shot down while Blue survives as ϕ_B ..Four situations lead to this result. These situations are

1. Blue fires first and hits Red before the latter fires back.
2. Blue fires first and Red executes pre-termination counter-fire. Blue hits and Red misses.
3. Red fires first and misses, and Blue executes pre-termination counter-fire; Blue hits.
4. Red fires first and misses, and Blue executes post-termination counter-fire; Blue hits.

The probabilities of these four mutual exclusive situations are summarized below to obtain ϕ_B

$$\phi_B = \left[\begin{array}{l} \underbrace{\Pr\{X_B < \min(X_R, T_a) \cap Y_R > \tau_B(X_B)\} p_B^A}_{\text{Blue fires first and Red does not fire back. Blue hits}} + \underbrace{\Pr\{X_B < \min(X_R, T_a) \cap Y_R < \tau_B(X_B)\} p_B^A \overline{p_R^U}}_{\text{Blue fires first and Red fires back before the missile terminates Blue hits and Red misses.}} \\ + \underbrace{\Pr\{X_R < min(X_B, T_a) \cap Y_B < \tau_R(X_R)\} \overline{p_R^A} p_B^U}_{\text{Red fires first and Blue fires back before the missile terminates. Red misses and Blue hits.}} \\ + \underbrace{\Pr\{X_R < \min(X_B, T_a) \cap \tau_R(X_R) < Y_B < T_a - X_R\} \overline{p_R^A} p_B^A}_{\text{Red fires first andBlue fires back after the missile terminates. Red misses and Blue hits.}} \end{array} \right]$$

To compute the probability of each situation, we need to express each of these probabilistic expressions in integral forms. Note that although the counter-firing time is assumed independent of the BVR engagement time, the events in each of the summands are not independent. This is chiefly because the missile termination time, $\tau_B(\tau_R)$, is a linear function of the BVR engagement time and it is used in the joint terms to compute the probability of a counter-fire.

For this outcome, we present the explicit integral forms of the probabilities. In addition, we also show in the first probability formulation how the comparison of minimums is expressed as the sum of two probability terms. For all other outcomes presented in the following subsections, the mathematical formulations are presented in Appendix A. The mathematical expressions of the four probability terms are:

$$\begin{aligned} &\Pr\{X_B < \min(X_R, T_a) \cap Y_R > \tau_B(X_B)\} p_B^A \\ &= \Pr\{X_B < X_R \le T_a \cap Y_B > \tau_B(X_B)\} P_B^A + \Pr\{X_B < T_a < X_R \cap Y_B > \tau_B(X_B)\} P_B^A \\ &= p_B^A \left[\int_0^{T_a} \int_0^{x_R} \overline{F}_{Y_R}\left(\tau_B(X_B)\right) f_{X_B}\left(x_B\right) f_{X_R}\left(x_R\right) dx_B dx_R + \int_{T_a}^{\infty} \int_0^{T_a} \overline{F}_{Y_R}\left(\tau_B(X_B)\right) f_{X_B}\left(x_B\right) f_{X_R}\left(x_R\right) dx_B dx_R \right] \end{aligned}$$

$$\begin{aligned} &\Pr\{X_B < \min(X_R, T_a) \cap Y_R < \tau_B(X_B)\} p_B^A \overline{p_R^U} \\ &= p_B^A \overline{p_R^U} \left[\int_0^{T_a} \int_0^{x_R} F_{Y_R}\left(\tau_B(X_B)\right) f_{X_B}\left(x_B\right) f_{X_R}\left(x_R\right) dx_B dx_R + \int_{T_a}^{\infty} \int_0^{T_a} F_{Y_R}\left(\tau_B(X_B)\right) f_{X_B}\left(x_B\right) f_{X_R}\left(x_R\right) dx_B dx_R \right] \end{aligned}$$

$$\Pr\{X_R < \min(X_B, T_a) \cap Y_B < \tau_R(X_R)\}\overline{p_R^A}\, p_B^U$$
$$= \overline{p_R^A}\, p_B^U \left[\int_0^{T_a}\int_0^{x_B} F_{Y_B}\left(\tau_R(X_R)\right) f_{X_R}\left(x_R\right) f_{X_B}\left(x_B\right) dx_R dx_B + \int_{T_a}^{\infty}\int_0^{T_a} F_{Y_B}\left(\tau_R(X_R)\right) f_{X_R}\left(x_R\right) f_{X_B}\left(x_B\right) dx_R dx_B \right]$$

$$\Pr\{X_R < \min(X_B, T_a) \cap \tau_R(X_R) < Y_B < T_a - X_R\}\overline{p_R^A}\, p_B^A$$
$$= \overline{p_R^A}\, p_B^A \left[\begin{array}{l} \displaystyle\int_0^{T_a}\int_0^{x_B} \left(F_{Y_B}\left(T_a - X_R\right) - F_{Y_B}\left(\tau_R(X_R)\right)\right) f_{X_R}\left(x_R\right) f_{X_B}\left(x_B\right) dx_R dx_B \\ \displaystyle + \int_{T_a}^{\infty}\int_0^{T_a} \left(F_{Y_B}\left(T_a - X_R\right) - F_{Y_B}\left(\tau_R(X_R)\right)\right) f_{X_R}\left(x_R\right) f_{X_B}\left(x_B\right) dx_R dx_B \end{array} \right]$$

where $F(\cdot)$ and $f(\cdot)$ denote the CDF and pdf, respectively, of appropriate probability distributions

b. Blue Shot Down, Red Survives.

This is a symmetrical outcome to the one described above, so ϕ_R is obtained by interchanging the subscripts $R \leftrightarrow B$.

$$\phi_R = \left[\begin{array}{l} \underbrace{\Pr\{X_R < \min(X_B, T_a) \cap Y_B > \tau_R(X_R)\}\, p_R^A}_{\text{Red fires first and Blue does not fire back. Red hits}} + \underbrace{\Pr\{X_R < \min(X_B, T_a) \cap Y_B < \tau_R(X_R)\}\, p_R^A\, \overline{p_B^U}}_{\begin{array}{c}\text{Red fires first and Blue fires back before the missile terminates}\\ \text{Red hits and Blue misses.}\end{array}} \\ + \underbrace{\Pr\{X_B < min(X_R, T_a) \cap \{Y_R < \tau_B(X_B)\}\overline{p_B^A}\, p_R^U}_{\begin{array}{c}\text{Blue fires first and Red fires back before the missile terminates.}\\ \text{Blue misses and Red hits.}\end{array}} \\ + \underbrace{\Pr\{X_B < \min(X_R, T_a) \cap \tau_B(X_B) < Y_R < T_a - X_B\}\overline{p_B^A}\, p_R^A}_{\begin{array}{c}\text{Blue fires first and Re}d\text{ fires back after the missile terminates.}\\ \text{Blue misses and Red hits.}\end{array}} \end{array} \right]$$

c. Both Aircraft Shot Down

We define ϕ_K as the probability of having both aircraft being shot down by each other. Two situations lead to this outcome. They are:

1. Blue fires first and Red fires back before Blue's missile terminates; both missiles hit.

2. Red fires first and Blue fires back before Red's missile terminates; both missiles hit.

The probability of this outcome is:

$$\phi_K = \underbrace{\Pr\{X_B < min(X_R, T_a) \cap Y_R < \tau_B(X_B)\} p_B^A p_R^U}_{\substack{\text{Blue fires first and Red fires back before the missile terminates.} \\ \text{Both hits.}}} + \underbrace{\Pr\{X_R < \min(X_B, T_a) \cap Y_B < \tau_R(X_R)\} p_R^A p_B^U}_{\substack{\text{Red fires first and Blue fires back before the missile terminates} \\ \text{Both hits.}}}$$

d. None of the Aircraft Fires

We define the probability of both aircraft surviving Phase 1 with no missiles fired as ϕ_{00}. The situations corresponding to this outcome is simply the case where both the Blue and Red aircraft's engagement times exceed the time limit of the Approach phase. This is written as:

$$\phi_{00} = \Pr\{T_a < \min(X_B, X_R)\}$$

e. Both Aircraft Survive—Only One Fires

We define the probability of both aircraft surviving Phase 1 with only Blue (Red) firing a missile as ϕ_{10} (ϕ_{01}). The only event that contributes to this probability is for Blue (Red) to fire first and misses its shot, while Red (Blue) does not fire back at all. Thus, these are written as:

$$\phi_{10} = \Pr\{X_B < min(X_R, T_a) \cap Y_R > \max(\tau_B(X_B), T_a - X_B)\} \bar{p}_B^A$$
$$\phi_{01} = \Pr\{X_R < min(X_B, T_a) \cap Y_B > \max(\tau_R(X_R), T_a - X_R)\} \bar{p}_R^A$$

f. Both Aircraft Survive—Both Fired One Missile

The last outcome from Phase 1 is where both aircraft survive Phase 1 and both fire one missile each. We define this as ϕ_{11}. Two situations lead to this outcome; they are:

1. Blue fires first and misses; Red fires either before or after Blue's missile terminates and misses as well.
2. Red fires first and misses; Blue fires either before or after Red's missile terminates and misses as well.

This probabilistic argument is written as:

$$\phi_{11} = \left[\begin{array}{l} \overbrace{\Pr\{X_B < min(X_R, T_a) \cap Y_R < \max(\tau_B(X_B), T_a - X_B)\} \overline{p_B^A}\, \overline{p_R^U}}^{\text{Blue fires first and Red fires back before missile terminates or approach ends. Both misses}} \\ \underbrace{+\Pr\{X_R < min(X_B, T_a) \cap Y_B < \max(\tau_R(X_R), T_a - X_R)\} \overline{p_R^A}\, \overline{p_B^U}}_{\text{Red fires first and Blue fires back before missile terminates or approach ends. Both misses}} \end{array} \right]$$

B. PHASE 2—DOGFIGHT

1. Methodology

Phase 2—Dogfight—is the part of the duel where the complexity of the combat dynamics escalates. Our model must capture sufficient dynamics in the dogfight while retaining model tractability. To achieve this, we incorporate basic flight theories into the DTMC. Specifically, flight theories involving aircraft turning performance are most critical and useful.

The use of basic flight theories allows us to formulate the probabilistic arguments within the DTMC together with the scenario assumptions mentioned in Chapter III. This is the key enabler to bridge the gap between engineering-level specifications and mission-level measures of effectiveness in our model.

We select appropriate parameters that can characterize the measures of effectiveness in the Dogfight phase, and subsequently, use them to formulate the DTMC and state transition probabilities in conjunction with the relevant flight theories.

2. Flight Theories and Their Relevance to Our Study

Flight theories involving aircraft turning performance is a critical part of the Phase 2 model formulation. Prior to presenting the model, we present in this section a brief description of relevant flight theories.

Two physical specifications of an aircraft are of most interest, namely 1) the maximum load factor of the aircraft's structure and 2) the velocity of the aircraft. These two specifications serve as variables in the turn radius and rate equations, which are subsequently used in our stochastic model.

For clarity and consistency, we retain notations typically used in engineering contexts. While the notation of some variables may overlap with the notations used in our model, the definitions used in this section are solely for elaborating flight theories and are not introduced verbatim into our model.

a. Basic Aerodynamic Forces and Kinematics

We first consider the basic aerodynamic forces acting on an aircraft during its turn, as shown in Figure 14. We denote W as the weight of the aircraft measured in Newtons [N], L_{eff} as the effective lift force, L_T as the total lift force, ϕ as the bank angle, F_{CG} as the centrifugal force, F_{CP} as the centripetal force, g as the gravitational constant of 9.81 m/s^2, V as the flight velocity, R as the turning radius, and a_r as the radial acceleration of the aircraft.

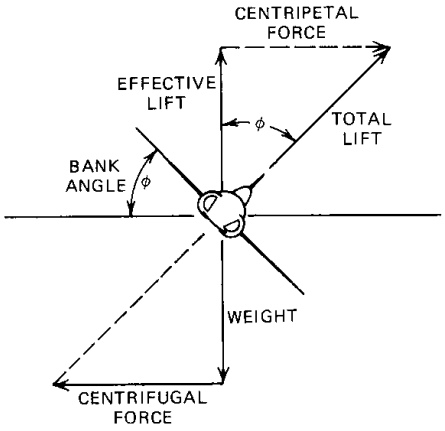

Figure 14 Aerodynamic forces acting on an aircraft performing a turn. Source: Dole and Lewis (2000).

According to Dole and Lewis (2000), the turn equation may be derived by comparing the two force vectors, namely the centripetal force and the centrifugal force. For a particle traveling in a circular path with velocity, V, and radius, R, its radial acceleration is:

$$a_r = \frac{V^2}{R}$$

By Newton's 2nd law, the centrifugal force is:

$$F_{CG} = ma_r = \frac{W}{g}\frac{V^2}{R}$$

Solving trigonometrically using the force vectors shown in Figure 14, the centripetal force is:

$$F_{CP} = L_T sin\phi$$

And by Newton's 1st law, the centripetal force must be equal to the centrifugal force for the aircraft to maintain its turn trajectory. This gives:

$$L_T sin\phi = \frac{W}{g}\frac{V^2}{R}$$

By resolving the weight vector in terms of the total lift force, the turn equation becomes

$$L_T sin\phi = \frac{L_T cos\phi}{g}\frac{V^2}{R}$$

which can be rearranged to:

$$R = \frac{V^2}{gtan\phi}$$

Now, consider the load factor acting on an aircraft, which is the ratio between the total lift force and its weight, given as:

$$G = \frac{L}{W} = \frac{1}{cos\phi}$$

where $Gsin\phi = tan\phi$. By trigonometry, $\cos\phi = \frac{1}{G}$, $\cos^2\phi = \frac{1}{G^2} = 1 - \sin^2\phi$. Therefore, $\sin\phi = \sqrt{1 - \frac{1}{G^2}}$. Substituting into the turn equation yields:

$$R = \frac{V^2}{g\sqrt{G^2 - 1}}$$

By relating the angular velocity with the tangential velocity and turning radius, the turn rate can be expressed as follows:

$$\omega = \frac{d\theta}{dt} = \frac{V}{R} = \frac{g\sqrt{G^2 - 1}}{V}$$

At this point, we have an expression for the turning radius and turn rate of an aircraft, respectively, as a function of two very important aircraft performance parameters—V, the velocity at which it executes a turn, and G, its structural load factor.

For our model, we consider the maximum load factor, G_{Max}, of the aircraft as the primary limiting factor to the turning radius and rates, given any velocity. This assumes that during the dogfight, both aircraft will attempt, given their velocity, to maximize the turn rate and/or minimize the turn radius.

b. Bounds of Turning Radius and Turning Rates

We further derive the bounds of an aircraft's turning radius and turn rates based on the minimum and maximum velocities of an aircraft. These bounds serve as the finite support range of the distributions for the random variable representing the velocities of the aircraft in our stochastic model. This improves realism to the model because an aircraft in flight is physically limited by its stall (minimum) velocity and maximum velocity. We assume that it is easier to obtain data on level-flight velocities than on level-turn velocities from an aircraft's flight control system; therefore, we further make a conversion of the turn equations that use level-flight velocities as its argument.

According to Hurt (1960), the relationship between the maneuver (turn) speed and stall speed is given as:

$$V_{(turn)} = V\sqrt{G_{Max}}$$

Substituting this into the turn equation yields the relationship of a level-flight velocity to the minimum and maximum turn radius and rates as follows:

$$R_{min} = \frac{V_s^{\,2}}{g\sqrt{1-\frac{1}{G_{Max}^2}}}, R_{\max} = \frac{V_{max}^{\,2}}{g\sqrt{1-\frac{1}{G_{Max}^2}}}$$

$$\omega_{max} = \frac{g\sqrt{G_{Max}^2-1}}{V_s}, \omega_{\min} = \frac{g\sqrt{G_{Max}^2-1}}{V_{\max}}$$

3. Phase 2 Parameters

Eleven parameters are required to construct the Phase 2 model. Two are random variables with distributions with non-negative support, and the remaining nine are deterministic inputs. Table 3 summarizes these 11 parameters used in the Phase 2 model.

Table 3 Parameters used in the Phase 2 model.

S/N		PARAMETER	NOTATION [UNITS]	PURPOSE
	1	Flight Velocity	V_B, V_R [meters per second]	Pursuit-Evade
	2	Dogfight Engagement Time	Z_B, Z_R [seconds]	Pursuit-Evade
	1	Single Shot Kill Probability	p_B, p_R	Pursuit-Evade, Disengagement
	2	Probability of Turn Types	$P(NtN),\ P(NtT)$	Pursuit-Evader
	3	Maximum Load Factor	G_{max}	Pursuit-Evade
	4	Target Acquisition Angle	θ [radians]	Pursuit-Evade
	5	Disengagement velocity	$\hat{v}_B, \hat{v}_R$ [meters per second]	Disengagement
	6	Maximum Engagement Range	d_B, d_R [meters]	Disengagement
	7	Initial Separation Distance	D_0 [meters]	Disengagement
	8	Maximum Pursuit Distance	D_{Max} [meters]	Disengagement
	9	Onboard Payload	i, j	Throughout

a. Random Variables

The two random variables characterizing the maneuvering and engagement capabilities of each aircraft are elaborated as follows:

1. **Flight Velocity**, $V_B(V_R)$, measured in meters per seconds (m/s). This is a random variable defined as the level-flight velocity that an aircraft may execute during the dogfight. This parameter characterizes the uncertainty

in the aircraft's velocity during a dogfight and is influenced by several factors such as 1) the aircraft's flight control system, 2) the pilot's skills, and 3) tactical doctrines. The distributions of these random variables have supports bounded by the minimum (stall) velocity and maximum velocity. For any unimodal distribution, the mode velocity is used to characterize the most likely executable velocity during the maneuvers in a dogfight. Estimates of such distributions are obtained from flight control data.

2. **Dogfight Engagement Time,** $Z_B\left(Z_R\right)$, measured in seconds. This is the time between the moment a pursuing aircraft initiates a firing drill and the moment it fires off a missile. This is time is a function of only the onboard target acquisition system, and is not to be confused with the BVR engagement time, X_B, used in the Phase 1 model.

b. Inputs

The remaining nine deterministic inputs are as follows:

1. **Single Shot Kill Probability**, $p_B\left(p_R\right)$. This is the probability that a Blue(Red) missile hits its target. This probability is identical to the single shot kill probability of an aimed shot, $p_B^A\left(p_R^A\right)$, defined in the Phase 1 model.

2. **Probability of Turn Types**, $P\left(NtN\right)$ and $P\left(NtT\right)$. The probability of a nose-to-nose turn (NtN) and a nose-to-tail (NtT) turn. This probability depends on the aircraft-type, tactics, and pilot skills. Formally, $P\left(NtN\right)=1-P\left(NtT\right)$.

3. **Maximum Load Factor**, $G_B\left(G_R\right)$, with values $G\geq 1$. This is the maximum possible ratio between the total lift force and the weight of the aircraft. It measures the gravitational acceleration, g, that an aircraft's structure may withstand. This is the aircraft specification that limits its turning radius or rate at any given velocity.

4. **Onboard Payload**, $i\left(j\right)$, used as a subscript of the aircraft's state to indicate the number of missiles remaining on Blue (Red) aircraft during the dogfight.

5. **Target Acquisition Angle**, $\theta_B\left(\theta_R\right)$, measured in radians. This is the half angle, measured from the center of the aircraft's cockpit, at which the aircraft's target acquisition system may detect and lock-on to a target. Refer to Figure 15 for the depiction of the target acquisition angle.

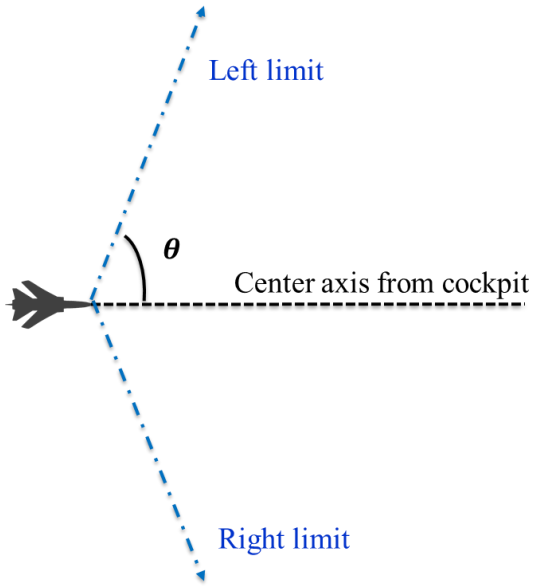

Figure 15 Target acquisition angle, θ, of an aircraft defined as the half angle measured from the left/right limit to the central axis of the direction of flight.

6. **Disengagement Velocity**, $\hat{v}_B\left(\hat{v}_R\right)$, measured in meters per second $\left(m/s\right)$. This is defined as the velocity that an aircraft may fly at during a disengagement pursuit regardless whether it is the Pursuer or Evader. We assume that an aircraft will attempt to fly at its top speed during a disengagement.

7. **Maximum Weapon Range**, $d_B\left(d_R\right)$, measured in meters. This is the maximum range at which Blue (Red) can fire at its opponent. This parameter is used during a disengagement pursuit.

8. **Initial Separation Distance**, D_0, measured in meters. This is the initial distance at which the two aircraft are apart during the start of a disengagement pursuit. This parameter is determined based on the combat tactics and historical data. For simplicity of the ensuing model, we treat this parameter to be deterministic.

9. **Maximum Pursuit Distance**, D_{Max}, measured in meters. This is the maximum distance the Pursuer can travel during a disengagement pursuit. Tactically, this refers to the boundary of the combat zone beyond which a Pursuer may be subjected the Evader's supporting or reinforcing assets such as ground air defense systems. For the model, we assume that D_{Max} is

the same for the Blue and Red aircraft. Figure 16 presents a graphical representation of the maximum disengagement distance.

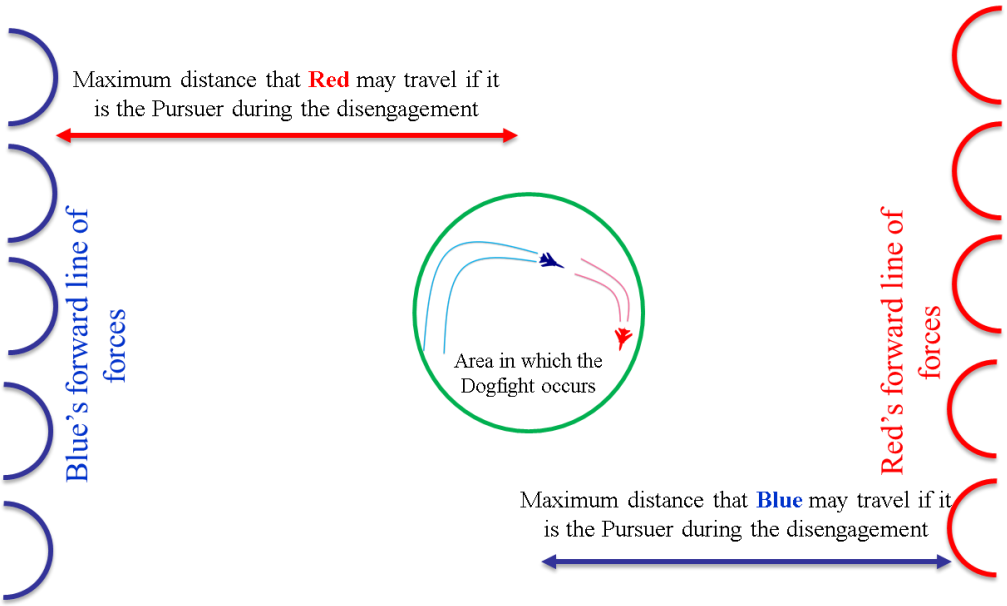

Figure 16 Maximum pursuit distance, D_{Max}, defined as the maximum distance that a Pursuer may travel during a disengagement.

d. Functions

Two important functions are derived using the flight velocity, $V_B\left(V_R\right)$ and the maximum load factor, $G_B\left(G_R\right)$. These are the turning radius, $\mathrm{R}_B\left(\mathrm{R}_R\right)$—script font used to distinguish the turning radius from the notation used for Red, R—and turning rates, $\Omega_B\left(\Omega_R\right)$, expressed as a function of the flight velocity, maximum load factor, and the gravitational constant, based on the flight theories discussed in Section 2.

We define Blue's turning radius as a function of its flight velocity, $\mathrm{R}_B\left(V_B\right)$, and turning rate as a function of its flight velocity, $\Omega_B\left(V_B\right)$, where

$$\mathrm{R}_B\left(V_B\right)=\frac{V_B^2}{g\sqrt{1-\frac{1}{G_B^2}}}$$

$$\Omega_B(V_B) = \frac{g\sqrt{G_B^2 - 1}}{V_B}$$

Similar expressions are used for the Red aircraft's turning radius and rate.

4. Events in Phase 2

a. Lead Turn and Maneuvers

In this event, both aircraft are in the state of neutrality while executing a move to attempt to become the Pursuer. The event happens when the two aircraft transits into Phase 2 from Phase 1, or after the Evader breaks off from the Pursuer. The model considers the maneuvering event from the time both aircraft begin the turn. As mentioned in Chapter III, two turn types—nose-to-nose and nose-to-tail—may happen. The identity of the Pursuer at the end of the event depends on the type of turn that occurs. When a nose-to-nose turn happens, the event is a contest of two turn radii. When a nose-to-tail occurs, it is a contest of two turn rates. Figure 17 shows the two turn types and their corresponding parameters of interest.

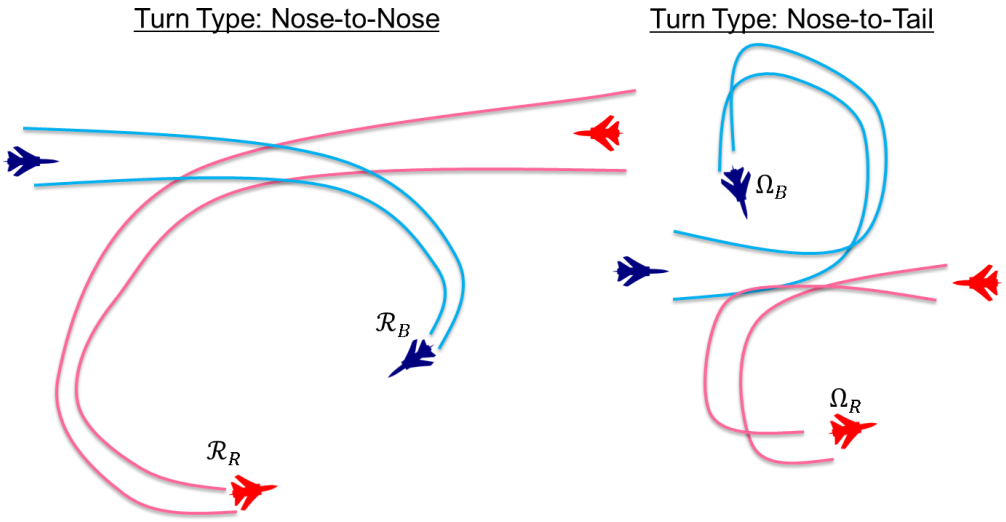

Figure 17 The flight trajectories of the two aircraft during a nose-to-nose turn and a nose-to-tail turn, and their corresponding parameters of interest. In a nose-to-nose turn, the turning radius R is used as the parameter of interest in determining the outcome of the turn. For a nose-to-tail turn, the turning rate, Ω, is used, instead.

Two potential outcomes may occur from this transitional event. First, in a nose-to-nose turn, the side with the small turning radius will eventually become the Pursuer at the end of the turn. Second, in a nose-to-tail turn, the side with the highest turn rate will become the Pursuer at the end of the turn.

b. Pursuit-Evade and Break-offs

The second and most prominent event in Phase 2 is the pursuit curve. The Evader's main aim is to break off from the pursuit while the Pursuer attempts to stay on the pursuit and fire its missile on the Evader. The turn rates of the two aircraft affect whether the Evader could break off, and the Pursuer' angle of target acquisition will determine the time window that it has to lock-on and fire at the Evader. Figure 18 demonstrates the relationships of the parameters in a pursuit curve with Blue as the Pursuer.

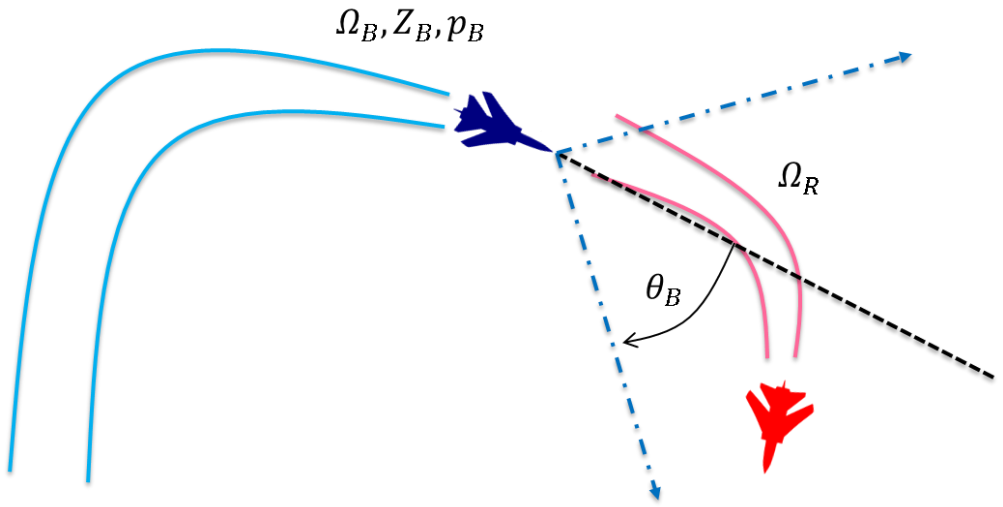

Figure 18 A pursuit curve with Blue as the Pursuer. During this event, both aircraft turn rates; and Blue's angle of target acquisition, engagement time, and probability of kill are of interests

In terms of the pursuit, two potential outcomes may occur. First, the Pursuer manages to fire at the Evader before the latter turns out of the target acquisition angle. Second, the Pursuer does not manage to fire before the Evader turns out of the target

acquisition angle. In the first case, if the Pursuer's missile hits the Evader, then the Evader is shot down. Otherwise, the two aircraft remain in the pursuit curve with the Pursuer reducing its payload of missiles by one. In the second case, we assume that if the Pursuer does not fire before the Evader turns out of the target acquisition angle, the Evader will eventually break-off from the pursuit curve, and the two aircraft will transit into a neutral state, thus leading to the contest of the lead turn again, as described in Subsection a.

c. Disengagements

In the last type of events for Phase 2, we have the disengagement pursuit with two aircraft flying in a straight-line vector in the same direction. The Evader is attempting to disengage from the duel after expending all its ammunition, while the Pursuer, with more than one missile left, attempts to shoot down the Evader before the Evader escapes out of the Pursuer's maximum weapon range and/or maximum pursuit distance.

Using the scenario in Chapter III and the parameters in Section 3 of this Chapter, we can formulate the relationships of the parameters characterizing this event as shown in Figure 19.

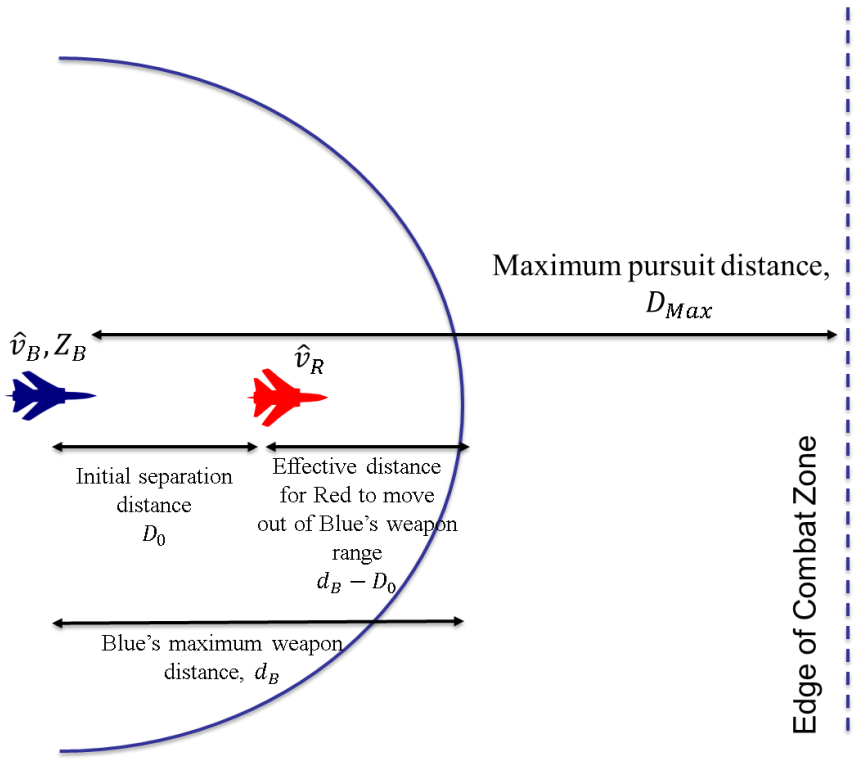

Figure 19 A disengagement of Red and pursuit by Blue. In this figure, Blue is the Pursuer, and Red is the disengaging Evader. For Blue to successfully fire at Red, it must fire within two time-windows. The first time-window corresponds to the time until Red aircraft flies out its weapon's maximum range. The second time-window is before Blue itself flies beyond its maximum pursuit distance.

Suppose Blue is the Pursuer, to compute whether Blue can fire at Red within the boundaries of this event, it is necessary to convert the spatial parameters into temporal forms. Using kinematics, we further define the time until Red moves out of Blue's maximum weapon range as

$$T_{*,D} = \frac{\left(d_B - D_0\right)}{\max\left\{\hat{v}_R - \hat{v}_B, 0\right\}}$$

In addition, we also define the time until Blue (Pursuer) reaches the maximum pursuit distance as:

$$T_{MPD,B} = \max\left\{\frac{D_{max}}{\hat{v}_B}, \frac{D_{max} - D_0}{\hat{v}_R}\right\}$$

The first term in the max-function corresponds to the time taken for Blue to move beyond its maximum pursuit distance into Reds operating boundary. The second term corresponds to the time taken for Red to move beyond its maximum pursuit distance into its own operating boundary. By taking the maximum of these two terms, we account for the both cases where $\hat{\nu}_B \le \hat{\nu}_R$ and $\hat{\nu}_B > \hat{\nu}_R$.

5. Discrete-Time Markov Chain (DTMC)

We define the DTMC for Phase 2 of the duel as $\{Y_n : n \ge 0\}$, using a state vector, (B_i, R_j), to represent the states of the Blue (Red) aircraft with $i(j)$ number of missiles remaining. For each aircraft, $B_i(R_j)$, the states that it may take on are

$$B_i = \begin{cases} M_i, E_i, D, K, * & \forall i \\ P_i & \forall i > 0 \end{cases}$$
$$R_j = \begin{cases} M_j, E_j, D, K, * & \forall j \\ P_j & \forall j > 0 \end{cases}$$

where $i(j) = \{m_{B(R)}, m_{B(R)} - 1, \ldots, 0\}$, M indicates a maneuvering state, P indicates a Pursuer state, E indicates an Evader state, D represents a successful disengagement, K represents the aircraft being shot down by its opponent, and * denotes any states other than D or K. In addition, $m_{B(R)}$ represent the number of missiles payload loaded on the Blue (Red) aircraft when the duel begins.

The resulting state space, $\{Y_n\}$, has the general form

$$\{(M_i, M_j), (P_i, E_j), (E_i, P_j), (*, D), (D, *), (D, D), (*, K), (K, *)\}$$

Note that there is no (K, K) state in the Dogfight phase, in contrary to the state space in Phase 1, because we assume it is not possible to have both aircraft being shot down simultaneously during the dogfight. Table 4 provides a detailed description of the individual state vectors in $\{Y_n\}$.

The last five states in Table 4 are absorbing states. Note that it is not possible to have the states (P_0, E_j), (P_0, E_0), (E_i, P_0), (E_0, P_0), and (M_0, M_0). This follows from the model assumption made previously that a Pursuer with no more missiles will attempt to disengage from the flight, and the two aircraft will not carry on the duel if neither has any missiles left.

Table 4 Descriptions of the individual state vectors for Phase 2 DTMC.

STATES $(\boldsymbol{B_i}, \boldsymbol{R_j})$	**DESCRIPTIONS**
(M_i, M_j)	Both aircraft are in the state of neutrality, maneuvering to achieve an advantageous position as the Pursuer i missiles remaining on Blue and j missiles remaining on Red.
(P_i, E_j)	Blue aircraft pursuing Red with i missiles remaining on Blue and j missiles remaining on Red.
(E_i, P_j)	Red aircraft pursuing Blue with i missiles remaining on Blue and j missiles remaining on Red.
$(*, D)$	Red aircraft successfully disengaged from the fight, regardless of Blue's state.
$(D, *)$	Blue aircraft successfully disengaged from the fight, regardless of Red's state.
(D, D)	Both aircraft disengage from the fight. The fight ends with no casualty.
$(*, K)$	Red aircraft shot down by Blue.
$(K, *)$	Blue aircraft shot down by Red.

6. The State Transition Probabilities

We now compute the transition probabilities of Phase 2.

a. Transitions from $\left(M_i, M_j\right)$

From the maneuvering states, $\left(M_i, M_j\right)$, for $i, j \neq 0$, it is possible to transit to the states $\left(P_i, E_j\right)$ and $\left(E_i, P_j\right)$, taking into account the probability of each turn type occurring during the dogfight. To reduce redundancy, we define the state transitions from the perspectives of Blue using the turning radius function, turning rate function, and the probability distribution of turn types as defined in Section 3.c. The probability of Blue becoming the Pursuer at the end of the maneuver is written as:

$$P_{M_i M_j \to P_i E_j} = P_{NtN} \cdot \Pr\{\mathrm{R}_B < \mathrm{R}_R \mid NtN) + P_{NtT} \cdot \Pr\{\Omega_B > \Omega_R \mid NtT\}$$

This transition probability comprises the probability of Blue executing a smaller turn radius than Red conditioned on a nose-to-nose turn, and the probability of Blue executing a faster turn than Red conditioned on a nose-to-tail turn. We further formulate the individual probabilities using our definitions in Section 3.c as follows:

$$\Pr\left\{\mathrm{R}_B(V_B) < \mathrm{R}_R(V_R)\right\} = \int_0^\infty \Pr\left\{\mathrm{R}_B(V_B) < \mathrm{R}_R(V_R) \mid \mathrm{R}_R(V_R) = r_R\right\} f_{\mathrm{R}_R}(r_R) d_{\mathrm{R}_R}$$

$$\Pr\left\{\Omega_B(V_B) > \Omega_R(V_R)\right\} = \int_0^\infty \Pr\left\{\Omega_B(V_B) < \Omega_R(V_R) \mid \Omega_R(V_R) = \omega_R\right\} f_{\Omega_R}(\omega_R) d_{\Omega_R}$$

Noteworthy, the conditional probabilities are expressed for any general distributions with real, positive support. To obtain numerical solutions, distributions with bounded support are more appropriate and realistic because of the maximum and minimum velocities that an aircraft may fly.

By symmetry, the probability of Red becoming the Pursuer at the end of the maneuver is:

$$P_{M_i M_j \to E_i P_j} = 1 - P_{M_i M_j \to P_i E_j}$$

Furthermore, if one of the aircraft expands all of its missiles $i, (\ j) = 0$, then:

$$P_{M_i M_0 \to P_i E_0} = 1, \ \forall i > 0$$

$$P_{M_0 M_j \to E_0 P_j} = 1, \ \forall\ j > 0$$

b. Transitions from (P_i, E_j) and (E_i, P_j)

We next consider the transition probabilities from the Pursuer-Evader states using Blue's viewpoint and apply them symmetrically for Red. Three general types of state transitions may occur when the dogfight is in this state. These are the states where $\{i \neq 0, j \neq 0\}$, $\{i > 1, j = 0\}$, and $\{i = 1, j = 0\}$. The first transition type constitutes the main bulk of the dogfight where the two aircraft are engaged in a series of Pursuer-Evader maneuvers, attempting to shoot the opponent down. The second transition type represents the scenario where Red has no more missiles and is attempting to disengage from the duel while Blue pursues it and attempts to shoot Red down. In the last typeBlue pursues Red during a disengagement, with only one missile left onboard Blue.

First, for $\{i \neq 0, j \neq 0\}$ the state may transit to 1) (M_i, M_j) if Red successfully breaks off from the ongoing pursuit, 2) (P_{i-1}, E_j) if Blue fires at Red before Red breaks off from the pursuit and Blue misses, and 3) $(*, K)$ if Blue fires and hit Red before Red breaks off from the pursuit.

For the dogfight to transit into the maneuvering state, (M_i, M_j), we use the analysis from Section 4.b to compute the transition probabilities. From Figure 18, we obtain the probability of transitioning to (M_i, M_j) by computing the probability that Blue's close-range engagement time, Z_B, is longer than the time taken for Red to move out of Blue's target acquisition angle, θ_B. This yields:

$$P_{P_i E_j \to M_i M_j} = \Pr\left(Z_B > \frac{\theta_B}{\Omega_R - \Omega_B} \cap \Omega_R > \Omega_B \right)$$
$$= \int_0^\infty \int_{\omega_B}^\infty \overline{F}_{Z_B}\left(\frac{\theta_B}{\omega_R - \omega_B} \right) f_{\Omega_R}(\omega_R)\, f_{\Omega_B}(\omega_B)\, d\omega_R\, d\omega_B$$

For the case where Red does not break off before Blue shoot, the probability of transitioning to (P_{i-1}, E_j) is:

$$P_{P_i E_j \to P_{i-1} E_j} = \left(1 - P_{P_i E_j \to M_i M_j}\right)(1 - p_B)$$

While the probability of transitioning to $(*,K)$ is then:

$$P_{P_iE_j \to *K} = \left(1 - P_{P_iE_j \to M_iM_j}\right) p_B$$

When $\{i > 1, j = 0\}$, it is possible to have two types of transitions 1) transit to $(*,K)$ if Blue shoots Red down, and 2) transit to $(*,D)$ if Blue does not shoot Red down. In the second case, we assume that Blue can only fire one missile during the disengagement. To formulate the transition probabilities in this second type of transition, we use the Disengagement scenario as discussed in Section 4.c.

From our analysis in Section 4.c, we observe that the conditions for Blue (the Pursuer) to shoot Red (the Evader) down, thus transitioning to $(*,K)$, is for Blue to fire before exceeding its maximum pursuit distance and before Red moves out of Blue's maximum weapon distance. The two temporal parameters, T_{*D} and $T_{MPD,B}$, are deterministic qualities that represent the durations of the two separate conditions—Red moving out of Blue's maximum engagement distance and Blue exceeding its own maximum pursuit distance—that are used to determine whether Blue can fire at Red during the disengagement pursuit. Although it is possible to incorporate uncertainty in the separation distance between the two aircraft during the dogfight, thus converting T_{*D} into a random variable, we find that it is sufficient to use a deterministic quantity for our model for the simplicity of the model without losing too much fidelity. Furthermore, two possible sub-scenarios may occur: 1) the pursuit velocity of Blue is higher or equal to Red's ($\tilde{v}_B \geq \tilde{v}_R$) and 2) the pursuit velocity of Blue is lower than Red's ($\tilde{v}_B < \tilde{v}_R$). In the first sub-scenario, we assume that Red cannot move out of Blue's maximum engagement distance since Blue will always be able to catch up; therefore, the only condition for Blue not to fire at Red is by exceeding its maximum pursuit distance. In the second sub-scenario, Blue has to satisfy the two conditions to fire at Red. Therefore, the transition probability can be expressed as:

$$P_{P_iE_0\to *K} = \begin{cases} \Pr\left(Z_B < \min\left(T_{*D}, T_{MPD,B}\right)\right) p_B & ,\tilde{v}_B < \tilde{v}_R \\ \Pr\left(Z_B < T_{MPD,B}\right) p_B & ,\tilde{v}_B \geq \tilde{v}_R \end{cases}$$

$$= \begin{cases} F_{Z_B}\left(\min\left(T_{*D}, T_{MPD,B}\right)\right) p_B & ,\tilde{v}_B < \tilde{v}_R \\ F_{Z_B}\left(T_{MPD,B}\right) p_B & ,\tilde{v}_B \geq \tilde{v}_R \end{cases}$$

As long as Red manages to escape out of Blue's maximum engagement distance or Blue reaches its maximum pursuit distance, or if Blue's missile misses, we consider it a successful Red disengagement. The transition probability is therefore written as

$$P_{P_iE_0\to *D} = 1 - P_{P_iE_0\to *K}$$

Lastly, for the case of $\{i=1, j=0\}$, it is a special subset of the second transition type, except that the resulting state transition will lead to either $(*,K)$, $(*,D)$, or (D,D). This is due to the additional resolution of the states that we are capturing when both aircraft disengages from the duel. Noteworthy, the subtle difference $(*,D)$ and (D,D) must be emphasized. The state $(*,D)$ indicates that Red successfully evades Blue and disengages from the duel. The state (D,D) indicates that Blue fires but missed its shot, and the disengagement is due to Blue's failure to hit.

For the transition to $(*,K)$, it remains in the similar form as $P_{P_iE_0\to *K}$ given as

$$P_{P_1E_0\to *K} = \begin{cases} F_{Z_B}\left(\min\left(T_{*D},\ T_{MPD,B}\right)\right) p_B & ,\ \tilde{v}_B < \tilde{v}_R \\ F_{Z_B}\left(T_{MPD,B}\right) p_B & ,\ \tilde{v}_B \geq \tilde{v}_R \end{cases}$$

For the transition to $(*,D)$, it is expressed as:

$$P_{P_1E_0\to *D} = \begin{cases} \bar{F}_{Z_B}\left(\min\left(T_{*D},\ T_{MPD,B}\right)\right) & ,\ \tilde{v}_B < \tilde{v}_R \\ \bar{F}_{Z_B}\left(T_{MPD,B}\right) & ,\ \tilde{v}_B \geq \tilde{v}_R \end{cases}$$

Whereas for the transition to (D,D), we have:

$$P_{P_1E_0\to *D} = \begin{cases} F_{Z_B}\left(\min\left(T_{*D},\ T_{MPD,B}\right)\right)(1-p_B) & ,\ \tilde{v}_B < \tilde{v}_R \\ F_{Z_B}\left(T_{MPD,B}\right)(1-p_B) & ,\ \tilde{v}_B \geq \tilde{v}_R \end{cases}$$

C. THE COMBINED PHASE 1-2 MODEL

In this section, we present how the solutions from Phase 1 and Phase 2 are combined.

We solve the model separately for Phase 1 and Phase 2. However, Phase 2 only occurs if Phase 1 does not result in a kill on either or both sides. Therefore, to compute the overall solution to the duel, we use the Law of Total Probability calculation to connect the outputs of Phase 1 that do not result in a kill to the inputs of Phase 2 to begin the dogfight.

1. Phase 1 Solutions

For Phase 1, we obtain seven outputs of probability values, three of which determine the probability of a win on each side or having both aircraft shot down, while each of the remaining four probability values corresponds to the number of missiles fired on each side: (0,0)—no missile was fired, (1,0), (0,1), (1,1)—both aircraft fired a missile. These last four probabilities become the distribution of the initial state for Phase 2. Formally, we define the Phase 1 solutions as:

$$\phi = \{\phi_B, \phi_R, \phi_K, \phi_{00}, \phi_{10}, \phi_{01}, \phi_{11}\}$$

Each component in the solution sets are computed using the probability model discussed in Section A.4. The first three terms, $\{\phi_B, \phi_R, \phi_K\}$, refers to the probabilities of Blue winning in Phase 1, Red winning in Phase 1, and both getting shot down in Phase 1. The remaining four terms, $\{\phi_{00}, \phi_{10}, \phi_{01}, \phi_{11}\}$, correspond to the four aforementioned missile-expending states.

2. Phase 2 Solutions

For Phase 2, we obtain five outputs using the absorbing states in the DTMC. Two of the outputs correspond to the states where one of the aircraft is shot down, while the remaining three correspond to the states where one or both aircraft successfully disengage from the duel. We define ψ as the solution set to Phase 2 as follows:

$$\psi = \{\psi_B, \psi_R, \psi_{BD}, \psi_{RD}, \psi_{DD}\}$$

The first two terms, $\{\psi_B, \psi_R\}$, correspond to the probability of Blue and Red winning in Phase 2. The last three terms, $\{\psi_{BD}, \psi_{RD}, \psi_{DD}\}$, are the probabilities of having Blue (BD) and Red (RD) disengaging from the dogfight and both (DD) disengaging.

The Phase 2 DTMC in our model is an absorbing Markov chain and therefore not irreducible; therefore, there exists no limiting distribution. Our solution sets correspond to the absorbing states and are computed using first passage time probabilities by raising the DTMC to a large power, n. By denoting $\mathbf{D}^n$ as the state transition matrix of the DTMC, this follows:

$$\lim_{n\to\infty} \mathbf{D}^n = \mathbf{D}^\infty$$

Notwithstanding, the absorption probabilities do not suffice as the solution to the Phase 2 model because we do not know what the initial state is at the beginning of Phase 2. We use the Law of Total Probability to remove the conditioning on the initial states of Phase 2 by multiplying the appropriate terms by the probabilities obtained from Phase 1. As an example, the probability Blue wins in Phase 2, is:

$$\psi_B = \sum_{\phi_{ij}}^{i,j\in\{0,1\}} \Pr\left(\mathrm{Y}_\infty = (*, K) \,|\, \mathrm{Y}_0 = \left(M_{m_B - i}, M_{m_R - j}\right)\right)\phi_{ij}$$

3. Overall Solutions

The overall solution of the duel is the win probability of each aircraft and the probabilities of them disengaging or mutually shooting each other down. This gives us an overview of how the duel will likely unfold as a single event.

We define a set, $\mathbf{\Gamma}$, comprising six components, namely 1) blue wins, 2) red wins, 3) blue disengages, 4) red disengages, 5) both disengages and 6) both shot down.

For 1) and 2), we consider the sum of the win probabilities for two phases, after applying the conditional probability for Phase 2. For 3) to 5), the solutions are unique to Phase 2, conditioned on Phase 1, while for 6), the solution is directly obtained from Phase 1.

Explicitly, we have in the overall solution set

$$\mathbf{\Gamma} = \begin{bmatrix} \Gamma_1 \\ \Gamma_2 \\ \Gamma_3 \\ \Gamma_4 \\ \Gamma_5 \\ \Gamma_6 \end{bmatrix} = \begin{bmatrix} \phi_B + \psi_B \\ \phi_R + \psi_R \\ \psi_{BD} \\ \psi_{RD} \\ \psi_{DD} \\ \phi_K \end{bmatrix}$$

Subjected to the condition that

$$\sum_{i=1}^{6} \Gamma_i = 1$$

THIS PAGE INTENTIONALLY LEFT BLANK

V. NUMERICAL EXAMPLE

We present in this chapter a numerical example of our model for the one-on-one duel featuring two actual, dissimilar aircraft. We also discuss some of the key considerations in selecting the appropriate distributions for the random variables used in the model.

In the subsequent portion of this chapter, we also present a sensitivity analysis of our analytical model using Design of Experiment (DOE) methods (Sanchez et.al 2014). The advantage of using DOE method on our analytical model, especially one that has a relatively large number of input parameters to consider, is the ability to construct a deterministic meta-model that offers further insights into the model without a combinatorial expansion in the number of iterations required.

A. AIRCRAFT SPECIFICATIONS

We feature two dissimilar fighter aircraft as shown in Figure 20, namely 1) Multi-role EF-2000 Eurofighter for the Blue, and 2) Multi-role Su-30 / FLANKER-F for the Red.

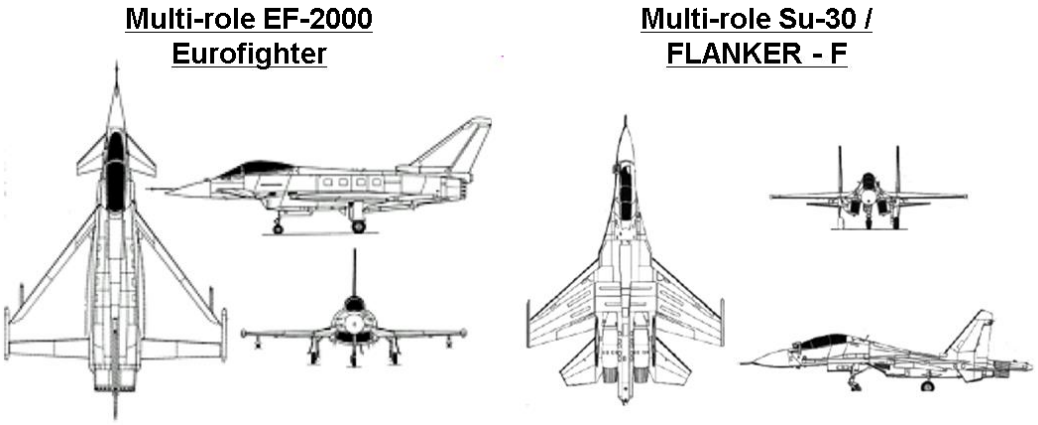

Figure 20 Blue aircraft—the Multi-role EF-2000 Eurofighter (left). Red aircraft—Multi-role Su-30/FLANKER-F (right). Source: U.S. Army TRADOC G-2 (2014).

We extract the relevant specifications of the two aircraft as shown in Table 5 .

Table 5 Summary of specifications for two aircraft

SPECIFICATIONS	BLUE—EF-2000	RED—SU-30/FF	SOURCES
Max G Loading	9	6.5	(U.S. Army TRADOC G-2 2014)
Max Speed (m/s)	592	590	(U.S. Army TRADOC G-2 2014)
Min Speed (m/s)	57	Assumed as 60	(GlobalSecurity.org 2013)
Payload	6 x BVRAAM + 6 x ASRAAM	6 x AA-12 Adder	(U.S. Army TRADOC G-2 2014)

Due to missing information from open sources regarding the minimum speed of the Red aircraft, we assume a relatively similar minimum speed as the Blue aircraft for our computation.

According to the Worldwide Equipment Guide, Vol. 2, (2014), the Blue aircraft is able to carry up to six Beyond-Visual-Range Air-to-Air Missiles (BVRAAM) and six Advanced Short Range Air-to-Air Missiles (ASRAAM). For our model, we assume that the Blue aircraft uses the BVRAAM during the Approach and both types of missiles during the dogfight. For the Red aircraft, according to the Worldwide Equipment Guide, Vol.2, (2014), it is able to carry up to six different variants of missiles. For simplicity, we assume that the Red aircraft carries a single variant—AA-12 Adder.

The missile specifications of the missiles used by the two aircraft appear in Table 6 . Specifically, the missile speed and the operating range—maximum weapon range—are used directly in our model.

Table 6 Performance of the missiles used by both aircraft.

SPECIFICATIONS	BVRAAM (Meteor)	ASRAAM (AIM-132)	AA-12 ADDER
Missile Speed	Mach 4	Mach 3	Mach 4
Operating Range	100km	50km	80km
Type	Active radar homing	Infrared homing with lock-on after launch	Active radar homing

B. PARAMETERS

We use the following parameters tabulated in Table 7 and Table 8 to perform the calculation in the Phase 1 and Phase 2 models respectively. Noteworthy, we have selected the Erlang distribution with shape parameter $k = 2$ for the BVR engagement time and Counter-firing time of both aircraft. Further discussions pertaining to the selection of these distributions will be covered in Section C.

Table 7 Parameters for the Phase 1 model.

PARAMETERS	BLUE	RED	REMARKS
Rate Parameter of BVR Engagement Time, λ	0.02	0.0125	$X_B \sim Erlang(2,\lambda_B)$ $X_R \sim Erlang(2,\lambda_R)$
Rate Parameter of Counter-fire Time, μ	0.067	0.067	$Y_B \sim Erlang(2,\mu_B)$ $Y_R \sim Erlang(2,\mu_R)$
Single Shot Kill Probability of Aimed shot, p^A	0.9	0.9	Assumed
Single Shot Kill Probability of Un-aimed Shot, p^U	0.75	0.85	Assumed
Aircraft Velocity, u	295.8 m/s	295.1 m/s	Half of maximum speed.
Missile velocity, w	Mach 3 (~1029m/s)	Mach 4 (~1372 m/s)	According to missile technical specifications
Missile Capacity, m	12	6	According to aircraft technical specifications
Initial Distance of Approach, D_a	100 km		Start of Approach
Minimum Distance at the End of Approach, $D_{\min}$	35 km		End of BVR

Table 8 Parameters for the Phase 2 model

PARAMETERS	BLUE	RED	REMARKS
Flight Velocity, V	$V_B \sim Tri(57,296,592)$	$V_R \sim Tri(60,295,590)$	Triangularly distributed with stall speed as the minimum, half of maximum speed as most likely, and top speed as the maximum.
Rate Parameter of Engagement during dogfight, γ	0.03	0.03	$Z_B \sim Exp(\gamma_B)$ $Z_R \sim Exp(\gamma_R)$
Single Shot Kill Probability, p	0.9	0.9	Same as $p_B^A\left(p_R^A\right)$
Probability of Turn Types	$P(NtN)=0.5, P(NtT)=0.5$		Assume equal distribution for both turn types.
Maximum Load Factor, G_{Max}	9	6.5	According to aircraft technical specifications
Target Acquisition Angle, θ	50 degrees	50 degrees	Assumed
Disengagement velocity, $\hat{v}$	592 m/s	590 m/s	Assume as top speed of aircraft
Maximum Engagement Range, d	100	80km	According to missile technical specifications
Initial Separation Distance, D_0	1.5km		Assumed as part of doctrines
Maximum Pursuit Distance, D_{max}	150km		50km beyond the initial approach distance.

C. SELECTION OF DISTRIBUTIONS FOR THE RANDOM VARIABLES

We provide a short elaboration of the distribution selection for the random variables used in this numerical example.

a. BVR Engagement Time and Counter-firing Time—Erlang-2

We select the Erlang distribution with a shape parameter, $k = 2$, and the corresponding rate parameters, λ and μ, for the BVR engagement time and counter-firing time, respectively. The Erlang-2 distribution is selected primarily to accommodate the nature of the approach where the time remaining in the approach decreases monotonously as the phase proceeds.

The Erlang-2 distribution allows us to capture the characteristics of the missile exchange in Phase 1 because the distribution is monotone increasingly in time. This characteristic agrees with the physical characteristics of the missile exchange where the probability for each aircraft to fire increases over the distance that they travel as the Approach phase unfolds. As a result, the memoryless property of the other more commonly used Exponential distribution for inter-firing times in a stochastic duel is not applicable in our model.

b. Flight Velocity—Triangular

We use the Triangular distribution for the flight velocity because of its finite bounds in the support. The use of this distribution allows us to compute the state transition probabilities from direct aircraft specifications.

Based on the nature of the aircraft specifications, we can determine the maximum and minimum speed at which an aircraft may operate during the dogfight. Furthermore, it is possible for analysts and engineers to extract data from flight control systems to determine what is the mode of the distribution—the most likely velocity during a dogfight.

Although other general distributions taking finite, bounded support are also acceptable, we deem that the triangular distribution will suffice for our model computation.

c. Dogfight Engagement Time—Exponential

We use the Exponential distribution for the dogfight engagement time in Phase 2. This, in contrast to the two random variables in Phase 1, is a valid and recommended distribution to characterize the firing rate of a Pursuer during the dogfight.

During a Pursuer-Evader maneuver, the Pursuer must constantly attempt to aim at the Evader while the Evader takes evasive actions. In this case, we assume that the Pursuer's target acquisition system experiences resetting of the aiming sequence during the evasions by the Evader. As such, the memoryless property of the Exponential distribution applies.

D. SOLUTIONS

Solving the probabilistic model analytically for Phase 1 yields the following distribution of the outcomes. With reference to Figure 21, our solution indicates that Blue has a reasonable advantage in Phase 1, with Blue having 31% and Red having 20%. Furthermore, the chances of both being shot down by each other is computed as 25%, and the aggregated probability of transitioning to Phase 2, regardless of the number of missiles fired in Phase 1, is 24%. Noteworthy, 21% corresponds to a transition to Phase 2 with neither side firing.

This probability distribution informs us the comparable performance of both the EF-2000 Eurofighter (Blue) and the Su-30 (Red) in an engagement at beyond-visual-range, with Blue having a relatively higher chance of shooting Red down because of its advantage in BVR engagement time. Specifically, Blue has a mean BVR engagement time of 100 seconds with a standard deviation of 70.71 seconds; Red has a mean BVR engagement time of 160 seconds with a standard deviation of 113.14 seconds. Furthermore, there is a significantly high probability that the duel will transition into Phase 2.

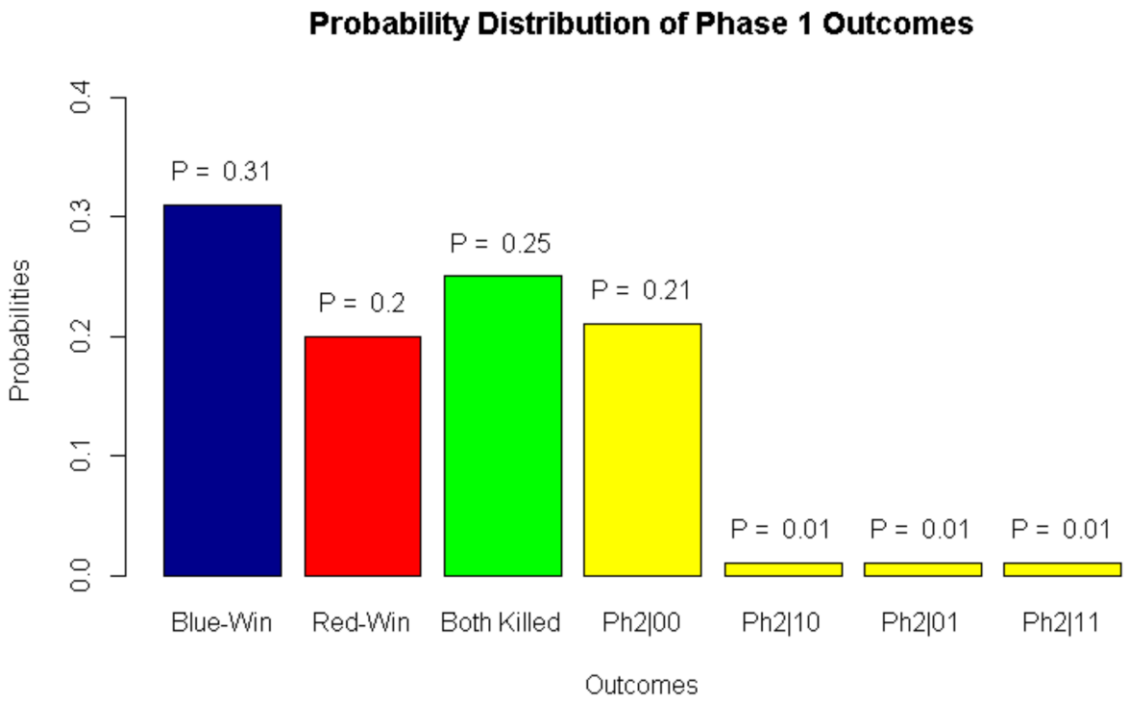

Figure 21 Probability distribution of the outcomes from Phase 1.

Subsequently, by solving the first passage time probabilities of the absorbing states in the Phase 2 model, and extracting the four possible initial conditions, we obtain the specific solutions to Phase 2. As an example, Figure 22 displays the probability distribution of the outcomes from Phase 2 conditioned on starting the dogfight with zero missiles fired on either side in Phase 1. Blue has a 68% chance of winning the dogfight, while Red only has a 31% chance of winning. Noteworthy, there is only a 1% chance that one or both aircraft disengage from the duel.

Based on our computation, we can clearly observe Blue's superiority over Red in a dogfight despite both aircraft having the same dogfight engagement time. The chief reason for the superior performance is due to the loading factor capacity of Blue resulting in a greater potential in its maneuverability.

Interestingly, the two aircraft are unlikely to disengage from the dogfight and the outcomes in this dogfight are not significantly sensitive to the number of missiles fired prior in Phase 1 during the Approach. This is likely due to the higher probability of kill of the missiles, and the relatively large number of missiles on both aircraft to last through

the duration of the dogfight. As such, we can observe that the fully loaded EF-2000 and Su-30 are both likely to have their missile payload last longer than the dogfight itself. In reality, a higher payload will alter the maneuverability of the aircraft because of the additional loading on the wings and pylons. Nonetheless, we gain the insights here that maneuverability is a critical factor to winning the dogfight while there is a need to balance that with the number of missiles on the payload.

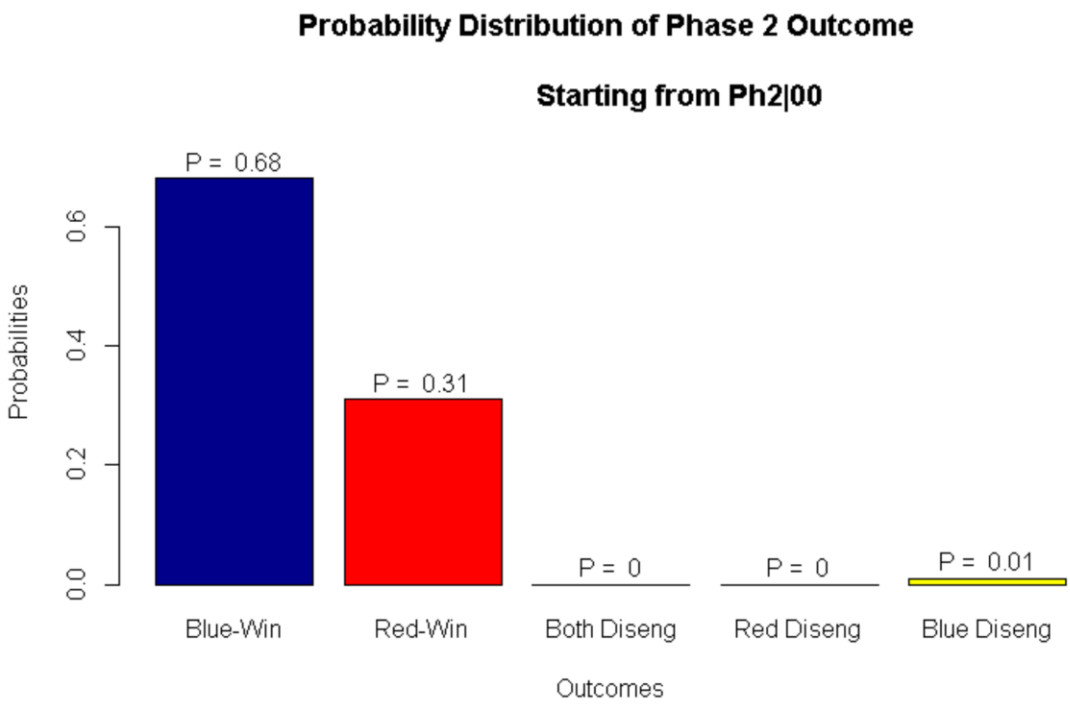

Figure 22 Probability distributions of the Phase 2 outcomes conditioned starting the dogfight with a neither side firing a missile in Phase 1.

Finally, we map the distribution of the Phase 2 solutions to the Phase 1 phase-transition outcomes to obtain the overall assessment of the duel as shown in Figure 23. The results of our computation for this duel indicate that Blue has about 47% chance of winning the duel, Red has approximately 28% chance of winning the duel, while it is possible that both are shot down by each other with a probability of 25%. In addition, the chances of a disengagement of any sort are negligible.

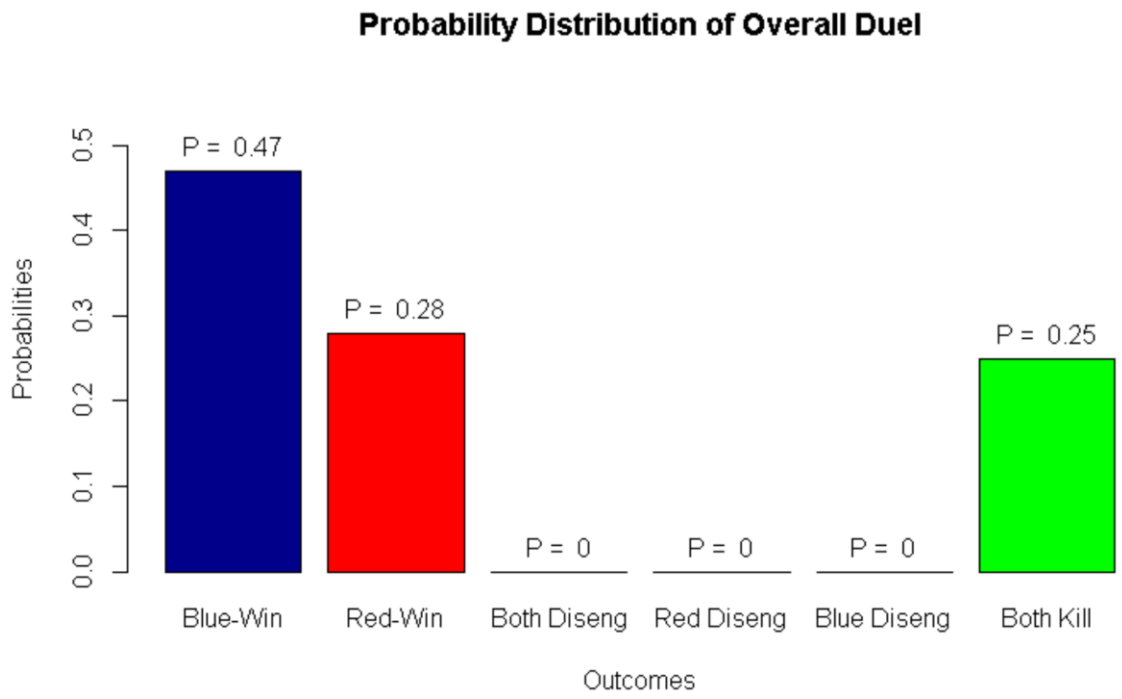

Figure 23 The overall probability distribution of the outcomes from the one-to-one duel. Blue is expected to win the duel with a probability of about 47%, Red has a probability of about 28% to win the duel. There is roughly 25% chance that both aircraft will shoot each other down, while it is unlikely that this duel will result in a disengagement of either of both sides.

We can make further observations and recommendations using our results. First, based on the performance of the EF-2000 (Blue) and the types of missiles it is likely to use, and those characteristics of the Su-30 (Red), we observe that both aircraft have comparable performance in the BVR engagement during Phase 1, with Blue having a reasonable advantage over Red. However, if both aircraft survive the first phase of approaching each other, the EF-2000 (Blue) is likely to out-maneuver the Su-30 (Red) in a close-range dogfight.

Second, with the assessment that the EF-2000 (Blue) will likely out-perform against its opponent in a close-range dogfight, it is important to focus any further enhancement to the aircraft on its survivability against the BVR Engagement in Phase 1.

In short, as long as the EF-2000 (Blue) can survive Phase 1, it is likely to dominate the Su-30 in a dogfight.

E. SENSITIVITY ANALYSIS USING DESIGN OF EXPERIMENT METHODS

1. Methodology

To perform our sensitivity analysis, we use a design of experiment (DOE) method to construct a meta-model of our analytical model. In specific, we use the Nearly-Orthogonal Latin Hypercube (NOLH) to generate a design matrix, and a multi-variate Least Square regression to construct the meta-models (Sanchez et al. 2014). Furthermore, the Bayesian Information Criterion (BIC) forward selection is used to perform the model selection for the least square regression.

The NOLH is one of the DOE methods for design point sampling that is characterized by its space-filling property. The space-filling property of the NOLH sampling method allows us to capture higher order interactions and relationships among the parameters within the sampling space, without having to enumerate an extensive run of computations (Law 2015). After the outputs from the NOLH sampling are obtained, we fit a multi-variate least square model considering all individual variables, two-way interactions, and 2nd order polynomial transformations of the terms.

Our current model requires a total of 31 parameters to compute the solutions; of which 13 are specific to each aircraft and five are global conditions. Our primary interest is to understand how one aircraft may perform against another; therefore, we perform the sensitivity analysis by fixing four global conditions, all 13 of the Red aircraft, and one belonging to the Blue aircraft. Specifically, the disengagement velocity of the Blue aircraft is fixed as a constant assuming that it will always execute the disengagement at its top speed. The four global conditions fixed as constants are, namely 1) initial distance of approach, 2) minimum distance until approach ends, 3) initial separation distance during the onset of a disengagement, 4) maximum pursuit distance. This construct will require us to perform the sensitivity analysis using 12 of Blue's parameters and one global parameter—the probability of turn type –, thus resulting in a total of 13 variables.

According to Sanchez et.al (2014) and Law (2015), the main benefit of such space-filling designs is the ability to capture higher order behaviors in the explanatory variables while demanding a much lower number of sampling (or runs). A simplistic sensitivity analysis using the 2^k factorial design (Sanchez et al. 2014) by varying every parameter by two levels will require up to 2^{13} runs to completely map out the response surface of our analytical model just to account for all the individual factors. Despite a large number of runs, the resulting response surface is only limited to 2-level, linear relationships between the response and the variables. This may result in the loss of meaningful higher-order interactions and relationships, which is the main limitation of using such designs.

2. Parameters, and Range of Values

We use a total of 13 parameters relating to the performance of the Blue aircraft and the probability of turn types to perform the sensitivity analysis against a fixed opponent and tactical situation. The 13 parameters and their range of values appear in Table 9 .

Noteworthy, we assume that the stall and maximum speed in the flight velocity's distribution are fixed; we use only the most likely flight velocity—mode of the flight velocity's triangular distribution—in this sensitivity analysis. This will reveal how the performance of the Blue aircraft may improve depending on probability the pilot can execute a turning maneuver at a favorable velocity, thus informing us about potential improvements in the flight controls and pilot's skills.

Table 9 Parameters and their range of values used for the sensitivity analysis.

S/N	PARAMETERS	LOWER BOUND	UPPER BOUND	REMARKS
1	Rate Parameter of BVR Engagement, λ_B	0.01	0.0154	130 - 200 sec
2	Rate Parameter of Counter-fire, μ_B	0.03	0.1	20—60 sec
3	Single Shot Kill Probability of Aimed shot, p_B^A	0.5	0.95	-
4	Single Shot Kill Probability Penalty, c_p [a]	0.5	0.95	-
5	Aircraft velocity, u_B	57 m/s	590 m/s	Stall to max speed
6	Missile velocity, w_B	1029 m/s	1715 m/s	Mach 3—5
7	Missile Capacity, m_B	6	15	Half capacity to 25% increase.
8	Likely Flight Velocity, v_B^f	57 m/s	590 m/s	Within current speed range.
9	Rate of Engagement during Dogfight, γ_B	0.02	0.067	30—90 sec
10	Probability of Nose-to-Nose Turn, $P(NtN)$	0.1	0.9	-
11	Maximum Load Factor, $G_{Max,B}$	6	10	-
12	Target Acquisition Angle, θ_B	40 degrees	70 degrees	-
13	Maximum Engagement Range, d_B	80 km	120 km	-

[a] Note: The Single Shot Kill Probability of an Un-aimed Shot is expressed as a function of the penalty coefficient and the kill probability of an aimed shot for the sensitivity analysis to satisfy $p^U \leq p^A$. Formally, $p^U = c_p \cdot p^A$

3. Nearly-Orthogonal Design Matrix

To satisfy the condition of near-orthogonality in the design matrix, according to Helcio et al. (2011), the maximum absolute pairwise correlation between any two factors needs to be $0 < \rho_{map} \leq 0.05$. By ensuring orthogonality, or near-orthogonality, we

minimize the drift-over effects on one subspace of the responses due to the perturbation of another adjacent subspace.

With the current set of parameters, we identify two of the parameters to be discrete, while the remaining eleven are continuous parameters. The base design has $\rho_{map} = 0.0891$ (Refer to Appendix B for the detailed properties of the base design matrix), thus not satisfying the condition for near-orthogonality.

To resolve this, we treat the design matrix by rotation and stacking of the design points, thus further expanding the number of design point combinations. As a result, our final design matrix has a total of 257 sets of design points with $\rho_{map} = 0.0433$, satisfying the condition for near-orthogonality in our design space. In addition, because of the rotation and stacking, we also enhance the space-filling property of the design matrix. This is as shown in Appendix B.

4. Key Insights from the Phase 1 Meta-Models

A total of seven meta-models, each corresponding to an outcome in Phase 1, is explored. However, we present here the key insights pertaining to our model by focusing on the Blue-Win and Red-Win meta-models which provide the most information about how Blue's parameter may be improved to win or deny Red to win, in Phase 1.

The Blue-Win meta-model provides us further insights in the model from an offensive point of view. With the design matrix sampled within the Blue aircraft's parameters, the Blue-Win meta-model shows how varying these parameters will increase the probability of Blue winning in Phase 1. On the other hand, the Red-Win meta-model provides us insights from a defensive point of view. This is because we are determining how Red's winning probability may change by changing Blue's parameters, and is valuable to the analysts in understanding how improving certain performance may deny Blue's opponent from winning in Phase 1.

For each meta-model, we also examine the two-way interactions of the parameters that are statistically significant from our model selection. These two-way interactions provide further useful information regarding how the change in one parameter may affect

the behavior of another. While all two-way interactions are considered, we make further recommendations in this chapter based on those that have tactical significance to our operational scenario.

a. Blue Win ϕ_B Meta-Model

We found all six parameters used in Phase 1 to be statistically significant in influencing the probability of Blue winning in Phase 1. Among the six, we observe three parameters to be most prominent, namely 1) the BVR engagement rate parameter, 2) the single shot kill probability, and 3) the aircraft velocity during the approach. Furthermore, we find that the parameters exhibit a linear relationship with respect to the probability of Blue winning in Phase 1. Figure 24 shows the graphical response surface of the ϕ_B meta-model.

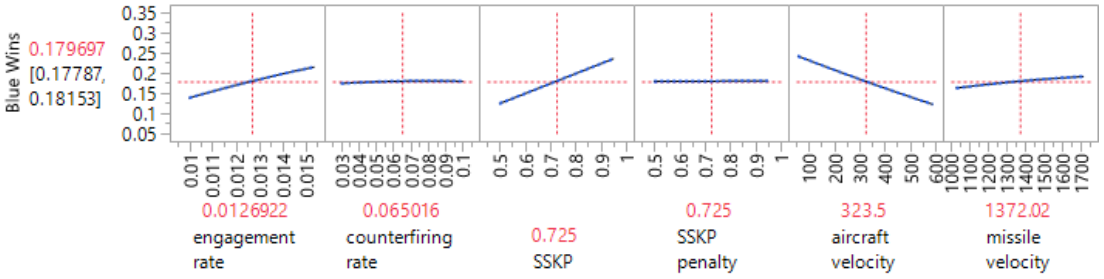

Figure 24 Meta-model for the probability of Blue win in Phase 1. All six Phase 1 parameters are statistically significant to the meta-model, among which, the BVR engagement rate parameter, SSKP, and aircraft velocity during Approach are the most influential.

Further analyses of the meta-model reveal six two-way interactions that are statistically significant. By inspecting the interaction plots, we find three interesting interactions that serve to inform us how the Blue aircraft may be improved to increase its chances of winning in Phase 1. These interactions are highlighted in Figure 25 with red boxes. The interpretations of these three interactions are as follows:

1. **BVR Engagement Rate Parameter and SSKP**. The effects of BVR engagement rate parameter on the probability of Blue winning in Phase 1 increase sharper when the SSKP is at a higher level. This implies that a

Blue aircraft equipped with an advanced missile system with high SSKP will experience a higher rate of increase in the probability of winning the duel in Phase 1 with each increase in its BVR engagement rate parameter. This interaction exemplifies the need to consider both the missile performance and its BVR engagement capabilities in parallel.

2. **BVR Engagement Rate Parameter and Missile Velocity**. A higher missile velocity increases the effects of BVR engagement rate parameter on the probability of Blue winning in Phase 1. This implies that if a Blue aircraft's missile is designed to perform at a higher Mach number, it is likely to dominate the duel in Phase 1 as its BVR engagement rate parameter increases. If the Blue aircraft's missile is of a lower Mach number design, the effects of the BVR engagement rate parameter will be undermined. This, again, illustrates how the missile performance and BVR engagement rate parameter must be considered in parallel.

3. **SSKP and Aircraft Velocity**. This interaction shows that a Blue aircraft flying at a lower speed will increase the effects of an increasing SSKP on the probability of Blue winning in Phase 1. We believe that this interaction is confounded with the BVR engagement rate parameter as well. We interpret this interaction that a Blue aircraft flying at a lower speed will have a higher chance of firing its missile before the phase ends, thus accentuating the effects of SSKP in this case.

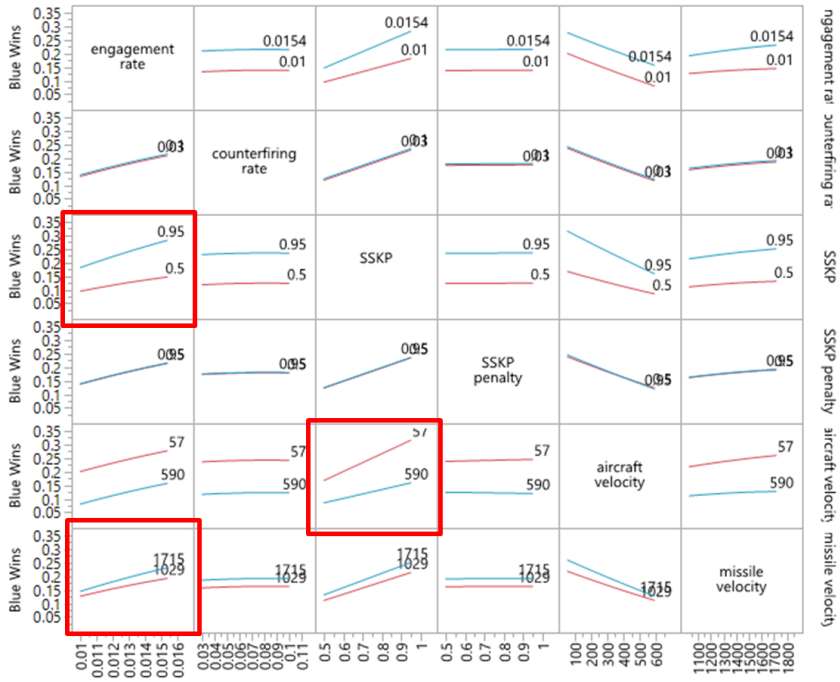

Figure 25 Interaction plots for the ϕ_B meta-model. The three influential interactions are highlighted in the red boxes. These are the interactions between the BVR engagement rate and SSKP, the BVR engagement rate and the missile velocity, and the SSKP and the aircraft velocity during Approach.

b. Red Win ϕ_R Meta-Model

From the ϕ_R meta-model, we gain insights from the defensive point of view for the Blue aircraft. The meta-model reveals how improving certain parameters of the Blue aircraft will also diminish Red's offensive capabilities to win the duel in Phase 1.

Five parameters are found to be statistically significant in this case. The missile velocity of Blue aircraft is deemed to be ineffective in influencing the chances that Red can win in Phase 1. Among the five significant parameters, the SSKP and Blue's aircraft velocity are the most influential. This is evident as shown in Figure 26 where the effects of increasing both the SSKP and aircraft velocity will drastically decrease the probability of Red winning the duel in Phase 1.

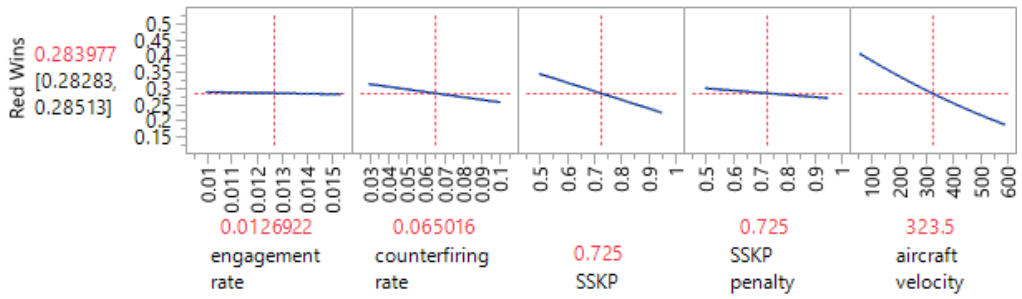

Figure 26 Meta-model for the probability of red win in Phase 1. Five parameters are statistically significant, of which, the SSKP and aircraft velocity are more influential in diminishing Red's probability of a win in Phase 1.

We find eight interactions between the five parameters to be statistically significant. Among the eight interactions, three of them highlighted in Figure 27 provide insights into the tactical significance of the Phase 1 duel. These three influential interactions are elaborated as follows:

1. **BVR Engagement Rate Parameter and SSKP**. We see an inverse relationship in the interaction between the BVR engagement rate parameter and the SSKP. With a low SSKP, Red's winning probability increases slightly with an increase in Blue's engagement rate. In contrast, with a high SSKP, Red's winning probability decreases with an increase in Blue's engagement rate parameter. This is a unique and counter-intuitive insight because it shows that Blue may create an opportunity for Red to shoot it down through counter-firing if Blue's SSKP is low and its engagement rate is high. It highlights the important interaction between shooting fast and shooting accurately, otherwise, the side initiating a shot is placed in a disadvantageous position.

2. **Counter-firing Rate Parameter and Aircraft Velocity**. We observe a difference in the rate of decrease in Red's probability of win with an increasing counter-firing rate parameter, with the aircraft velocity set at a different level. When Blue is flying at its maximum speed, Red's probability of win appeared indifferent to an increase in Blue's counter-firing rate parameter. However, with a low-speed approach by Blue, Red's probability of win decreases more significantly when an increasing Blue counter-firing rate parameter. This shows the value of Blue having the capability to fire back fast at Red if Red is the side which fires first.

3. **SSKP and Aircraft Velocity**. We observe the same interactive effects as per the Blue-Win meta-model. With a low-speed approach, Red's probability of win decreases drastically with an increase in Blue's SSKP.

On the other hand, Red's winning probability appears to be indifferent to the increase in Blue's SSKP when Blue is flying at its top speed. These behaviors are interacted with the BVR engagement rate parameter; when Blue is flying slower, yet shooting faster at BVR, it accentuates the effects of having a high SSKP of the missile.

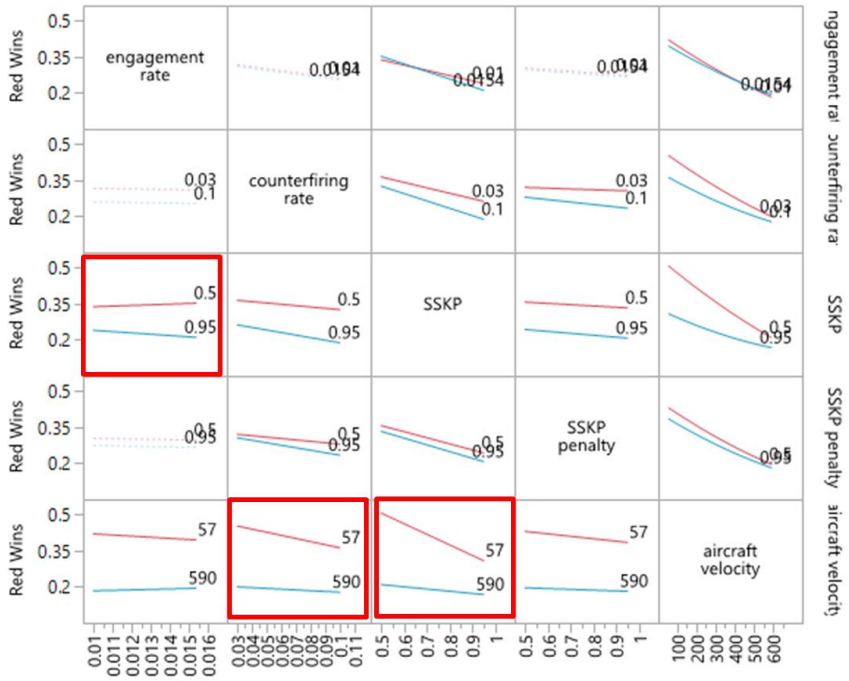

Figure 27 Interaction plots for the ϕ_R meta-model. The three influential interactions are highlighted in the red boxes. These are the interactions between the BVR engagement rate parameter and SSKP, the counter-firing rate parameter and the aircraft velocity, and the SSKP and the aircraft velocity.

5. Key Insights from the Overall Duel Meta-Models

For the overall duel, the Blue-Win and Red-Win meta-models are the most informative. As per the Phase 1 meta-models, these two models for the overall duel informs us of the characteristics of the model response from both the offensive and defensive point of view for the Blue aircraft.

The key difference between the overall meta-model and the Phase 1 meta-model is that only the response surfaces are of operational significance to our scenario. Because

of the structure of our two-phase model, the interactions among the parameters do not provide any critical insights.

a. Blue-Win Γ_1 Meta-Model

We find a total of seven parameters that are statistically significant in affecting Blue's probability of winning the whole duel. Specifically, four parameters are influential in changing Blue's winning probability while the other three provide insights that can put Blue's at an advantageous position. The four influential parameters are the SSKP, aircraft velocity, flight velocity, and maximum load factor. Figure 28 is the meta-model comprising the seven parameters.

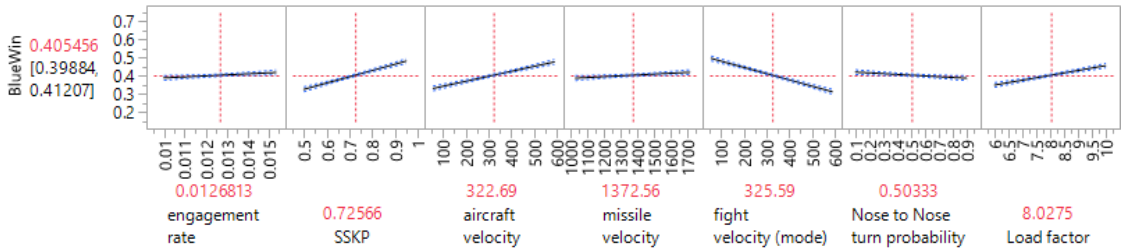

Figure 28 Blue-win meta-model for the overall duel. Seven parameters are statistically significant to the meta-model, among which, the SSKP, aircraft velocity, flight velocity, and maximum load factor are the most influential. The BVR engagement rate parameter, missile velocity, and turn-type probabilities provides further information on how Blue may be improved to have a greater advantage over Red.

Tactically, we find that the SSKP of the missile and the aircraft speed during the approach to play influential roles in increasing Blue's winning probability in the overall duel. This, however, does not undermine the importance of having higher rate of firing at BVR—as evident in the Phase 1 meta-model for Blue-Win—but, instead, informs us that the ability of Blue to win by shooting first is depends on its missile's kill probability and the speed at which it flies.

On the other hand, the flight velocity and maximum load factor inform us how critical flight control and aircraft structural design can drastically change Blue's probability of a win. Furthermore, we highlight the absence of the dogfight engagement

rate in the meta-model. This is counterintuitive, yet, represents a significant operational characteristic of the dogfight; the ability to out-maneuver one's opponent and sustain a Pursuer's role clearly stands out as a critical performance factor than to be able to simply shoot faster.

b. Red-Win Γ_2 Meta-Model

We find seven parameters that are statistically significant in the Red-Win meta-model. Three of these parameters appear to be most influential in denying Red' winning probability for the overall duel; these are the SSKP, flight velocity, and the maximum load factor of Blue aircraft. Figure 29 is the Red-Win meta-model.

Figure 29 Red-win meta-model for the overall duel. Seven parameters are statistically significant to the meta-model, among which, the SSKP, flight velocity, and maximum load factor of the Blue aircraft are the most influential in affecting Red's probability of a win. The BVR engagement rate parameter, counter-firing rate parameter, SSKP penalty, and the aircraft velocity provide information on how Red's performance may be further deterred by improving Blue's performance.

Tactically, the Blue's SSKP can deny Red's probability of win; this is applicable to both Phase 1 and Phase 2. Furthermore, the characteristics we see in the flight velocity and maximum load factor of Blue agree with the insights we gain from the Blue-Win meta-model, where by improving these aspects of the Blue aircraft not only increases Blue's winning probability but also reduces Red's winning probability.

THIS PAGE INTENTIONALLY LEFT BLANK

VI. CONCLUSIONS AND FUTURE WORK

Our work illustrates how a one-on-one duel between two fighter aircraft can be modeled using a variant of stochastic duels that incorporates kinematics and flight theories. This approach allows us to directly relate the physical characteristics of the aircraft to their mission-level performance; thus departing from the use of low-fidelity parameters that are difficult to obtain in real-life. Furthermore, our model remains analytically tractable while maintaining the fidelity of the model to actual air combats. Our model provides air combat analysts and decision-makers an avenue to obtain first-order evaluations of fighter aircraft performance to reinforce their focal areas for larger-scale, higher-order evaluations.

Our model comprises two parts, namely 1) a probability model for the missile exchange during an approach between two aircraft, 2) a Discrete-Time Markov Chain model for the close-range dogfight. The first part of the model focuses on the missile exchange between the two aircraft at the beyond-visual range, with the kinematics of the aircraft and missiles in-flight modeled explicitly to improve the model's fidelity. The second part of the model concentrates on solving the dynamics of a dogfight using a Markov Chain augmented with flight theory, where the two aircraft are engaged in complex air combat maneuvers with the goal of shooting their opponent down.

We applied our model to a numerical example featuring two actual, dissimilar aircraft and perform a sensitivity analysis using smart experimental design methods. Our analysis reveals that in Phase 1 the BVR engagement rate parameter, SSKP of the aircraft's missile, and the aircraft's velocity have significant effects in influencing the probability of win of an aircraft. Furthermore, we find that increasing the SSKP and velocity of an aircraft may also diminish the win probability of the opponent. For the overall duel, we discover that the SSKP, aircraft velocity in Phase 1, flight velocity in Phase 2, and the maximum load factor of the aircraft to be most influential to the win probability of one side. In addition, by analyzing the effects on the opponent, we find the same four parameters to be influential in diminishing the win probability of the opponent.

Tactical assessments and evaluations are not limited to only one-on-one duels. Therefore, we propose two major areas of future research using similar approaches for force-level evaluations of air combats. These are 1) many-on-many air combat evaluations using stochastic duels and 2) air-to-ground mission evaluation using stochastic duels.

1. Many-on-Many Air Combat Evaluation Using Stochastic Duels

We propose an extension of our modeling approach to develop a many-on-many air combat stochastic duel. We highlight that this area of future research should be scoped to a moderate number of participants on both sides in each air combat scenario to enable the use of engineering-level specifications to compute mission-level performance.

A similar two-phase approach may also be adopted for this case. Phase 1 may feature a two-sided missile exchange with the distinction of coordinated and uncoordinated fires for the side initiating missile fires and the side firing back, respectively. This scenario may be developed using a binomial, combinatoric formulation to determine the number of kills on each side depending on their type of firing. We emphasize the need to model the velocities of the missiles with respect to the velocities of the aircraft to ensure sufficient fidelity in this model.

Phase 2's tactical maneuvers involving two or more aircraft could potentially be approximated using a slightly more complex version of the kinematic formulations. A good starting point will consider the key maneuvers in a two-on-one duel, followed by a two-on-two duel since a many-on-many air duel is made up of multiple individual duels.

2. Air-To-Ground Mission Evaluation Using Stochastic Duels

This recommendation extends beyond a pure air-to-air combat by considering the interactions of bombers against ground targets or opponents. A similar construct as the Phase 1 model is a potential approach, except that one side of the duel comprises static targets on the ground. Both Air-to-Surface and Surface-to-Air missiles may be used to model the missile exchange between the two sides. A model in this scenario will be

useful to the naval aviation community as the ground unit in the model can easily be adapted and extended to surface warships.

Researches in this area should consider the potential use of kinematic approximation in the stochastic duel to determine the probability of an aircraft evading a Surface-to-Air missile by maneuvering itself defensively, thus enhancing the fidelity of the air-to-ground model.

THIS PAGE INTENTIONALLY LEFT BLANK

APPENDIX A. DETAILED SOLUTIONS FOR THE EVENTS IN PHASE 1

A. BLUE SHOT DOWN WITH RED SURVIVING

$$\phi_R = \left[\begin{array}{l} \underbrace{\Pr\{X_R < \min(X_B, T_a) \cap Y_B > \tau_R(X_R)\} p_R^A}_{\text{Red fires first and Blue does not fire back. Red hits}} + \underbrace{\Pr\{X_R < \min(X_B, T_a) \cap Y_B < \tau_R(X_R)\} p_R^A \overline{p_B^U}}_{\text{Red fires first and Blue fires back before the missile terminates Red hits and Blue misses.}} \\ + \underbrace{\Pr\{X_B < min(X_R, T_a) \cap Y_R < \tau_B(X_B)\} \overline{p_B^A} p_R^U}_{\text{Blue fires first and Red fires back before the missile terminates. Blue misses and Red hits.}} \\ + \underbrace{\Pr\{X_B < \min(X_R, T_a) \cap \tau_B(X_B) < Y_R < T_a - X_B\} \overline{p_B^A} p_R^A}_{\text{Blue fires first and Red fires back after the missile terminates. Blue misses and Red hits.}} \end{array} \right]$$

$$\underbrace{\Pr\{X_R < \min(X_B, T_a) \cap Y_B > \tau_R(X_R)\} p_R^A}_{\text{Red fires first and Blue does not fire back. Red hits.}}$$

$$= p_R^A \left[\int_0^{T_a} \int_0^{x_B} \overline{F}_{Y_B}(\tau_R(X_R)) f_{X_R}(x_R) f_{X_B}(x_B) dx_R dx_B + \int_{T_a}^{\infty} \int_0^{T_a} \overline{F}_{Y_B}(\tau_R(X_R)) f_{X_R}(x_R) f_{X_B}(x_B) dx_R dx_B \right]$$

$$\underbrace{\Pr\{X_R < \min(X_B, T_a) \cap Y_B < \tau_R(X_R)\} p_R^A \overline{p}_B^U}_{\text{Red fires first and Blue fires back before missile termiantes. Red hits and Blue misses.}}$$

$$= p_R^A \overline{p}_B^U \left[\int_0^{T_a} \int_0^{x_B} F_{Y_B}(\tau_R(X_R)) f_{X_R}(x_R) f_{X_B}(x_B) dx_R dx_B + \int_{T_a}^{\infty} \int_0^{T_a} F_{Y_B}(\tau_R(X_R)) f_{X_R}(x_R) f_{X_B}(x_B) dx_R dx_B \right]$$

$$\underbrace{\Pr\{X_B < \min(X_R, T_a) \cap Y_R < \tau_B(X_B)\} \overline{p}_B^A p_R^U}_{\text{Blue fires first and Red fires back before missile terminates Blue misses and Red hits.}}$$

$$= \overline{p}_B^A p_R^U \left[\int_0^{T_a} \int_0^{x_R} F_{Y_R}(\tau_B(X_B)) f_{X_B}(x_B) f_{X_R}(x_R) dx_B dx_R + \int_{T_a}^{\infty} \int_0^{T_a} F_{Y_R}(\tau_B(X_B)) f_{X_B}(x_B) f_{X_R}(x_R) dx_B dx_R \right]$$

$$\underbrace{\Pr\{X_B < \min(X_R, T_a) \cap \tau_B(X_B) < Y_R < T_a - X_B\}\bar{p}_B^A p_R^A}_{\substack{\text{Blue fires first and Red fires back after missile terminates} \\ \text{Blue misses and Red hits.}}}$$

$$= \bar{p}_B^A p_R^A \left[\begin{array}{l} \int_0^{T_a}\int_0^{x_R} \left(F_{Y_R}(T_a - X_B) - F_{Y_R}(\tau_B(X_B))\right) f_{X_B}(x_B) f_{X_R}(x_R) dx_B dx_R \\ + \int_{T_a}^{\infty}\int_0^{T_a} \left(F_{Y_R}(T_a - X_B) - F_{Y_R}(\tau_B(X_B))\right) f_{X_B}(x_B) f_{X_R}(x_R) dx_B dx_R \end{array} \right]$$

B. BOTH AIRCRAFT SHOT DOWN

$$\phi_K = \underbrace{\Pr\{X_B < min(X_R, T_a) \cap Y_R < \tau_B(X_B)\} p_B^A p_R^U}_{\substack{\text{Blue fires first and Red fires back before the missile terminates.} \\ \text{Both hits.}}} + \underbrace{\Pr\{X_R < \min(X_B, T_a) \cap Y_B < \tau_R(X_R)\} p_R^A p_B^U}_{\substack{\text{Red fires first and Blue fires back before the missile terminates} \\ \text{Both hits.}}}$$

$$\underbrace{\Pr\{X_B < \min(X_R, T_a) \cap Y_R < \tau_B(X_B)\} p_B^A p_R^U}_{\substack{\text{Blue fires first and Red fires back before missile terminates} \\ \text{Both hits.}}}$$

$$= p_B^A p_R^U \left[\int_0^{T_a}\int_0^{x_R} F_{Y_R}(\tau_B(X_B)) f_{X_B}(x_B) f_{X_R}(x_R) dx_B dx_R + \int_{T_a}^{\infty}\int_0^{T_a} F_{Y_R}(\tau_B(X_B)) f_{X_B}(x_B) f_{X_R}(x_R) dx_B dx_R \right]$$

$$\underbrace{\Pr\{X_R < \min(X_B, T_a) \cap Y_B < \tau_R(X_R)\} p_R^A p_B^U}_{\substack{\text{Red fires first and Blue fires back before missile termiantes.} \\ \text{Red hits and Blue misses.}}}$$

$$= p_R^A p_B^U \left[\int_0^{T_a}\int_0^{x_B} F_{Y_B}(\tau_R(X_R)) f_{X_R}(x_R) f_{X_B}(x_B) dx_R dx_B + \int_{T_a}^{\infty}\int_0^{T_a} F_{Y_B}(\tau_R(X_R)) f_{X_R}(x_R) f_{X_B}(x_B) dx_R dx_B \right]$$

C. BOTH AIRCRAFT SURVIVE WITH NO FIRING BY EITHER SIDE

$$\phi_{00} = \Pr\{T_a < \min(X_B, X_R)\} = \int_0^{\infty}\int_0^{\infty} f_{X_B}(x_B) f_{X_R}(x_R) dx_B dx_R \overset{\text{indp}}{=} \bar{F}_{X_B}(x_B)\bar{F}_{X_R}(x_R)$$

D. BOTH AIRCRAFT SURVIVE WITH ONLY ONE SIDE FIRING

$$\phi_{10} = \underbrace{\Pr\left\{X_B < \min(X_R, T_a) \cap Y_R > \max\left(\tau_B(X_B), T_a - X_B\right)\right\} \bar{p}_B^A}_{\substack{\text{Blue fires first and Red does not fire back} \\ \text{Blue misses.}}}$$

$$= \bar{p}_B^A \left[\begin{array}{l} \int_0^{T_a} \int_0^{x_R} \bar{F}_{Y_R}\left(\max\left(\tau_B(X_B), T_a - X_B\right)\right) f_{X_B}(x_B)\, f_{X_R}(x_R)\, dx_B dx_R \\ + \int_{T_a}^{\infty} \int_0^{T_a} \bar{F}_{Y_R}\left(\max\left(\tau_B(X_B), T_a - X_B\right)\right) f_{X_B}(x_B)\, f_{X_R}(x_R)\, dx_B dx_R \end{array} \right]$$

$$\phi_{01} = \underbrace{\Pr\left\{X_R < \min(X_B, T_a) \cap Y_B > \max\left(\tau_R(X_R), T_a - X_R\right)\right\} \overline{p_R^A}}_{\substack{\text{Red fires first and Blue does not fire back} \\ \text{Red misses.}}}$$

$$= \overline{p_R^A} \left[\begin{array}{l} \int_0^{T_a} \int_0^{x_B} \bar{F}_{Y_B}\left(\max\left(\tau_R(X_R), T_a - X_R\right)\right) f_{X_R}(x_R)\, f_{X_B}(x_B)\, dx_R dx_B \\ + \int_{T_a}^{\infty} \int_0^{T_a} \bar{F}_{Y_B}\left(\max\left(\tau_R(X_R), T_a - X_R\right)\right) f_{X_R}(x_R)\, f_{X_B}(x_B)\, dx_R dx_B \end{array} \right]$$

E. BOTH AIRCRAFT SURVIVE WITH BOTH FIRING ONE MISSILE EACH

$$\phi_{11} = \left[\begin{array}{l} \overbrace{\Pr\{X_B < min(X_R, T_a) \cap Y_R < \max(\tau_B(X_B), T_a - X_B)\} \bar{p}_B^A \bar{p}_R^U}^{\text{Blue fires first and Red fires back before missile terminates or approach ends. Both misses}} \\ \underbrace{+\Pr\{X_R < min(X_B, T_a) \cap Y_B < \max(\tau_R(X_R), T_a - X_R)\} \bar{p}_R^A \bar{p}_B^U}_{\text{Red fires first and Blue fires back before missile terminates or approach ends. Both misses}} \end{array} \right]$$

$$\underbrace{\Pr\left\{X_B < \min(X_R, T_a) \cap Y_R < \max\left(\tau_B(X_B), T_a - X_B\right)\right\} \bar{p}_B^A \bar{p}_R^U}_{\substack{\text{Blue fires first and Red fires back before missile terminates or approach ends} \\ \text{Both miss.}}}$$

$$= \bar{p}_B^A \bar{p}_R^U \left[\begin{array}{l} \int_0^{T_a} \int_0^{x_R} F_{Y_R}\left(\max\left(\tau_B(X_B), T_a - X_B\right)\right) f_{X_B}(x_B)\, f_{X_R}(x_R)\, dx_B dx_R \\ + \int_{T_a}^{\infty} \int_0^{T_a} F_{Y_R}\left(\max\left(\tau_B(X_B), T_a - X_B\right)\right) f_{X_B}(x_B)\, f_{X_R}(x_R)\, dx_B dx_R \end{array} \right]$$

$$\underbrace{\Pr\left\{X_R < \min(X_B, T_a) \cap Y_B < \max\left(\tau_R(X_R), T_a - X_R\right)\right\} \bar{p}_B^A \bar{p}_B^U}_{\substack{\text{Red fires first and Blue fires back before missile terminates or approach ends} \\ \text{Both misses.}}}$$

$$= \bar{p}_B^A \bar{p}_B^U \left[\begin{array}{l} \int_0^{T_a} \int_0^{x_B} F_{Y_B}\left(\max\left(\tau_R(X_R), T_a - X_R\right)\right) f_{X_R}(x_R) f_{X_B}(x_B) dx_R dx_B \\ + \int_{T_a}^{\infty} \int_0^{T_a} F_{Y_B}\left(\max\left(\tau_R(X_R), T_a - X_R\right)\right) f_{X_R}(x_R) f_{X_B}(x_B) dx_R dx_B \end{array} \right]$$

APPENDIX B. DESIGN MATRICES FOR SENSITIVITY ANALYSIS

A. PROPERTIES OF BASE DESIGN MATRIX

The base design matrix of the 65-level NOLH yielded a maximum absolute pairwise correlation of 0.0891. The pairwise correlation value is highlighted in Figure 30. This violates the requirement for near orthogonality and needs to be further treated. However, we see that the space-filling property of the base design matrix is sufficiently satisfied as shown in Figure 31.

	engagement rate	counterfiring rate	SSKP	SSKP penalty	aircraft velocity	missile velocity	payload capacity	fi
engagement rate	1.0000	0.0013	0.0001	-0.0005	0.0005	-0.0004	0.0550	
counterfiring rate	0.0013	1.0000	-0.0013	0.0019	0.0021	0.0080	-0.0352	
SSKP	0.0001	-0.0013	1.0000	-0.0000	-0.0001	0.0120	-0.0195	
SSKP penalty	-0.0005	0.0019	-0.0000	1.0000	0.0001	-0.0037	0.0229	
aircraft velocity	0.0005	0.0021	-0.0001	0.0001	1.0000	-0.0018	0.0032	
missile velocity	-0.0004	0.0080	0.0120	-0.0037	-0.0018	1.0000	-0.0240	
payload capacity	0.0550	-0.0352	-0.0195	0.0229	0.0032	-0.0240	1.0000	
fight velocity (mode)	-0.0094	0.0073	-0.0059	0.0049	0.0034	0.0017	-0.0141	
dogfight engagement rate	-0.0072	-0.0142	0.0049	0.0031	-0.0015	-0.0006	0.0032	
Nose to Nose turn probability	-0.0010	-0.0121	0.0015	0.0050	-0.0062	-0.0024	0.0131	
load factor	0.0502	0.0139	-0.0085	0.0078	-0.0330	-0.0155	-0.0891	
target angle	-0.0019	0.0130	-0.0049	0.0080	-0.0025	-0.0228	0.0030	
weapon max range	0.0001	0.0042	0.0002	-0.0008	0.0001	0.0039	0.0155	

	ght velocity (mode)	dogfight engagement rate	Nose to Nose turn probability	load factor	target angle	weapon max range
engagement rate	-0.0094	-0.0072	-0.0010	0.0502	-0.0019	0.0001
counterfiring rate	0.0073	-0.0142	-0.0121	0.0139	0.0130	0.0042
SSKP	-0.0059	0.0049	0.0015	-0.0085	-0.0049	0.0002
SSKP penalty	0.0049	0.0031	0.0050	0.0078	0.0080	-0.0008
aircraft velocity	0.0034	-0.0015	-0.0062	-0.0330	-0.0025	0.0001
missile velocity	0.0017	-0.0006	-0.0024	-0.0155	-0.0228	0.0039
payload capacity	-0.0141	0.0032	0.0131	-0.0891	0.0030	0.0155
fight velocity (mode)	1.0000	-0.0013	0.0154	-0.0006	-0.0056	0.0067
dogfight engagement rate	-0.0013	1.0000	0.0147	0.0117	-0.0047	-0.0187
Nose to Nose turn probability	0.0154	0.0147	1.0000	-0.0551	0.0030	0.0017
load factor	-0.0006	0.0117	-0.0551	1.0000	-0.0506	0.0172
target angle	-0.0056	-0.0047	0.0030	-0.0506	1.0000	-0.0203
weapon max range	0.0067	-0.0187	0.0017	0.0172	-0.0203	1.0000

Figure 30 Correlation table of the design points in the base design matrix.

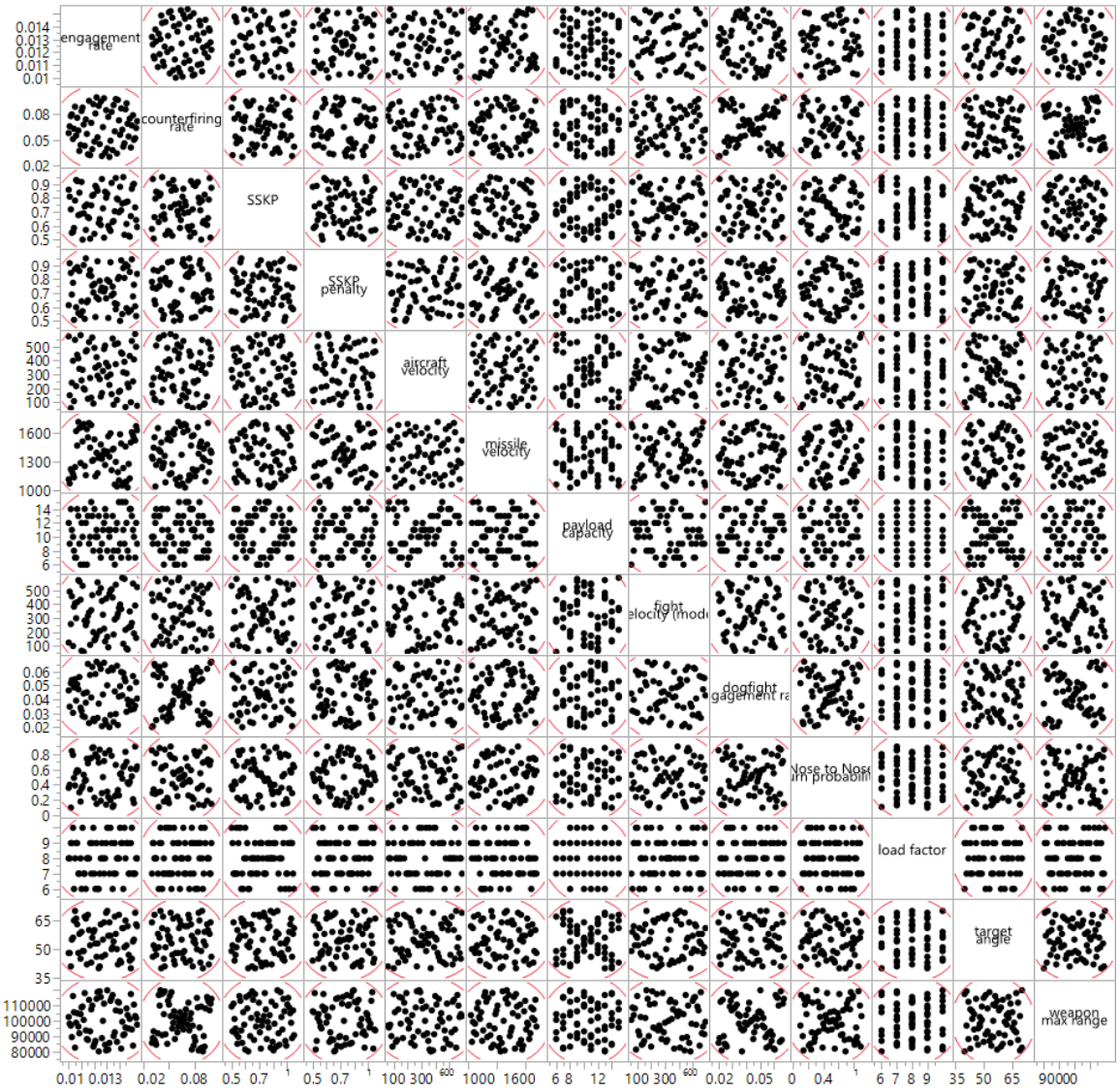

Figure 31 Multi-variate scatterplot of the base design matrix. Visual inspection of the scatterplot reveals acceptable space-filing property of the base design matrix.

B. PROPERTIES OF THE FINAL DESIGN MATRIX

To reduce the maximum absolute pairwise correlation among the explanatory variables in the design matrix, we rotated and stacked four times to capture more subsets of the sample space within the hypercube. The resulting final design matrix yields a maximum absolute pairwise correlation of 0.0433, as shown in Figure 32, thus satisfying near-orthogonality. In addition, the space-filling property of the design matrix is further

improved by rotation and stacking. The improved space-filling property is shown in Figure 33.

	engagement rate	counterfiring rate	SSKP	SSKP penalty	aircraft velocity	missile velocity	payload capacity
engagement rate	1.0000	0.0010	0.0012	-0.0038	-0.0030	-0.0000	0.0142
counterfiring rate	0.0010	1.0000	-0.0004	-0.0034	0.0049	0.0044	-0.0053
SSKP	0.0012	-0.0004	1.0000	-0.0020	-0.0024	0.0044	-0.0044
SSKP penalty	-0.0038	-0.0034	-0.0020	1.0000	-0.0038	-0.0066	0.0188
aircraft velocity	-0.0030	0.0049	-0.0024	-0.0038	1.0000	-0.0046	-0.0163
missile velocity	-0.0000	0.0044	0.0044	-0.0066	-0.0046	1.0000	-0.0074
payload capacity	0.0142	-0.0053	-0.0044	0.0188	-0.0163	-0.0074	1.0000
fight velocity (mode)	-0.0014	0.0025	0.0004	-0.0018	-0.0013	-0.0014	0.0096
dogfight engagement rate	0.0023	-0.0021	-0.0015	0.0002	-0.0030	-0.0035	0.0091
Nose to Nose turn probability	0.0045	-0.0047	0.0008	-0.0019	0.0010	-0.0072	0.0067
load factor	0.0284	-0.0053	-0.0223	0.0045	-0.0157	0.0127	-0.0433
target angle	-0.0003	0.0031	-0.0014	-0.0010	-0.0030	-0.0062	0.0107
weapon max range	-0.0026	0.0039	-0.0052	0.0027	-0.0008	-0.0047	0.0048

	fight velocity (mode)	dogfight engagement rate	Nose to Nose turn probability	load factor	target angle	weapon max range
engagement rate	-0.0014	0.0023	0.0045	0.0284	-0.0003	-0.0026
counterfiring rate	0.0025	-0.0021	-0.0047	-0.0053	0.0031	0.0039
SSKP	0.0004	-0.0015	0.0008	-0.0223	-0.0014	-0.0052
SSKP penalty	-0.0018	0.0002	-0.0019	0.0045	-0.0010	0.0027
aircraft velocity	-0.0013	-0.0030	0.0010	-0.0157	-0.0030	-0.0008
missile velocity	-0.0014	-0.0035	-0.0072	0.0127	-0.0062	-0.0047
payload capacity	0.0096	0.0091	0.0067	-0.0433	0.0107	0.0048
fight velocity (mode)	1.0000	0.0014	0.0049	0.0047	-0.0048	0.0014
dogfight engagement rate	0.0014	1.0000	0.0009	-0.0191	-0.0036	-0.0014
Nose to Nose turn probability	0.0049	0.0009	1.0000	-0.0165	-0.0008	0.0015
load factor	0.0047	-0.0191	-0.0165	1.0000	-0.0022	-0.0073
target angle	-0.0048	-0.0036	-0.0008	-0.0022	1.0000	-0.0074
weapon max range	0.0014	-0.0014	0.0015	-0.0073	-0.0074	1.0000

Figure 32 Correlation table of the design factors in the final design matrix.

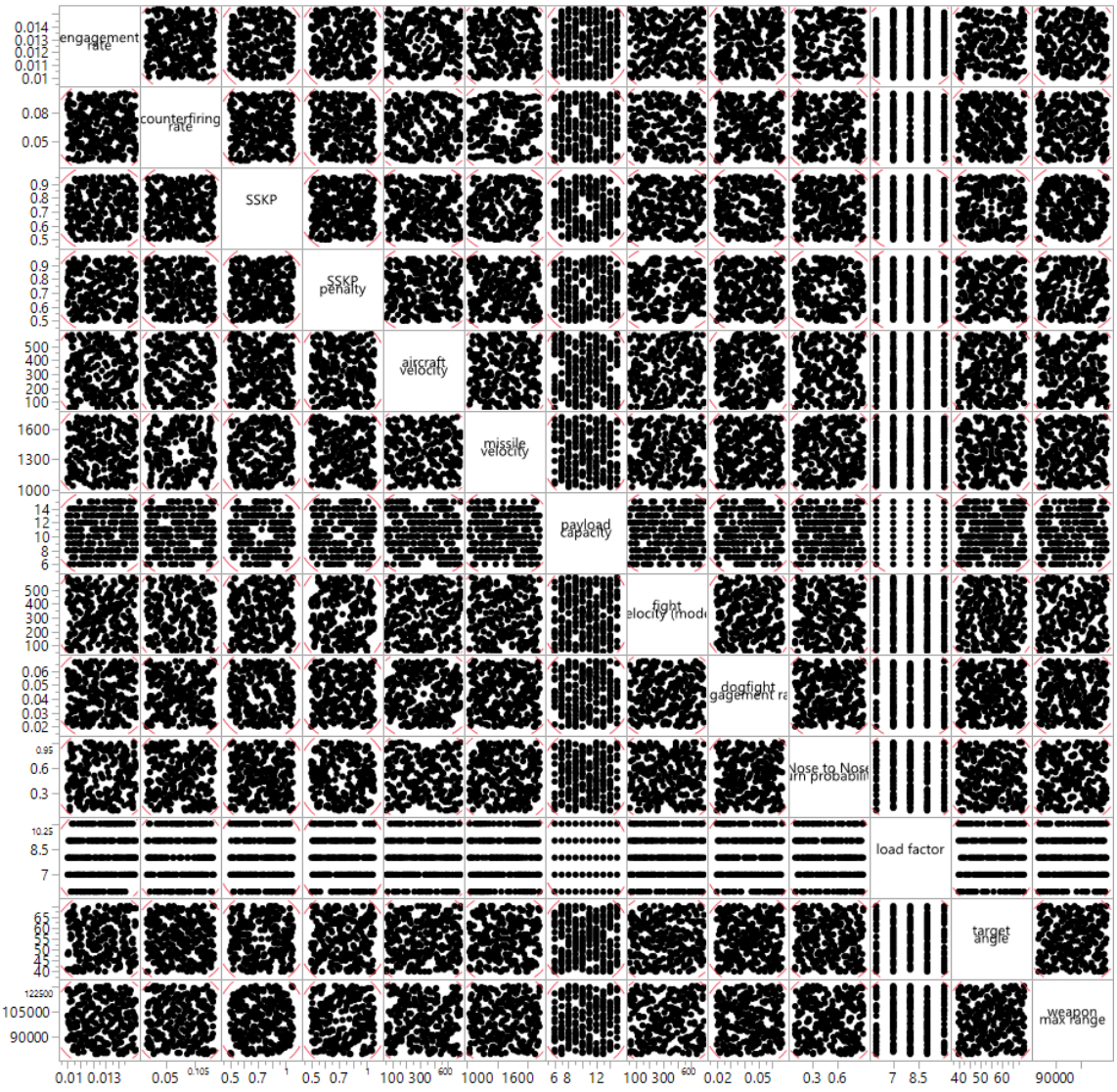

Figure 33 Multi-variate scatterplot of the final design matrix. Significant improvement to the space-filling property of the design matrix can be observed.

APPENDIX C. PHASE 1 META-MODELS

A. BLUE WIN (ϕ_B) META-MODEL

The Blue-Win (ϕ_B) meta-model has a R^2_{adj} of 0.993 as shown in the Summary of Fit in Figure 35, and this implies a good fit of the model. From the Actual vs Predicted plot and Residual plot, we further confirm the homoscedasticity of the fitted model. These characteristics give us the validation that the meta-model is fitted appropriately using the least-square regression.

The resulting meta-model takes in six individual factors, six two-way interactions, and four 2nd degree polynomial terms. All fitted parameters are statistically significant with $\Pr(>|t|) < 0.05$ except for the SSKP penalty term. However, we cannot remove the SSKP penalty due to the statistical significance of its interaction with the aircraft velocity.

The fitted Blue-Win meta-model is used to produce the prediction profiler as shown in Figure 24 in Chapter V. E.

Summary of Fit

RSquare	0.993374
RSquare Adj	0.992932
Root Mean Square Error	0.004626
Mean of Response	0.17754
Observations (or Sum Wgts)	257

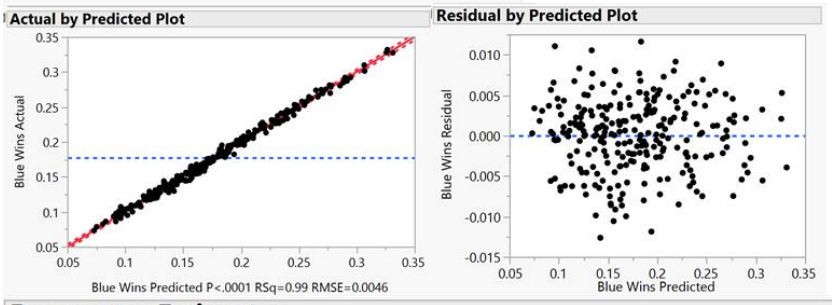

Parameter Estimates

Term	Estimate	Std Error	t Ratio	Prob>|t|
Intercept	-0.171595	0.004028	-42.60	<.0001*
engagement rate	14.18129	0.181771	78.02	<.0001*
counterfiring rate	0.0753985	0.013961	5.40	<.0001*
SSKP	0.2472689	0.002174	113.74	<.0001*
SSKP penalty	0.0034164	0.002174	1.57	0.1174
aircraft velocity	-0.000225	1.837e-6	-122.2	<.0001*
missile velocity	4.1754e-5	1.427e-6	29.27	<.0001*
(engagement rate-0.01269)*(SSKP-0.725)	19.844426	1.497537	13.25	<.0001*
(engagement rate-0.01269)*(missile velocity-1372.02)	0.0057947	0.000955	6.07	<.0001*
(SSKP-0.725)*(aircraft velocity-323.502)	-0.000311	1.364e-5	-22.83	<.0001*
(SSKP-0.725)*(missile velocity-1372.02)	5.3332e-5	1.274e-5	4.19	<.0001*
(SSKP penalty-0.725)*(aircraft velocity-323.502)	-4.862e-5	1.48e-5	-3.29	0.0012*
(aircraft velocity-323.502)*(missile velocity-1372.02)	-7.026e-8	9.692e-9	-7.25	<.0001*
(engagement rate-0.01269)*(engagement rate-0.01269)	-431.2961	139.2795	-3.10	0.0022*
(counterfiring rate-0.06502)*(counterfiring rate-0.06502)	-2.269257	0.826662	-2.75	0.0065*
(aircraft velocity-323.502)*(aircraft velocity-323.502)	3.4133e-8	1.402e-8	2.43	0.0156*
(missile velocity-1372.02)*(missile velocity-1372.02)	-2.402e-8	8.687e-9	-2.76	0.0061*

Figure 35 Statistical details of the least-square fitted model for the Phase 1 Blue-Win meta-model. The R^2_{adj} value of 0.993 implies a sufficiently good fit. The Actual versus Predicted plot and the Residual Plot also reveals a generally good fit with no significant non-linearity in the factors. Six factors, six two-way interactions and four 2nd-order polynomial terms are used to construct the meta-model.

B. RED WIN (ϕ_R) META-MODEL

The Red-Win (ϕ_R) meta-model has a R^2_{adj} of 0.994 as shown in the Summary of Fit in Figure 36, and this implies a good fit of the model. Similar observations on the homoscedasticity of the fitted model, as compared to the Blue-Win meta-model, can be made, thus validating the Red-Win meta-model.

The resulting meta-model takes in five individual factors, eight two-way interactions, and one 2[nd]-degree polynomial terms. All fitted parameters are statistically significant with $\Pr(>|t|) < 0.05$.

The fitted Red-Win meta-model is used to produce the prediction profiler, as shown in Figure 26 in Chapter V. E.

Summary of Fit

RSquare	0.994389
RSquare Adj	0.994064
Root Mean Square Error	0.006009
Mean of Response	0.288458
Observations (or Sum Wgts)	257

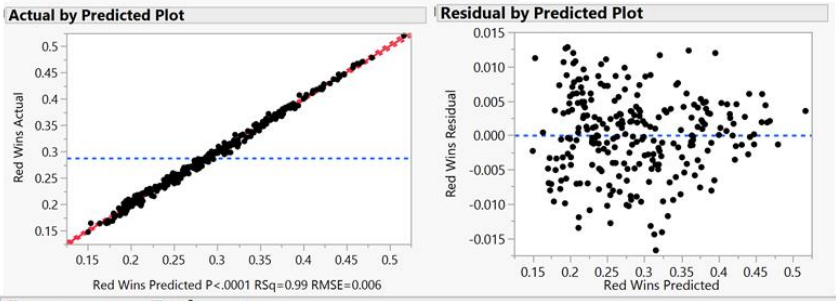

Parameter Estimates

Term	Estimate	Std Error	t Ratio	Prob>|t|
Intercept	0.7280878	0.004447	163.74	<.0001*
engagement rate	-1.336353	0.236088	-5.66	<.0001*
counterfiring rate	-0.806656	0.018133	-44.49	<.0001*
SSKP	-0.266494	0.002824	-94.38	<.0001*
SSKP penalty	-0.06705	0.002824	-23.75	<.0001*
aircraft velocity	-0.000411	2.386e-6	-172.2	<.0001*
(engagement rate-0.01269)*(SSKP-0.725)	-18.19283	1.959398	-9.28	<.0001*
(engagement rate-0.01269)*(aircraft velocity-323.502)	0.0124829	0.001646	7.58	<.0001*
(counterfiring rate-0.06502)*(SSKP-0.725)	-1.158003	0.141021	-8.21	<.0001*
(counterfiring rate-0.06502)*(SSKP penalty-0.725)	-0.997347	0.148009	-6.74	<.0001*
(counterfiring rate-0.06502)*(aircraft velocity-323.502)	0.0018478	0.000131	14.16	<.0001*
(SSKP-0.725)*(SSKP penalty-0.725)	-0.058863	0.022112	-2.66	0.0083*
(SSKP-0.725)*(aircraft velocity-323.502)	0.0006549	1.762e-5	37.16	<.0001*
(SSKP penalty-0.725)*(aircraft velocity-323.502)	0.0001319	1.949e-5	6.77	<.0001*
(aircraft velocity-323.502)*(aircraft velocity-323.502)	1.8214e-7	1.807e-8	10.08	<.0001*

Figure 36 Statistical details of the least-square fitted model for the Phase 1 Red-Win meta-model. The R^2_{adj} value of 0.994 implies a sufficiently good fit. The Actual versus Predicted plot and the Residual Plot also reveals a generally good fit with no significant non-linearity in the factors. Five factors, eight two-way interactions and one 2nd[d]-order polynomial terms are used to construct the meta-model.

THIS PAGE INTENTIONALLY LEFT BLANK

APPENDIX D. OVERALL DUEL META-MODEL

A. BLUE WIN (Γ_1) META-MODEL

The Blue-Win (Γ_1) meta-model for the overall duel has a R^2_{adj} of 0.752 as shown in the Summary of Fit in Figure 37. The R^2_{adj} is not high, however, it is sufficiently well-fitted to provide insights to our model. From the Actual versus Predicted plot and Residual plot, we further confirm the homoscedasticity of the fitted model; however, we also observe that the deviance in the model

The resulting meta-model takes in seven individual factors and three two-way interactions. All fitted parameters are statistically significant with $\Pr(>|t|) < 0.05$.

The fitted Blue-Win (Γ_1) meta-model is used to produce the prediction profiler as shown in Figure 28 in Chapter V. E.

Summary of Fit

RSquare	0.762023
RSquare Adj	0.75227
Root Mean Square Error	0.053633
Mean of Response	0.405236
Observations (or Sum Wgts)	255

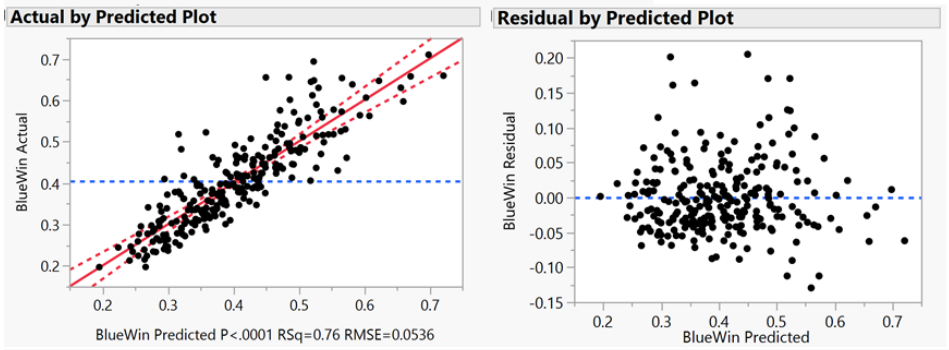

Parameter Estimates

Term	Estimate	Std Error	t Ratio	Prob>|t|
Intercept	-0.148916	0.046762	-3.18	0.0016*
engagement rate	5.5253791	2.12014	2.61	0.0097*
SSKP	0.3447112	0.02537	13.59	<.0001*
aircraft velocity	0.0002737	2.139e-5	12.80	<.0001*
missile velocity	4.7062e-5	1.655e-5	2.84	0.0048*
fight velocity (mode)	-0.000344	2.155e-5	-15.97	<.0001*
Nose to Nose turn probability	-0.041793	0.014268	-2.93	0.0037*
Load factor	0.0266955	0.002688	9.93	<.0001*
(aircraft velocity-322.686)*(fight velocity (mode)-325.592)	-7.175e-7	1.463e-7	-4.90	<.0001*
(aircraft velocity-322.686)*(Load factor-8.02745)	8.6652e-5	1.758e-5	4.93	<.0001*
(Nose to Nose turn probability-0.50333)*(Load factor-8.02745)	-0.040796	0.011448	-3.56	0.0004*

Figure 37 Statistical details of the least-square fitted model for the overall Blue-Win meta-model. The R^2_{adj} value of 0.752 implies a sufficient fit for our purpose. The Actual versus Predicted plot and the Residual plot also reveals a generally good fit with no significant non-linearity in the factors. Seven factors and three two-way interactions are used to construct the meta-model.

B. RED WIN (Γ_2) META-MODEL

The Red-Win (Γ_2) meta-model for the overall duel has a R^2_{adj} of 0.592 as shown in the Summary of Fit in Figure 38. The R^2_{adj} is relatively low, implying a low goodness of fit; however, it is sufficiently to provide insights to how changing the Blue parameter may affect Red's win probability.

The resulting meta-model takes in seven individual factors and three two-way interactions. All fitted parameters are statistically significant with $\Pr(>|t|) < 0.05$ except for the aircraft velocity of Blue. However, the factor cannot be removed due to the statistical significance of its interactions with the SSKP and flight velocity.

The fitted Red-Win (Γ_2) meta-model is used to produce the prediction profiler as shown in Figure 29 in Chapter V. E.

Summary of Fit

RSquare	0.608373
RSquare Adj	0.592322
Root Mean Square Error	0.076749
Mean of Response	0.461129
Observations (or Sum Wgts)	255

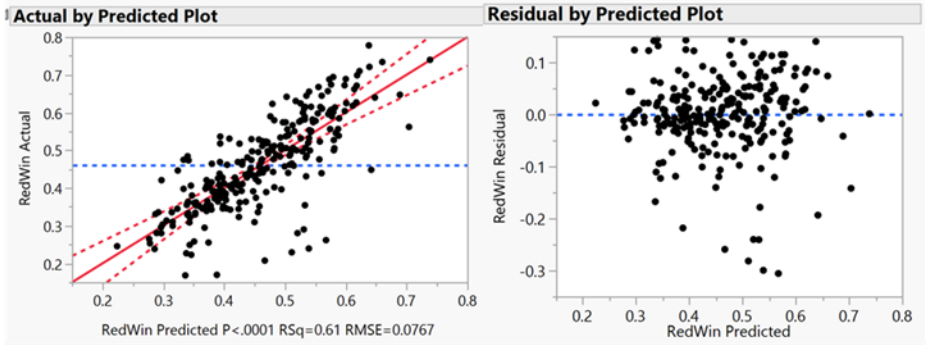

Parameter Estimates

Term	Estimate	Std Error	t Ratio	Prob>|t|
Intercept	1.0783519	0.060144	17.93	<.0001*
engagement rate	-11.8877	3.0337	-3.92	0.0001*
counterfiring rate	-1.047303	0.232598	-4.50	<.0001*
SSKP	-0.383159	0.036307	-10.55	<.0001*
Log(SSKP penalty)	-0.060726	0.025569	-2.37	0.0183*
aircraft velocity	-0.000047	3.06e-5	-1.54	0.1259
fight velocity (mode)	0.0003638	3.083e-5	11.80	<.0001*
Load factor	-0.030399	0.003847	-7.90	<.0001*
(SSKP-0.72566)*(aircraft velocity-322.686)	0.0005494	0.000228	2.41	0.0168*
(SSKP-0.72566)*(Load factor-8.02745)	0.0862504	0.029148	2.96	0.0034*
(aircraft velocity-322.686)*(fight velocity (mode)-325.592)	8.2771e-7	2.151e-7	3.85	0.0002*

Figure 38 Statistical details of the least-square fitted model for the overall Red-Win meta-model. The R^2_{adj} value of 0.592 implies a sufficient fit for our purpose. The Actual versus Predicted plot and the Residual plot also reveals a generally good fit with no significant non-linearity in the factors. Seven factors and three two-way interactions are used to construct the meta-model.

LIST OF REFERENCES

Ancker CJ Jr, Gafarian AV (1983) The two-on-one stochastic duel. Report, US Army TRADOC Systems Analysis Activity, Department of the Army, New Mexico.

Baron S, Kleinman DL, Serben S (1972) A study of the Markov Game approach to tactical maneuvering problems. Report, National Aeronautics and Space Administration, Washington DC.

Dole CE, Lewis JE (2000) Maneuvering performance. *Flight Theory Aerodynamics: A Practical Guide Operational Safety* (John Wiley & Sons, New York), 226–230.

Feigin PD, Shinar J (1984) A simple Markov model for the analysis of multiple air combat. *Naval Research Logistics Quarterly.* 31:413–429.

Gilbert RE (2011) Strategic implications of US fighter force reductions: air-to-air combat modeling using Lanchester equations. Masters Thesis, Air Force Institute of Technology, Ohio.

GlobalSecurity.org (2013) Eurofighter Typhoon EF-2000 - Specifications. Europe. Retrieved (August 5, 2017), http://www.globalsecurity.org/military/world/europe/eurofighter-specs.htm.

Helcio VJ, Sanchez SM, Kienitz KH (2011) Improved efficient, nearly orthogonal, nearly balanced mixed designs. *Winter Simulation. Conference.*3605–3616.

Hurt HH J (1960) Maneuvering performance. *Aerodynamics for Naval Aviators* (The Office of the Chief Of Naval Operations Aviation Training Division, Los Angeles), 180.

Johnson IR, MacKay NJ (2008) Lanchester models and the Battle of Britain. *Naval Research Logistics.* 58:210–222.

Moritz K, Polis R, Well KH (1987) Pursuit-Evasion in a medium range air-combat scenario. *Computational Mathematical Applications.* 13(1):167–180.

Kress M (1992) A many-on-many stochastic duel model for a mountain battle. *Naval Research Logistics*. 39:437–446.

Lanchester FW (1916) The principle of concentration. *Aircraft in Warfare: The Dawn of the Fourth Arm*. (Constable and Company Limited, London), 39–53.

Law AM (2015) Response surfaces and meta-models. *Simulation Modeling and Analysis* (McFraw-Hill Higher Education, New York), 656–679.

Li J, Liu L (2012) The many-on-one stochastic duel model with information sharing. *Applied Mathematics.* 3:637–640.

Liu L (2006) A kind of stochastic duel model for guerrilla war. *European Journal of Operations Research.* 171(60174028):430–438.

Sanchez SM, Sánchez PJ, Wan H (2014) Simulation experiments: better insights by design. *Proceedings of the 2014 Summer Simulation Multiconference*. 53.

Shaw RL (1985) Basic fighter maneuvers. *Fighter Combat: Tactics and Maneuvering*. (United States Naval Institute., Maryland), 62–97.

U.S. Army TRADOC G-2 (2014) Worldwide Equipment Guide Volume 2: Airspace and Air Defense Systems. Report, TRADOC Intelligence Support Activity, Department of the Army, Kansas City.

Virtanen K, Karelahti J, Raivio T (2006) Modeling air combat by a moving horizon influence diagram game. *Journal of Guidance, Control, and Dynamics*. 29(5):1080–1091.

Williams T, Ancker CJ Jr (1963) Stochastic duels. *Operations Research* 11(5):803–817.

Zabinski H (2015) Capital investment planning aid for naval aircraft. Master Thesis, Naval Postgraduate School, Monterey.

INITIAL DISTRIBUTION LIST

1. Defense Technical Information Center
   Ft. Belvoir, Virginia

2. Dudley Knox Library
   Naval Postgraduate School
   Monterey, California